REPORT DOCUMENTATION PAGE

Form Approved OMB NO. 0704-0188

The public reporting burden for this collection of information is estimated to average 1 hour per response, including the time for reviewing instructions, searching existing data sources, gathering and maintaining the data needed, and completing and reviewing the collection of information. Send comments regarding this burden estimate or any other aspect of this collection of information, including suggesstions for reducing this burden, to Washington Headquarters Services, Directorate for Information Operations and Reports, 1215 Jefferson Davis Highway, Suite 1204, Arlington VA, 22202-4302. Respondents should be aware that notwithstanding any other provision of law, no person shall be subject to any oenalty for failing to comply with a collection of information if it does not display a currently valid OMB control number.
PLEASE DO NOT RETURN YOUR FORM TO THE ABOVE ADDRESS.

1. REPORT DATE (DD-MM-YYYY)	2. REPORT TYPE	3. DATES COVERED (From - To)
14-02-2011	Final Report	1-Sep-2005 - 31-Aug-2008

4. TITLE AND SUBTITLE
Novel low Cost High Efficiency Tunable RF Devices and Antenna Arrays Design based on the Ferroelectric Materials and the CTS Technologies

5a. CONTRACT NUMBER
W911NF-05-1-0495

5b. GRANT NUMBER

5c. PROGRAM ELEMENT NUMBER
611102

6. AUTHORS
Magdy F. Iskander

5d. PROJECT NUMBER

5e. TASK NUMBER

5f. WORK UNIT NUMBER

7. PERFORMING ORGANIZATION NAMES AND ADDRESSES
University of Hawaii - Honolulu
2530 Dole Street
Sakamaki D200
Honolulu, HI 96822 -2225

8. PERFORMING ORGANIZATION REPORT NUMBER

9. SPONSORING/MONITORING AGENCY NAME(S) AND ADDRESS(ES)
U.S. Army Research Office
P.O. Box 12211
Research Triangle Park, NC 27709-2211

10. SPONSOR/MONITOR'S ACRONYM(S)
ARO

11. SPONSOR/MONITOR'S REPORT NUMBER(S)
49304-EL.1

12. DISTRIBUTION AVAILABILITY STATEMENT
Approved for Public Release; Distribution Unlimited

13. SUPPLEMENTARY NOTES
The views, opinions and/or findings contained in this report are those of the author(s) and should not contrued as an official Department of the Army position, policy or decision, unless so designated by other documentation.

14. ABSTRACT
In our research, we investigate development of the low cost ferroelectric tunable RF devices and integrated phased antenna arrays with beam steering capabilities. Accomplished tasks include a successful design of the Ka-band CTS antenna array with over 1 GHz bandwidth, the simulation of the integrated CTS antenna array performance with multi-dielectric layer ferroelectric phase shifters, conducting a comparative study between the multi- and single- layer coplanar waveguide ferroelectric phase shifters design. Simulation results demonstrated the feasibility

15. SUBJECT TERMS
Tunable RF phase shifter, ferroelectric material, antenna array

16. SECURITY CLASSIFICATION OF: a. REPORT	b. ABSTRACT	c. THIS PAGE	17. LIMITATION OF ABSTRACT	15. NUMBER OF PAGES	19a. NAME OF RESPONSIBLE PERSON
UU	UU	UU	UU		Magdy Iskander
					19b. TELEPHONE NUMBER 808-956-3434

Standard Form 298 (Rev 8/98)
Prescribed by ANSI Std. Z39.18

Report Title

Novel low Cost High Efficiency Tunable RF Devices and Antenna Arrays Design based on the Ferroelectric Materials and the CTS Technologies

ABSTRACT

In our research, we investigate development of the low cost ferroelectric tunable RF devices and integrated phased antenna arrays with beam steering capabilities. Accomplished tasks include a successful design of the Ka-band CTS antenna array with over 1 GHz bandwidth, the simulation of the integrated CTS antenna array performance with multi-dielectric layer ferroelectric phase shifters, conducting a comparative study between the multi- and single- layer coplanar waveguide ferroelectric phase shifters design. Simulation results demonstrated the feasibility of using the integrated CTS and ferroelectric materials approach for designing high performance phased antenna array. Conventional ferroelectric devices were facing low input impedance values, and high ohmic losses. In order to address these issues, we developed a new phase-shifter design procedure that was based on the use of "multi-dielectric" layers substrate including a middle layer of highly tunable ferroelectric material and numerically verified that this approach significantly reduced the insertion losses, while maintaining a large percentage (85%) of the tunability. Our research indicated that the application of the multi-dielectric layers in this new CPW-CTS antenna design will provide the much anticipated breakthrough in developing low cost antenna arrays with beam steering capabilities.

List of papers submitted or published that acknowledge ARO support during this reporting period. List the papers, including journal references, in the following categories:

(a) Papers published in peer-reviewed journals (N/A for none)

M. F. Iskander, Z. Zhang, Z. Yun, and R. Isom, "Coaxial Continuous Transverse Stub (CTS) Array." IEEE Micro. Wireless. Lett., vol. 11, no. 12, pp. 489-491, Dec. 2001.

R. Ison, M. Iskander, Z. Yun, and Z. Zhang, " Design and Development of Multiband Coaxial Continuous Transverse Stub (CTS) Antenna Arrays," IEEE Trans. on Antennas and propagation, vol. 52, no.8, pp. 2180-2184, Aug. 2004

W. Kim, M. Iskander, and C. Tanaka, "High-performance Low-Cost Phase-Shifter Design Based on the Ferroelectric Materials Technology," Elelctronics Letters, Vol. 40, no. 21,pp. 1345-1347, Oct. 2004.

W. Kim, M.F. Iskander, "A new Coplanar Waveguide Continuous Transverse Stub (CPW-CTS) Antenna for Wireless Communications." IEEE Ant.. & Prop. Lett., vol. 4, pp. 172-174, 2005.

W. Kim, M. Iskander, C. Krowne, "Modified Green's Function and Spectral-Domain Approach for Analyzing Anisotropic and Multidielectric Layer Coplanar Waveguide Ferroelectric Phase Shifters," EEE Transactions on Microwave Theory and Techniques,"vol. 55, pp. 402-409, 2007

W. Kim and M. Iskander, "Integrated Phased Array Antenna Design Using Ferroelectric Materials and the Continuous Transverse Stub Technology," IEEE Trans. on Antennas and propagation, vol. 54, no. 11, pp. 3095-3105, 2006

Number of Papers published in peer-reviewed journals: 6.00

(b) Papers published in non-peer-reviewed journals or in conference proceedings (N/A for none)

Number of Papers published in non peer-reviewed journals: 0.00

(c) Presentations

Number of Presentations: 0.00

Non Peer-Reviewed Conference Proceeding publications (other than abstracts):

Number of Non Peer-Reviewed Conference Proceeding publications (other than abstracts): 0

Peer-Reviewed Conference Proceeding publications (other than abstracts):

W. Kim, M. Iskander, "Novel High performance Low Cost Phase-Shifter Design Based on the Ferroelectric Materials Technology Using the WIPL-D Code," Applided Computational Elelctromagnetics Society, Syracuse, NY, 2004.

M. F. Iskander, W. Kim, J. Bell, N. Celik, Z. Yun, and H. Youn, "Antenna arrays technologies for advanced wireless systems," The 2nd International IEEE Conference on Microwaves, Communications, Antennas and Electronic Systems (IEEE COMCAS'09), Tel Aviv, Israel, Nov. 9-11, 2009.

W. C. Kim, and m. F. Iskander, "A Technique for Modeling Multi-Dielectric Layers Coplanar Waveguide Ferroelectric Phase Shifters," IEEE Antennas and Propagation International Symposium, Honolulu, HI, June 10-16, 2007.

W. C. Kim, and M. Iskander, " Integrated Phased Antenna Array Design Using Ferroelectric Materials and the Coplanar Waveguide Continuous Transverse Stub Technologies," IEEE Int'l Symposium on Antennas and Propagation, Albuquerque, NM, July 2006.

M. Rezk, W. Kim, Z. Yun, M. F. Iskander, "Narrow Beam Adaptive Array for Advanced Wireless Applications," 2005 IEEE/ACES International Conference on Wireless Communications and Applied Computational Electromagnetics, pp. 594-597, April 3-7, 2005, Honolulu, Hawaii.

Number of Peer-Reviewed Conference Proceeding publications (other than abstracts): 5

(d) Manuscripts

Number of Manuscripts: 0.00

Patents Submitted

W. Kim and M. F. Iskander,"A new Coplanar Waveguide Continuous Transverse Stub (CWP-CTS) antenna for wireless communications," U.S. Patent 7,079,082, Jul. 18, 2006

Patents Awarded

W. Kim and M. F. Iskander,"A new Coplanar Waveguide Continuous Transverse Stub (CWP-CTS) antenna for wireless communications," U.S. Patent 7,079,082, Jul. 18, 2006

Awards

Graduate Students

NAME	PERCENT_SUPPORTED
FTE Equivalent:	
Total Number:	

Names of Post Doctorates

NAME	PERCENT_SUPPORTED
FTE Equivalent:	
Total Number:	

Names of Faculty Supported

NAME	PERCENT_SUPPORTED	National Academy Member
Magdy F. Iskander		No
FTE Equivalent:		
Total Number:	**1**	

Names of Under Graduate students supported

NAME	PERCENT_SUPPORTED
FTE Equivalent:	
Total Number:	

Student Metrics

This section only applies to graduating undergraduates supported by this agreement in this reporting period

The number of undergraduates funded by this agreement who graduated during this period: ......

The number of undergraduates funded by this agreement who graduated during this period with a degree in science, mathematics, engineering, or technology fields:......

The number of undergraduates funded by your agreement who graduated during this period and will continue to pursue a graduate or Ph.D. degree in science, mathematics, engineering, or technology fields:......

Number of graduating undergraduates who achieved a 3.5 GPA to 4.0 (4.0 max scale):......

Number of graduating undergraduates funded by a DoD funded Center of Excellence grant for Education, Research and Engineering:......

The number of undergraduates funded by your agreement who graduated during this period and intend to work for the Department of Defense ......

The number of undergraduates funded by your agreement who graduated during this period and will receive scholarships or fellowships for further studies in science, mathematics, engineering or technology fields: ......

Names of Personnel receiving masters degrees

NAME	
Total Number:	

Names of personnel receiving PHDs

NAME	
Wayne Kim	
Total Number:	**1**

Names of other research staff

NAME	PERCENT_SUPPORTED
FTE Equivalent:	
Total Number:	

Sub Contractors (DD882)

Inventions (DD882)

5 **A new Coplanar Waveguide Continuous Transverse Stub (CWP-CTS) antenna for wireless communications**

Patent Filed in US? (5d-1) Y

Patent Filed in Foreign Countries? (5d-2) N

Was the assignment forwarded to the contracting officer? (5e) N

Foreign Countries of application (5g-2):

5a: W. Kim and M. F. Iskander

5f-1a: University of Hawaii

5f-c: |1680 East West Rd

honolulu HI 96822

Scientific Progress

Technology Transfer

REPORT DOCUMENTATION PAGE

Form Approved
OMB No. 0704-0188

The public reporting burden for this collection of information is estimated to average 1 hour per response, including the time for reviewing instructions, searching existing data sources, gathering and maintaining the data needed, and completing and reviewing the collection of information. Send comments regarding this burden estimate or any other aspect of this collection of information, including suggestions for reducing the burden, to Department of Defense, Washington Headquarters Services, Directorate for Information Operations and Reports (0704-0188), 1215 Jefferson Davis Highway, Suite 1204, Arlington, VA 22202-4302. Respondents should be aware that notwithstanding any other provision of law, no person shall be subject to any penalty for failing to comply with a collection of information if it does not display a currently valid OMB control number.

PLEASE DO NOT RETURN YOUR FORM TO THE ABOVE ADDRESS.

1. REPORT DATE *(DD-MM-YYYY)*: 01-15/2011

2. REPORT TYPE: Final Technical Report

3. DATES COVERED *(From - To)*: September 2005 - August 2007

4. TITLE AND SUBTITLE
Novel Low Cost High Efficiency Tunable RF Devices and Antenna Arrays Design based on the Ferroelectric Materials and the CTS Technologies

5a. CONTRACT NUMBER: W911NF-05-1-0495

5b. GRANT NUMBER: n/a

5c. PROGRAM ELEMENT NUMBER: n/a

5d. PROJECT NUMBER: E49304-EL-05-152

5e. TASK NUMBER: n/a

5f. WORK UNIT NUMBER: n/a

6. AUTHOR(S)
Iskander, Magdy F.

7. PERFORMING ORGANIZATION NAME(S) AND ADDRESS(ES)
University of Hawaii
2530 Dole Street, Sakamaki Hall D-200
Honolulu, Hawaii 96822

8. PERFORMING ORGANIZATION REPORT NUMBER: 0W411

9. SPONSORING/MONITORING AGENCY NAME(S) AND ADDRESS(ES)
ONRRO Seattle
1107 NE 45th Street, Suite 350
Seattle, Washington 98105-4631

10. SPONSOR/MONITOR'S ACRONYM(S): ONRRO

11. SPONSOR/MONITOR'S REPORT NUMBER(S): N63374

12. DISTRIBUTION/AVAILABILITY STATEMENT

13. SUPPLEMENTARY NOTES

14. ABSTRACT
In our research, we investigate development of the low cost ferroelectric tunable RF devices and integrated phased antenna arrays with beam steering capabilities. Accomplished tasks include a successful design of the Ka-band CTS antenna array with over 1 GHz bandwidth, the simulation of the integrated CTS antenna array performance with multi-dielectric layer ferroelectric phase shifters, conducting a comparative study between the multi- and single- layer coplanar waveguide ferroelectric phase shifters design. Simulation results demonstrated the feasibility of using the integrated CTS and ferroelectric materials approach for designing high performance phased antenna array. Conventional ferroelectric devices were facing low input impedance values, and high ohmic losses. In order to address these issues, we developed a new phase-shifter design procedure that was based on the use of "multi-dielectric" layers substrate including a middle layer of highly tunable ferroelectric material and numerically verified that this approach significantly reduced the insertion losses, while maintaining a large percentage (85%) of the tunability. Our research indicated that the application of the multi-dielectric layers in this new CPW-CTS antenna design will provide the much anticipated

15. SUBJECT TERMS

16. SECURITY CLASSIFICATION OF: a. REPORT	b. ABSTRACT	c. THIS PAGE	17. LIMITATION OF ABSTRACT	18. NUMBER OF PAGES	19a. NAME OF RESPONSIBLE PERSON
U	U	U	UU		Magdy F. Iskander

19b. TELEPHONE NUMBER *(Include area code)*: 808-956-3434

Reset

INSTRUCTIONS FOR COMPLETING SF 298

1. REPORT DATE. Full publication date, including day, month, if available. Must cite at least the year and be Year 2000 compliant, e.g. 30-06-1998; xx-06-1998; xx-xx-1998.

2. REPORT TYPE. State the type of report, such as final, technical, interim, memorandum, master's thesis, progress, quarterly, research, special, group study, etc.

3. DATES COVERED. Indicate the time during which the work was performed and the report was written, e.g., Jun 1997 - Jun 1998; 1-10 Jun 1996; May - Nov 1998; Nov 1998.

4. TITLE. Enter title and subtitle with volume number and part number, if applicable. On classified documents, enter the title classification in parentheses.

5a. CONTRACT NUMBER. Enter all contract numbers as they appear in the report, e.g. F33615-86-C-5169.

5b. GRANT NUMBER. Enter all grant numbers as they appear in the report, e.g. AFOSR-82-1234.

5c. PROGRAM ELEMENT NUMBER. Enter all program element numbers as they appear in the report, e.g. 61101A.

5d. PROJECT NUMBER. Enter all project numbers as they appear in the report, e.g. 1F665702D1257; ILIR.

5e. TASK NUMBER. Enter all task numbers as they appear in the report, e.g. 05; RF0330201; T4112.

5f. WORK UNIT NUMBER. Enter all work unit numbers as they appear in the report, e.g. 001; AFAPL30480105.

6. AUTHOR(S). Enter name(s) of person(s) responsible for writing the report, performing the research, or credited with the content of the report. The form of entry is the last name, first name, middle initial, and additional qualifiers separated by commas, e.g. Smith, Richard, J, Jr.

7. PERFORMING ORGANIZATION NAME(S) AND ADDRESS(ES). Self-explanatory.

8. PERFORMING ORGANIZATION REPORT NUMBER. Enter all unique alphanumeric report numbers assigned by the performing organization, e.g. BRL-1234; AFWL-TR-85-4017-Vol-21-PT-2.

9. SPONSORING/MONITORING AGENCY NAME(S) AND ADDRESS(ES). Enter the name and address of the organization(s) financially responsible for and monitoring the work.

10. SPONSOR/MONITOR'S ACRONYM(S). Enter, if available, e.g. BRL, ARDEC, NADC.

11. SPONSOR/MONITOR'S REPORT NUMBER(S). Enter report number as assigned by the sponsoring/ monitoring agency, if available, e.g. BRL-TR-829; -215.

12. DISTRIBUTION/AVAILABILITY STATEMENT. Use agency-mandated availability statements to indicate the public availability or distribution limitations of the report. If additional limitations/ restrictions or special markings are indicated, follow agency authorization procedures, e.g. RD/FRD, PROPIN, ITAR, etc. Include copyright information.

13. SUPPLEMENTARY NOTES. Enter information not included elsewhere such as: prepared in cooperation with; translation of; report supersedes; old edition number, etc.

14. ABSTRACT. A brief (approximately 200 words) factual summary of the most significant information.

15. SUBJECT TERMS. Key words or phrases identifying major concepts in the report.

16. SECURITY CLASSIFICATION. Enter security classification in accordance with security classification regulations, e.g. U, C, S, etc. If this form contains classified information, stamp classification level on the top and bottom of this page.

17. LIMITATION OF ABSTRACT. This block must be completed to assign a distribution limitation to the abstract. Enter UU (Unclassified Unlimited) or SAR (Same as Report). An entry in this block is necessary if the abstract is to be limited.

REPORT DOCUMENTATION PAGE (SF298)
(Continuation Sheet)

Final Report (9/1/04-8/31/07):

Novel low Cost High Efficiency Tunable RF Devices and Antenna Arrays Design based on the Ferroelectric Materials and the CTS Technologies

Magdy Iskander PI.

Table of Contents

List of Figures

Statement of the problem studied

Low cost and high performance steerable antennas have been a critically important and challenging topic in satellite communication, radar, navigation, remote sensing, and space exploration. Ferroelectric tunable RF devices such as phase shifters and RF switches incorporated into high performance phased-array antennas with beam steering capabilities are one promising technology to satisfy these requirements. While many emerging designs and alternative approaches are being developed to help achieve the desired high RF performance and low cost objectives, there is still a need for fresh ideas that may provide complementary avenues to other ongoing research. For example, while some are continuing with the development of the MEMs technology with focus on overcoming some of the remaining difficulties including RF packaging, reliability, reducing the response time, and lowering the required switching voltages, others are pursuing the development of metamaterials and Electromagnetic Band Gap Surfaces (EPG) to help develop new devices say with reduced size, multiband capabilities, or to enhance the performance by increasing gain and mitigating interferences.

In our research, we investigate development of the low cost ferroelectric tunable RF devices and integrated phased antenna arrays with beam steering capabilities. Ferroelectric materials are characterized by change in permittivity with an applied dc-bias voltage. This change in permittivity can be used to change the electrical length of a transmission line and, hence, in the design of low-cost phase shifters. Furthermore, the ferroelectric material can be embedded in phased array antenna designs such as that based on the Continuous Transverse Stub (CTS) technology [1-4], leading to an integrated antenna array design with beam steering capability. [5-8]

The most popular ferroelectric material for room temperature operation is $Ba_xSr_{1-x}TiO_3$ (BSTO) where varying *x* can vary the maximum of the dielectric constant. However, BSTO films had suffered from a high loss tangent. Many researches have been conducted to improve the high loss characteristics of BSTO and recent advances in the development of this material have resulted in decreasing the loss tangent (0.001) by using dopants [9], and increasing the tunability by annealing process [10]. It was, however, generally felt that designs based on this technology, although low cost, still exhibited unacceptably high insertion losses and impractical low input impedance values. Specifically, input impedance values for microstrip and parallel plate waveguide type structures were too small for utilization in practical designs. Furthermore, Ohmic losses are unacceptably high in addition to the input impedance issues. Therefore, in order to address such high insertion losses and the unacceptably low input impedance values, HCAC proposed a new phase-shifter design procedure that was based on the use of “multi-dielectric” layers substrate including a middle layer of highly tunable ferroelectric material [6-8] and numerically verified that this approach significantly reduced the insertion losses, while maintaining a large percentage (85%) of the tunability.[8] This multilayer-dielectric loading technique involves a novel biasing procedure for the ferroelectric layer beneath the low dielectric layer. The recently developed coplanar waveguide (CPW) version of the CTS technology [3,4] can be integrated with this multilayer ferroelectric tunable RF component to achieve high performance and low cost phased antenna arrays. It is believed that the application of the multi-dielectric layers in this new CPW-CTS antenna design is ready to provide the much anticipated breakthrough in developing low cost antenna arrays with beam steering capabilities. Unlike any other approach, the multilayer ferroelectric

CPW-CTS antenna is based on “integrating the phase shifters with the antenna element,” rather than as part of the electronics package, and as a result is expected to achieve a high system performance in addition to satisfying the much desired goal of reducing the cost.

The objective of this research is to develop a high performance low cost antenna array using integrated Continuous Transverse Stub (CTS) and Ferroelectric material technologies. Tasks included the design of a CTS antenna array in the Ka-Band with bandwidth of over 1GHz, simulation of the beam steering capability of an integrated CTS array with ferroelectric phase shifters placed between the antenna array elements, characterization of multi-dielectric layers ferroelectric phase shifters, and the possible evaluation of the complete integrated antenna array design.

Summary of the most important results

The goal of this work is to investigate development of the low cost ferroelectric tunable RF devices and integrated phased antenna arrays with beam steering capabilities. Ferroelectric materials are characterized by change in permittivity with an applied dc-bias voltage. This change in permittivity can be used to change the electrical length of a transmission line and, hence, in the design of low-cost phase shifters. Such ferroelectric material can be embedded in phased array antenna designs such as that based on the Continuous Transverse Stub (CTS) technology, leading to an integrated antenna array design with beam steering capability. The most popular ferroelectric material for room temperature operation is $Ba_xSr_{1-x}TiO_3$ (BSTO) where varying *x* can vary the maximum of the dielectric constant. However, BSTO films had suffered from a high loss tangent. It was generally felt that designs based on this technology, although low cost, still exhibited unacceptably high insertion losses and impractical low input impedance values. Specifically, input impedance values for microstrip and parallel plate waveguide type structures were too small for utilization in practical designs. Furthermore, Ohmic losses are unacceptably high in addition to the input impedance issues. Therefore, main focus of this project was to investigate and develop a method to overcome these issues.

Our approach to address such high insertion losses and the unacceptably low input impedance values was based on the use of "multi-dielectric" layers substrate including a middle layer of highly tunable ferroelectric material. Fig. 1 depicts a multidielectric ferroelectric phase-shifter design that employs the placement of a low-loss nontunable dielectric layer in between the ferroelectric material and the coplanar electrodes to reduce the attenuation constant and improve the figure of Merit (FoM).

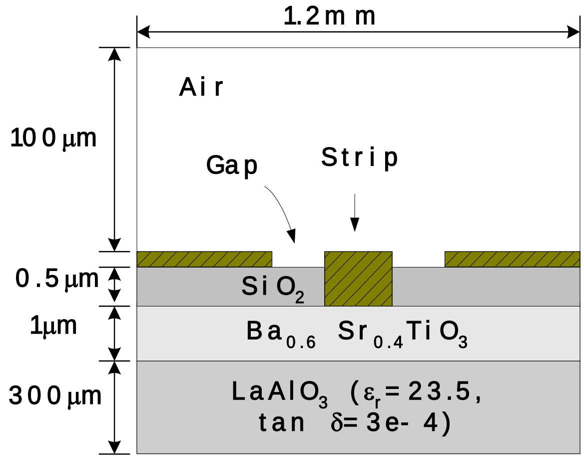

Fig. 1 Cross section of multidielectric employing a via through the silicon–dioxide layer for simple ferroelectric biasing.

The FoM is defined as the amount of phase shift per decibel loss, where the loss is calculated based on the unbiased condition. This new design was modeled using the method of finite differences and newly developed spectral matrix method. Simulation results showed the potential distribution penetrates deeper into the ferroelectric material for the multilayer design. These results indicate that adequate polarization across ferroelectric material may be realized with the formation of a via through the silicon dioxide layer, under the center conductor. Based on these promising simulation results, we next examined feasibility on integration of a phase shifter using the mulitdielectric biasing method and the coplanar waveguide continuous transverse stub (CPW-CTS) antenna technology. We proceeded to simulate the desired integrated phased array antenna with beam steering capabilities. (See Fig. 2) The simulated phased array produced nearly ±20 ° (or 40 °) of beam scanning in conjunction with possessing good impedance match. The use of a thinner ferroelectric layer results in a smaller scan of ± 15 ° but higher gain and lower scan loss. These results were published in IEEE transaction Antenna and propagation in 2007 (see Appendix).

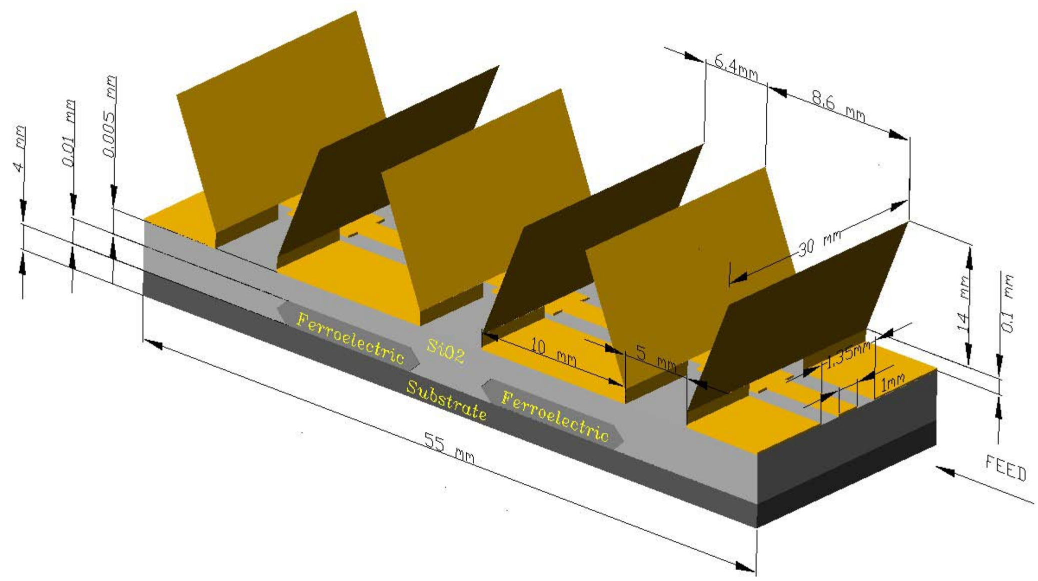

Fig. 2 Layout of the CPW-CTS phased array antenna for simulations.

Accomplished tasks include a successful design of the Ka-band CTS antenna array with over 1 GHz bandwidth, the simulation of the integrated CTS antenna array performance with multi-dielectric layer ferroelectric phase shifters, conducting a comparative study between the multi- and single- layer coplanar waveguide ferroelectric phase shifters design, and the more recent successful fabrication and characterization of ferroelectric phase shifters. Results from the CTS antenna design work may be found in references [1-4], and results from the comparative study of the single- and multilayer ferroelectric phase shifters may be found in [5-7]. Simulation results that demonstrate the feasibility of using the integrated CTS and ferroelectric materials approach for designing high performance phased antenna array can also be found in reference [8]. In this case it is shown that while this approach is feasible, inclusion of thicker layer of ferroelectric material will be required to achieve beam steering more than $\pm 20^0$. To avoid the use of thicker ferroelectric layers and the corresponding need for a larger DC bias voltage, an approach in which analog phase shifting would be accomplished using the proposed technology while larger phase shifts would be achieved using available digital technologies. It is believed that this combined analog (small beam steering angles) and digital (large steering angles) would lead to optimum phased antenna array designs with performance, cost, and required DC bias voltage all taken into consideration.

Publications

Peer-reviewed journals:

M. F. Iskander, Z. Zhang, Z. Yun, and R. Isom, “Coaxial Continuous Transverse Stub (CTS) Array.” *IEEE Micro. Wireless. Lett.,* vol. 11, no. 12, pp. 489-491, Dec. 2001.

R. Ison, M. Iskander, Z. Yun, and Z. Zhang, " Design and Development of Multiband Coaxial Continuous Transverse Stub (CTS) Antenna Arrays," IEEE Trans. on Antennas and propagation, vol. 52, no.8, pp. 2180-2184, Aug. 2004

W. Kim, M. Iskander, and C. Tanaka, "High-performance Low-Cost Phase-Shifter Design Based on the Ferroelectric Materials Technology," Elelctronics Letters, Vol. 40, no. 21,pp. 1345-1347, Oct. 2004.

W. Kim, M.F. Iskander, “A new Coplanar Waveguide Continuous Transverse Stub (CPW-CTS) Antenna for Wireless Communications.” *IEEE Ant.. & Prop. Lett.,* vol. 4, pp. 172-174, 2005.

W. Kim, M. Iskander, C. Krowne, “Modified Green's Function and Spectral-Domain Approach for Analyzing Anisotropic and Multidielectric Layer Coplanar Waveguide Ferroelectric Phase Shifters,*” EEE Transactions on Microwave Theory and Techniques*,”vol. 55, pp. 402-409, 2007

W. Kim and M. Iskander, "Integrated Phased Array Antenna Design Using Ferroelectric Materials and the Continuous Transverse Stub Technology," IEEE Trans. on Antennas and propagation, vol. 54, no. 11, pp. 3095-3105, 2006

Conference proceedings:

W. Kim, M. Iskander, "Novel High performance Low Cost Phase-Shifter Design Based on the Ferroelectric Materials Technology Using the WIPL-D Code," Applided Computational Elelctromagnetics Society, Syracuse, NY, 2004.

M. F. Iskander, W. Kim, J. Bell, N. Celik, Z. Yun, and H. Youn, “Antenna arrays technologies for advanced wireless systems,” *The 2nd International IEEE Conference on Microwaves, Communications, Antennas and Electronic Systems* (IEEE COMCAS’09), Tel Aviv, Israel, Nov. 9-11, 2009.

W. C. Kim, and m. F. Iskander, “A Technique for Modeling Multi-Dielectric Layers Coplanar Waveguide Ferroelectric Phase Shifters,” *IEEE Antennas and Propagation International Symposium*, Honolulu, HI, June 10-16, 2007.

W. C. Kim, and M. Iskander, “ Integrated Phased Antenna Array Design Using Ferroelectric Materials and the Coplanar Waveguide Continuous Transverse Stub Technologies,” *IEEE Int’l Symposium on Antennas and Propagation*, Albuquerque, NM, July 2006.

M. Rezk, W. Kim, Z. Yun, M. F. Iskander, “Narrow Beam Adaptive Array for Advanced Wireless Applications,” *2005 IEEE/ACES International Conference on Wireless Communications and Applied Computational Electromagnetics*, pp. 594-597, April 3-7, 2005, Honolulu, Hawaii.

Book Chapter:

Magdy F. Iskander, Wayne Kim, Jodie Bell, Nuri Celik, and Zhengqing Yun, "*Antenna Arrays Technologies for Advanced Wireless Systems",* Modern Antenna Handbook, Constantine Balanis, Editor, John Wiley & Sons publication, July 2008.

Ph.D. Awarded:

Wayne Kim (Dec. 2006)

Report of Inventions

W. Kim and M. F. Iskander,"A new Coplanar Waveguide Continuous Transverse Stub (CWP-CTS) antenna for wireless communications," U.S. Patent 7,079,082, Jul. 18, 2006

Bibliography

[1] M. F. Iskander, Z. Zhang, Z. Yun, and R. Isom, “Coaxial Continuous   Transverse Stub (CTS) Array.” *IEEE Micro. Wireless. Lett.,* vol. 11, no. 12, pp. 489-491, Dec. 2001.

[2] R. Ison, M. Iskander, Z. Yun, and Z. Zhang, " Design and Development of Multiband Coaxial Continuous Transverse Stub (CTS) Antenna Arrays," IEEE Trans. on Antennas and propagation, vol. 52, no.8, pp. 2180-2184, Aug. 2004

[3] W. Kim, M.F. Iskander, “A new Coplanar Waveguide Continuous Transverse Stub (CPW-CTS) Antenna for Wireless Communications.” *IEEE Ant.. & Prop. Lett.,* vol. 4, pp. 172-174, 2005.

[4] W. Kim and M. F. Iskander,”A new Coplanar Waveguide Continuous Transverse Stub (CWP-CTS) antenna for wireless communications,” U.S. Patent 7,079,082, Jul. 18, 2006

[5] W. Kim, M. Iskander, and C. Tanaka, "High-performance Low-Cost Phase-Shifter Design Based on the Ferroelectric Materials Technology," Elelctronics Letters, Vol. 40, no. 21,pp. 1345-1347, Oct. 2004.

[6] W. Kim, M. Iskander, C. Krowne, “Modified Green's Function and Spectral-Domain Approach for Analyzing Anisotropic and Multidielectric Layer Coplanar Waveguide Ferroelectric Phase Shifters,” *EEE Transactions on Microwave Theory and Techniques*,”vol. 55, pp. 402-409, 2007

[7] W. Kim, M. Iskander, "Novel High performance Low Cost Phase-Shifter Design Based on the Ferroelectric Materials Technology Using the WIPL-D Code," Applided Computational Elelctromagnetics Society, Syracuse, NY, 2004.

[8] W. Kim and M. Iskander, "Integrated Phased Array Antenna Design Using Ferroelectric Materials and the Continuous Transverse Stub Technology," IEEE Trans. on Antennas and propagation, vol. 54, no. 11, pp. 3095-3105, 2006

[9] F. W. Van Keuls, C. H. Mueller, F. A. Miranda, R. R. Romanofsky, C. L. Canedy, S. Aggarwal, T. Venkatesan, R. Ramesh, J. S. Horwitz, W. Change, and W. J. Kim, “Room temperature thin film BaxSr1-xTiO3 Ku- band coupled microstrip phase shifters: Effects of film thickness, doping, annealing and substrate choice,” in *IEEE MTT-S Int. Microwave Symp*. Vol. 2, pp. 737-740, Jun. 1999.

[10] S.W. Kirchoeferm J. M. Pond, H. S. Newman, W. J. Kim and J. S. Horwitz, “Ferroelectric/ferrite tunable phase shifters,” in IEEE MTT-S Int. Microwave Symp. Vol. pp. 1359-1362, Jun. 2000.

Modified Green's Function and Spectral-Domain Approach for Analyzing Anisotropic and Multidielectric Layer Coplanar Waveguide Ferroelectric Phase Shifters

Wayne Kim, *Member, IEEE*, Magdy F. Iskander, *Fellow, IEEE*, and Clifford M. Krowne, *Senior Member, IEEE*

***Abstract*—Phase-shifter design based on ferroelectric materials technology has shown promising performance characteristics and the potential for achieving the long standing goal of realizing high performance, low-cost microwave phase shifters, and phased-array antennas. In this paper, we present a unifying spectral-domain approach and a newly derived Green's function that provide a "first principles" method for the design and analysis of ferroelectric material based coplanar waveguide phase shifters. The modified Green's function not only accounts for the finite thickness of the conductors, but also for the "current crowding" phenomena that results from using the very high dielectric constant ferroelectric film. Both isotropic and anisotropic effects were analyzed and the developed theoretical results were in excellent agreement with measured data. It is also shown that the multidielectric layer-based design of these phase shifters may provide nearly threefold increase in the figure-of-merit compared with the direct metallization case. A new biasing approach is proposed to achieve effective biasing of the ferroelectric layer and without excessive field concentration in the overlaying low dielectric layer. The formulation, procedure for the calculation of the current and charge distributions, and comparison between simulation and experimental results are described and presented in detail.**

***Index Terms*—Anisotropic, coplanar waveguide (CPW), ferroelectric, Green's function, phase shifter, spectral domain.**

I. Introduction

MODELING ferroelectric coplanar waveguide (CPW) phase shifters has been and continues to be a computationally challenging endeavor because of the very thin layers (around 0.5–2 μm) in conjunction with possessing large dielectric-constant materials ranging from 100 to several thousand, depending on composition, applied voltage, operating temperature, and more importantly, the crystalline quality. In addition to the challenge of modeling these thin-film devices, the ability to accurately predict and identify the various loss mechanisms become computationally intensive as the device structures become increasingly complex. Losses in ferroelectric coplanar devices have consistently shown to be dominated by ohmic (conductor) losses associated with the guiding coplanar metal, as compared to other possible loss mechanisms [1], [2], particularly with recent advances in producing low-loss tangent ferroelectric materials. The attenuation due to ohmic losses may contribute up to 90% of the total loss budget [1].

In [1], the self-consistent dyadic Green's function contained in the spectral matrix method automatically calculates the substrate and ferroelectric material bulk losses. The ohmic (conductor loss), on the other hand, was treated in an alternative fashion. To model attenuation due to conductor losses, the self-consistent Green's function was modified to take into account both the intrinsic and extrinsic parameters of the coplanar device. The modified term was found to simultaneously model the attenuation and propagation characteristics with excellent accuracy. Although this method was effective, the extrinsic parameters were selected to fit measured data and did not allow the user to model the attenuation performance toward a desired goal.

In [2], the attenuation in ferroelectric coplanar devices is modeled based on the current crowding depth or the depth from the center and ground conductor edges at which 63% of the current flows. The current density was translated from the charge distribution on the electrodes by means of the quasi-TEM approximation [3]. It was found that the charge distribution was very high near the edges of the electrodes as the permittivity of the ferroelectric film increased in conjunction with implementation in thin-film technology. In terms of coplanar devices, these effects were considered extrinsic parameters. Although this method was effective, it will not accurately calculate the attenuation when the frequency increases significantly if the ferroelectric exhibits a high degree of anisotropy or if the ferroelectric device demonstrates multimode propagation.

In this paper, we combine the two models described above [1], [2] to form a new modified dyadic Green's function term that includes both the intrinsic and extrinsic parameters and develop a "first principles" approach to device modeling. The "first principles" approach refers to the ability to effectively design ferroelectric coplanar devices with prior knowledge of only a few measurements based on information such as basic materials properties and deposition techniques. The new Green's function will then be compared with measured results for verification. There are several available design options in the literature [4]–[6] and we have applied the new Green's function approach to the design in [1].

Manuscript received March 14, 2006; revised October 30, 2006. This work was supported by the National Science Foundation under Grant ECS05-25270 and by the Army Research Office under Grant W911NF-05-1-0495.

W. Kim and M. F. Iskander are with the Hawaii Center for Advanced Communications, College of Engineering, University of Hawaii at Manoa, Honolulu, HI 96822 USA (e-mail: kimwayne@hawaii.edu; magdy.iskander@gmail.com).

C. M. Krowne is with the Microwave Technology Branch, Electronics Science and Technology Division, Naval Research Laboratory, Washington, DC 20375-5347 USA (e-mail: krowne@webbsight.nrl.navy.mil).

Digital Object Identifier 10.1109/TMTT.2006.889305

0018-9480/$25.00 © 2007 IEEE

Authorized licensed use limited to: UNIV OF HAWAII LIBRARY. Downloaded on June 18,2010 at 22:24:49 UTC from IEEE Xplore. Restrictions apply.

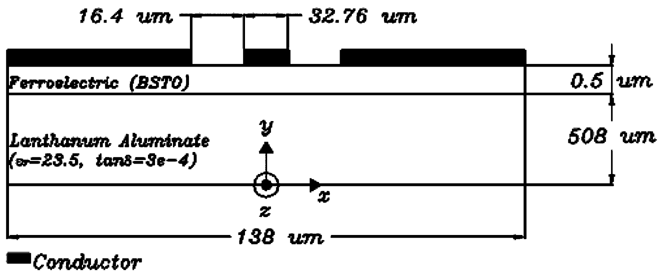

Fig. 1. Cross section of ferroelectric CPW phase shifter employing thin-film ferroelectric technology over lanthanum–aluminate substrate.

Following the development of the modified dyadic Green's function term, a study on the effects of the anisotropic and isotropic permittivity representations of the ferroelectric thin-film material will be presented. It would be beneficial to gain physical insight into which the tensor component dominates the overall device performance. The anisotropic and isotropic models will be compared with the measured results presented in [1].

The coplanar ferroelectric phase shifter exhibited high ohmic losses and could be deemed undesirable for implementation in practical wireless communication systems particularly in phased-array antennas. In an attempt to reduce the associated losses, the newly developed spectral matrix method will be used to effectively model a novel multidielectric design that will reduce the attenuation constant and improve the figure-of-merit (FoM). The multidielectric phase shifter employs a layer of low loss, nontunable dielectric material placed in between the ferroelectric material [$\mathrm{Ba}_x\mathrm{Sr}_{1x}\mathrm{TiO}_3$ (barium–strontium–titanate)], and the coplanar electrodes. Although this design has been described earlier [7], in this paper, we present a first attempt to fully analyze its performance using the spectral-domain approach together with the newly developed Green's function formulation.

II. Ferroelectric Coplanar Device Modeling

Fig. 1 illustrates the geometry of the thin-film ferroelectric coplanar phase shifter [1]. The structure uses barium–strontium–titanate $(\mathrm{Ba}_x\mathrm{Sr}_{1x}\mathrm{TiO}_3)$ with a compositional ratio of $x = 0.6$ over a lanthanum–aluminate (LaAlO_3) substrate.

The total device width was 138 μm, the ferroelectric layer thickness was 0.5 μm, and the LaAlO_3 substrate layer thickness was 508 μm. The relative dielectric constant for the LaAlO_3 substrate was $\varepsilon_r = 23.5$ with $\tan\delta = 3e-4$. The $\tan\delta_{\mathrm{fe}}$ for the $\mathrm{Ba}_{0.6}\mathrm{Sr}_{0.4}\mathrm{TiO}_3$ material was 0.01. The center strip width was 32.76 μm, the gapwidth was 16.4 μm, and the conductor thickness was 1.5 μm and was made of pure silver with resistivity $\rho = 1.629 \times 10^{-6}\ \Omega \cdot$ cm.

For the coplanar device, which was modeled as two coupled slots, with the fields in the slot locations expanded in a complete set of basis functions, the dyadic Green's function in admittance form is given by [1], [8]

$$G'_{ad} = \frac{1}{\det G'} \begin{bmatrix} G'_{zz} & -G'_{xz} \\ -G'_{zx} & G'_{xx} \end{bmatrix} \tag{1}$$

where

$$\det G' = G'_{xx}G'_{zz} - G'_{xz}G'_{zx}. \tag{2}$$

The Green's function in (1) is used in a system of homogenous equations to compute the propagation constant in the coplanar device as a function of frequency [8].

For modeling attenuation, it is important to note that in the spectral-domain approach described in [1], it was necessary to modify the self-consistent admittance Green's function terms in (1) to account for extrinsic parameters such as the finite thickness of the conductors and to account for the substantial amount of field lines that couple between and penetrate laterally into the coplanar arrangement. This modification was implemented to the diagonal elements of (1) and is given by

$$G'_{zz} = G_{zz} - \frac{1}{\sigma w_{\mathrm{eff}}} \left\{ (1+j)\,\frac{t}{4\delta} + c(f)\frac{w_{cs}}{w_{cs} + 2w_{\mathrm{slot}}} \cdot \left[\frac{\frac{(1+j)\,w_{cs}}{\delta}}{\tanh\left[\frac{(1+j)\,w_{cs}}{\delta}\right]} \right] \right\} \tag{3}$$

where

$$c(f) = \left(\frac{f}{f_o}\right)^k \qquad \delta = \frac{1}{\sqrt{\pi f \mu_o \sigma}} \tag{4}$$

and where w_{cs} is the center conductor strip width, w_{slot} is the gapwidth of the CPW device, and w_{eff} is the newly quantified term, defined as the summation of the current crowding depths of the center and ground conductors [2]. A similar expression may also be used to modify the second diagonal term G'_{xx}.

The relation between current and charge density distributions may be given by

$$j_s(x) = qn_s(x)v = \rho_s v \tag{5}$$

where $n_s(x)$ is the surface charge concentration and q is the electronic charge. Based on a study on the applicability of using a quasi-TEM approximation [3], we can assume no transverse currents in the CPW device; hence, the charge velocity v has only a longitudinal component and, therefore, the charge and current distributions are identical [2].

To calculate the charge/current distributions and, hence, to quantify w_{eff} in the two layer substrate illustrated in Fig. 1, we have employed the method of the finite-difference numerical method for multilayered structures. Since the finite-difference method is widely used and its derivation may be found elsewhere [9], [10], it will not be derived here. Considering computational efficiency, an unequal arm grid was employed taking into account the estimated concentration of charges, as shown in Fig. 2.

Shorter grids were implemented in regions where charges undergo rapid changes and wider grids in regions where the charges are relatively uniformly distributed or where the absolute value of the charge density is expected to be small. Along the x-direction, a fine grid was formed near the conductor–gap

Authorized licensed use limited to: UNIV OF HAWAII LIBRARY. Downloaded on June 18,2010 at 22:24:49 UTC from IEEE Xplore. Restrictions apply.

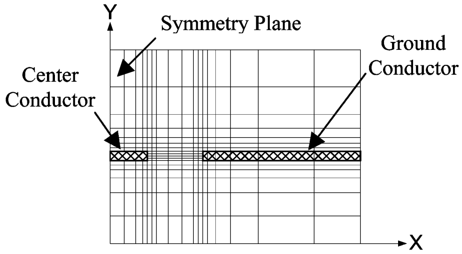

Fig. 2. Unequal arm grid illustrating the grid spacing with a high confinement of cells near the conductor to gap interface (x-direction) in conjunction with high confinement of cells near the conductor to substrate interfaces (y-direction). Symmetry was employed to further improve computation efficiency.

interfaces with a relatively coarser grid formed away from these regions. Along the y-direction, a fine grid was formed near the conductors and substrate interfaces and a relatively coarser grid further away. If N segments are taken for the number of cells in a specified region, then the cell spacings may be mapped according to the relation

$$\begin{pmatrix} x_i \\ y_i \end{pmatrix} = -a\cos\frac{i\pi}{N}, \qquad i = 0,\ldots,N; \quad \begin{pmatrix} -a < x < a \\ -a < y < a \end{pmatrix} \tag{6}$$

where x_i and y_i are the local coordinates.

To quantify the effect of current crowding, a current crowding depth (δ_{cc}), defined as the depth from the conductor edges at which 63% of the current is concentrated, may be defined as [2]

$$\int_{s-\delta_{\mathrm{cc}}}^{s} j_s(x)dx = \left(1-\frac{1}{e}\right)\int_0^s j_s(x)dx \tag{7}$$

where $j_s(x)$ is the surface current density, s is the width of the conductor, and $e = 2.718$.

Based on the current crowding expression in (7), the effective width w_{eff} in the modifying Green's function term (3) may be expressed by

$$w_{\mathrm{eff}} = \delta_s + \delta_g \tag{8}$$

where w_{cs} is the width of the center strip, δ_s is the current crowding depth of the center strip, w_{gp} is the width of the ground plane, and δ_g is the current crowding depth of the ground plane.

III. Charge Distributions

The charge/current distribution of the coplanar electrodes is illustrated in Fig. 3 for the center conductor and Fig. 4 for the ground-plane conductor. The charge distribution is evaluated by multiplying the normal component of the electric field with the equivalent permittivity surrounding the electrodes and is given by

$$\varepsilon_o \varepsilon_r E_{\mathrm{norm}} = \rho_s. \tag{9}$$

The permittivity for the ferroelectric unbiased case was set to $\varepsilon_r\ (V_{\mathrm{dc}} = 0\ \mathrm{V}) = 440 - j440\tan\delta_{\mathrm{fe}}$, and the permittivity for the biased case was set to $\varepsilon_r(V_{\mathrm{dc}} = 40\ \mathrm{V}) = 187.4 - j187.4\tan\delta_{\mathrm{fe}}$, as was reported in [1], to satisfy both α and β simultaneously. The current crowding effect may be explained

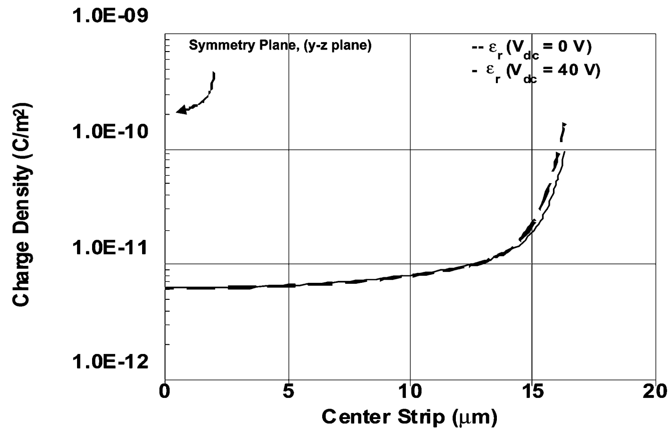

Fig. 3. Charge distributions on the center strip conductor for both biased and unbiased cases. Taking symmetry into account (see Fig. 1), only one-half of the center strip (from $x = 0$ to $x = 16.38$ μm) is illustrated.

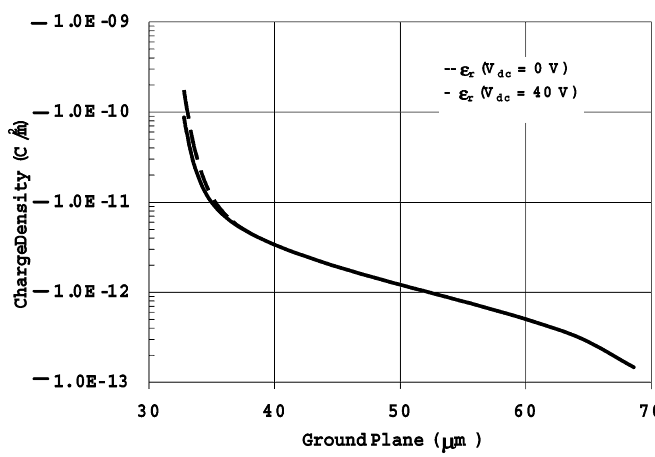

Fig. 4. Charge distributions on the ground-plane conductor for both biased and unbiased cases. Taking symmetry into account (see Fig. 1), only one side of the ground plane (from $x = 32.78$ to $x = 69$ μm) is illustrated.

by the extremely high field confinement in the ferroelectric material as a result of the increase in permittivity. With increased film permittivity, the electric field is forced towards the edges of the electrodes, thus increasing the current crowding near the edges.

IV. Anisotropic and Isotropic Permittivity Comparative Study

In [1], the unbiased ferroelectric case was modeled using a scalar permittivity given by $\varepsilon_r(V_{\mathrm{dc}} = 0\,\mathrm{V}) = 440 - j440\tan\delta_{\mathrm{fe}}$, and the biased ferroelectric case was modeled using a tensor permittivity given by

$$\varepsilon_r(V = 40\ \mathrm{V}) = \begin{bmatrix} 187.4 & 0 & 0 \\ 0 & 440 & 0 \\ 0 & 0 & 440 \end{bmatrix} - j\begin{bmatrix} 187.4 & 0 & 0 \\ 0 & 440 & 0 \\ 0 & 0 & 440 \end{bmatrix}\tan\delta_{\mathrm{fe}}. \tag{10}$$

The anisotropic values were determined based on a permittivity extraction algorithm described in [1]. Basically, the permittivity

Authorized licensed use limited to: UNIV OF HAWAII LIBRARY. Downloaded on June 18,2010 at 22:24:49 UTC from IEEE Xplore. Restrictions apply.

values were iterated until the theoretical phase propagation constant agreed with the experimental results. We compare the tensor permittivity in (10) for the biased case to a scalar representation given by

$$\varepsilon_r(V = 40\ \mathrm{V}) = \begin{bmatrix} 187.4 & 0 & 0 \\ 0 & 187.4 & 0 \\ 0 & 0 & 187.4 \end{bmatrix} - j \begin{bmatrix} 187.4 & 0 & 0 \\ 0 & 187.4 & 0 \\ 0 & 0 & 187.4 \end{bmatrix} \tan\delta_{\mathrm{fe}}. \quad (11)$$

V. Results and Discussions

w_{eff} is determined by first calculating δ_s and δ_g by substituting (9) into (5) and using (7). w_{eff} is then determined using (8). With $f_o = 10$ GHz, $w_{\mathrm{eff}} = 2.2\ \mu$m, and $k = 0.373$ for the unbiased case and with $f_o = 10$ GHz, $w_{\mathrm{eff}} = 2.9\ \mu$m, and $k = 0.3428$ for the biased case, Fig. 5(a) and (b) shows the attenuation constant for the unbiased and biased cases, respectively, comparing measurement to theoretical results based on the above calculations. In matching the theoretical results to measurements, it was suggested in [1] that the excessive measured data excursions between approximately 5 and 10 GHz were questionable due to experimental errors, as well as device mismatches. Therefore, this data was not considered in the comparison. Similarly the presented simulation results ignored these questionable data. Fig. 5(c) depicts the measured phase shift compared to theory. The attenuation and phase shift show very good agreement between the experimental data and the presented theoretical results.

Fig. 5(b) and (c) also illustrates the comparison between anisotropic and isotropic ferroelectric permittivity models for the biased case.

It can be seen in Fig. 5(a) that the tensor and scalar representation of the ferroelectric permittivity are in exact agreement (same curve) and both are in good agreement with measured results.

The phase shift changes by up to $\sim 1.1^\circ/\mathrm{mm}$ at 20 GHz and is not considered a significant difference. Additional simulation results in which elements of the tensor dielectric matrix were changed one element at a time showed that the lateral tensor element (ε_{xx}) dominate the performance of the coplanar device as compared to the other tensor elements.

It should be noted that different ferroelectric film properties, as well as coplanar geometry may not result in such a strong ε_{xx} dependence. For the case of gap/ferroelectric film thickness ratio less than unity, it is expected that the rather strong transverse electric field components will be inhomogeneous with variations that are coordinate dependent and, hence, the need for a more careful anisotropic analysis. For example, results in which the gap/ferroelectric film thickness ratio was decreased to below unity demonstrates that the attenuation may change by up to ~0.75 dB/mm and that the phase shift may change by up to $\sim 20^\circ/\mathrm{mm}$ at 20 GHz, respectively, as a result of the large dependence on the perpendicular tensor components. These results are considered significant and would require anisotropic modeling. However, for the aforementioned coplanar geometry, the degree of anisotropy under biased conditions does not cause significant deviation from the isotropic model.

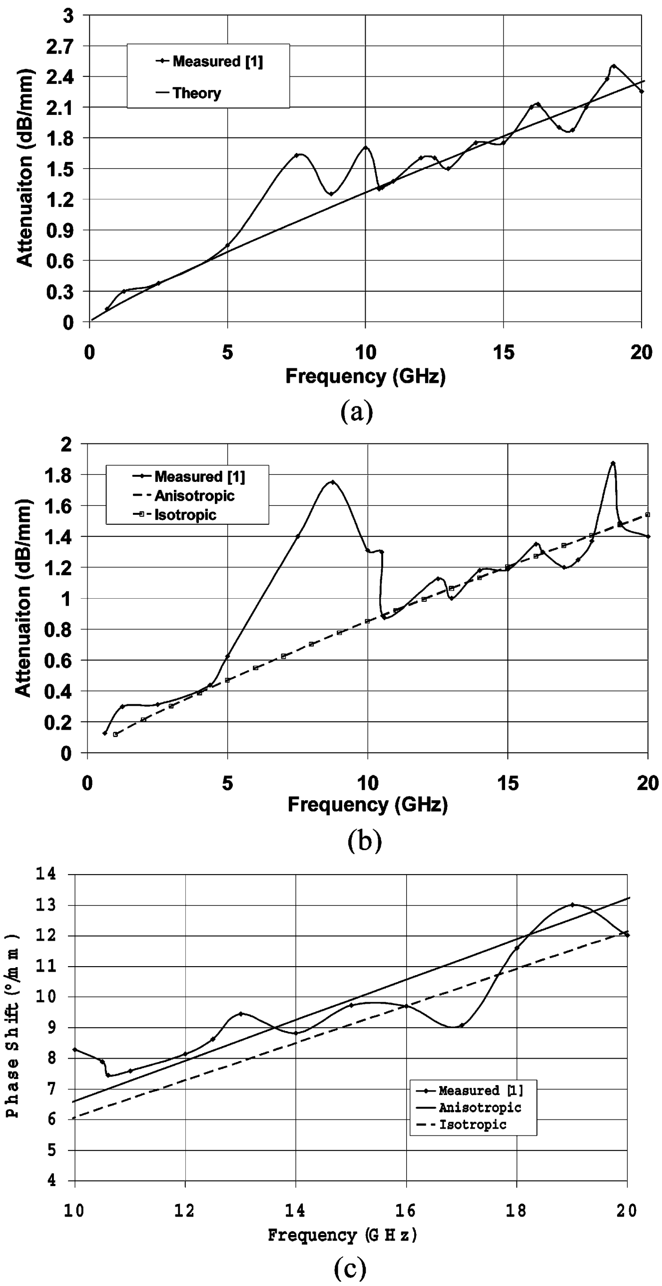

Fig. 5. (a) Attenuation constant for the unbiased case ε_r ($V_{\mathrm{dc}} = 0$ V). (b) Attenuation constant for the biased case ε_r ($V_{\mathrm{dc}} = 40$ V). (c) Phase shift versus frequency comparing experimental data to theory. The results also illustrate a comparison between anisotropic and isotropic ferroelectric permittivity representations.

Both the spectral matrix and the method of finite difference were formulated in MATLAB. For the spectral matrix code, the number of basis functions used to expand the x and z components of the electric field in the CPW slots were set to $n_x = n_z = 3$, and the number of Fourier spectral terms was set to $n = 200$.

VI. Multidielectric Coplanar Phase Shifter

The attenuation constant illustrated in Fig. 5 may be considered too high for implementation in phased-array antenna

Authorized licensed use limited to: UNIV OF HAWAII LIBRARY. Downloaded on June 18,2010 at 22:24:49 UTC from IEEE Xplore. Restrictions apply.

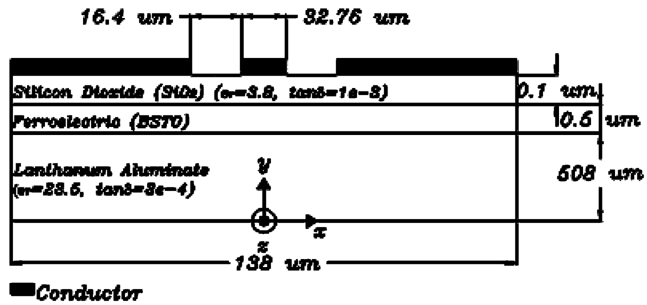

(a)

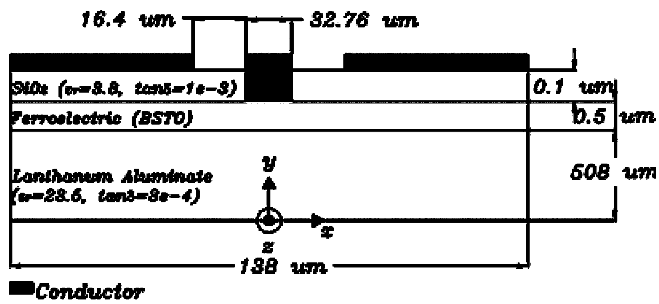

(b)

Fig. 6. Cross section of: (a) multidielectric ferroelectric CPW phase shifter employing very thin low-loss nontunable layer between the ferroelectric film and the coplanar electrodes and (b) multidielectric employing a via through the silicon–dioxide layer for simple ferroelectric biasing.

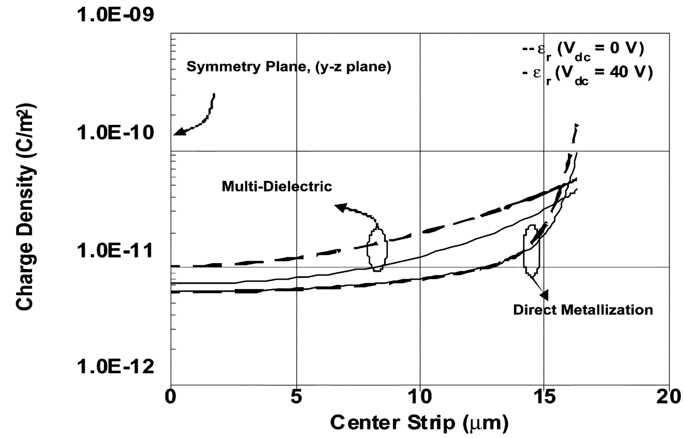

Fig. 7. Charge distributions on the center strip conductor for both biased and unbiased cases comparing the multidielectric and direct metallization cases. Taking symmetry into account (see Fig. 1), only one-half of the center strip (from $x = 0$ to $x = 16.38\ \mu$m) is illustrated.

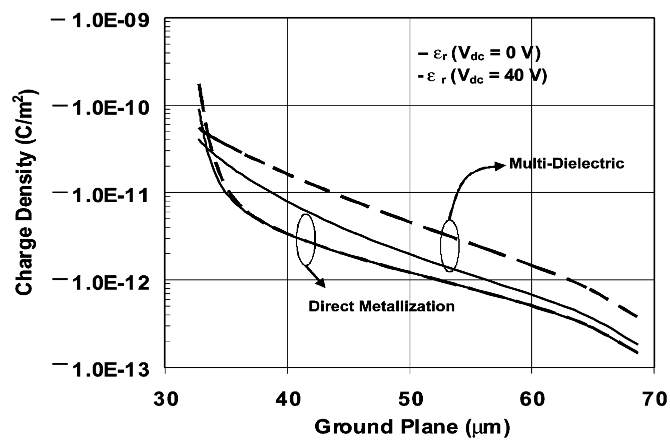

Fig. 8. Charge distributions on the ground-plane conductor for both biased and unbiased cases comparing the multidielectric and the direct metallization cases. Taking symmetry into account (see Fig. 1), only one side of the ground plane (from $x = 32.78$ to $x = 69\ \mu$m) is illustrated.

systems due to the anticipated high scan loss in conjunction with low radiation efficiencies. In an attempt to improve the phase-shifter performance, an alternate multidielectric layers design was proposed in [7]. Fig. 6(a) depicts a multidielectric ferroelectric phase-shifter design that employs the placement of a low-loss nontunable dielectric layer in between the ferroelectric material [$Ba_xSr_{1x}TiO_3$ (barium–strontium–titanate)] and the coplanar electrodes to reduce the attenuation constant and improve the FoM. The FoM is defined as the amount of phase shift per decibel loss, where the loss is calculated based on the unbiased condition. This new design was modeled in this paper using the method of finite differences and newly developed spectral matrix method.

The charge/current distribution on the coplanar electrodes is illustrated in Fig. 7 for the center conductor and Fig. 8 for the ground-plane conductor. Both Figs. 7 and 8 show results that compare the direct metallization case with the multidielectric case. The permittivity for the unbiased case was $\varepsilon_r\ (V = 0\ \text{V}) = 440 - j440 \tan\delta_{\text{fe}}$, and the permittivity for the biased case was $\varepsilon_r\ (V = 40\ \text{V}) = 187.4 - j187.4 \tan\delta_{\text{fe}}$.

For direct metallization, the charge distribution is forced towards the edges of the electrodes with increasing permittivity, thus increasing the current crowding near the edges. For the multidielectric situation [see Fig. 6(a)], the charge distribution is spread out across the electrodes and, hence, not highly concentrated near the edges and, thus, significantly reducing the current crowding effect.

Based on the charge distribution profiles and (8), with $f_o = 10$ GHz, $w_{\text{eff}} = 12.4\ \mu$m, and $k = 0.373$ for the unbiased case and with $f_o = 10$ GHz, $w_{\text{eff}} = 10 \mu$m, and $k = 0.3428$ for the biased case, Fig. 9 compares the attenuation constant of the direct metallization design illustrated in Fig. 1 to the multidielectric approach illustrated in Fig. 6(a) for the unbiased and biased cases. The attenuation constant decreased by ~1.85 dB/mm at 20 GHz for the unbiased case and decreased by ~1.07 dB/mm at 20 GHz for the biased condition.

The FoM results in Fig. 10 demonstrate a significant increase when using the multidielectric approach. The overall phase shift for the multidielectric design decreased by only $\sim 3.6^\circ$/mm at 20 GHz compared to the direct metallization case, while there was a large decrease in the attenuation constant, and this is what resulted in the significant overall increase in the FoM ($^\circ$/dB). The FoM improved from $\sim 6^\circ$/dB to $\sim 20^\circ$/dB at 20 GHz and illustrates that the multidielectric design improves the overall phase-shifter performance.

As expected, the inclusion of the low-loss SiO_2 layer would complicate the implementation of the biasing circuit. For the direct metallization approach, the ferroelectric may be tuned using a simple bias-tee arrangement. However, in the multidielectric

Authorized licensed use limited to: UNIV OF HAWAII LIBRARY. Downloaded on June 18,2010 at 22:24:49 UTC from IEEE Xplore. Restrictions apply.

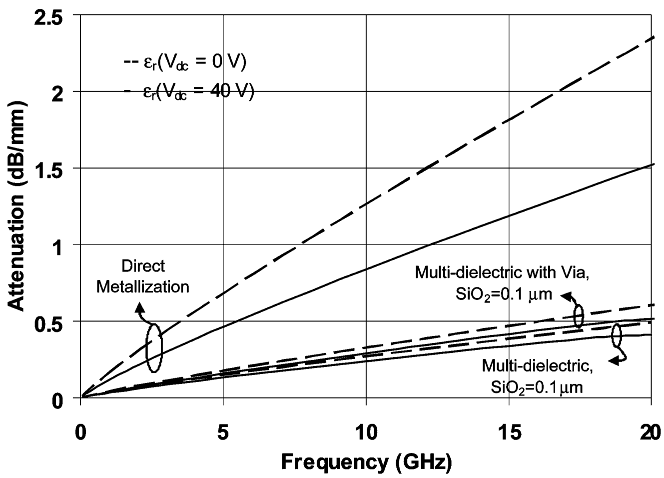

Fig. 9. Attenuation constant α for the unbiased $\varepsilon_r(V_{\mathrm{dc}} = 0\ \mathrm{V})$ and biased $\varepsilon_r\ (V_{\mathrm{dc}} = 40\ \mathrm{V})$ cases, comparing the direct metallization design shown in Fig. 1, the multidielectric design shown in Fig. 6(a), and the multidielectric with via design shown in Fig. 6(b).

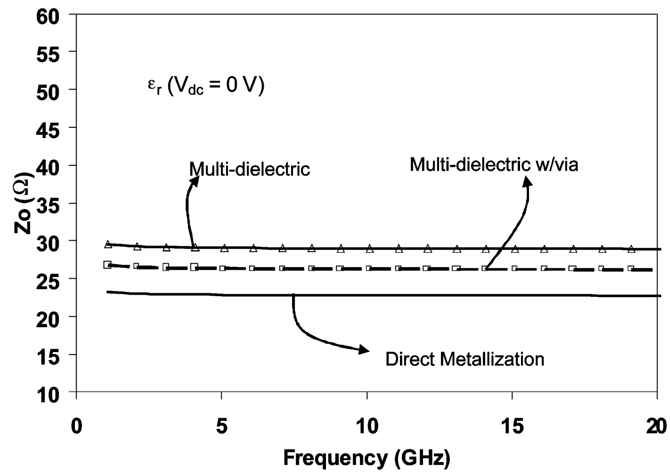

Fig. 11. Characteristic impedance Z_o for the unbiased $\varepsilon_r(V_{\mathrm{dc}} = 0\ \mathrm{V})$ case comparing the direct metallization design shown in Fig. 1, the multidielectric design shown in Fig. 6(a), and the multidielectric with via design shown in Fig. 6(b).

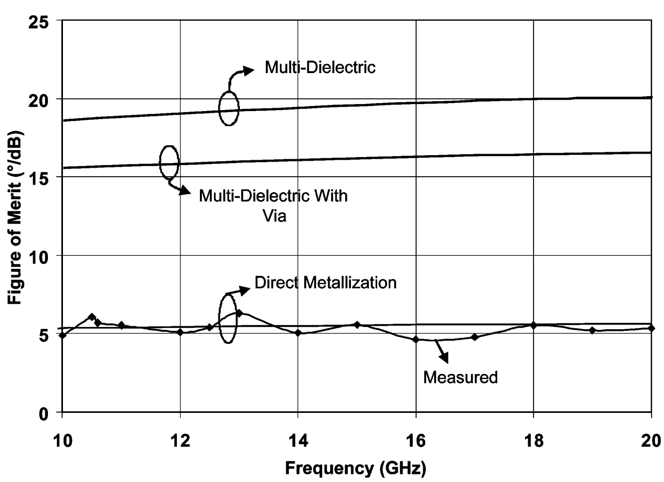

Fig. 10. FoM comparing the direct metallization design shown in Fig. 1, the multidielectric design shown in Fig. 6(a), and the multidielectric with via design shown in Fig. 6(b).

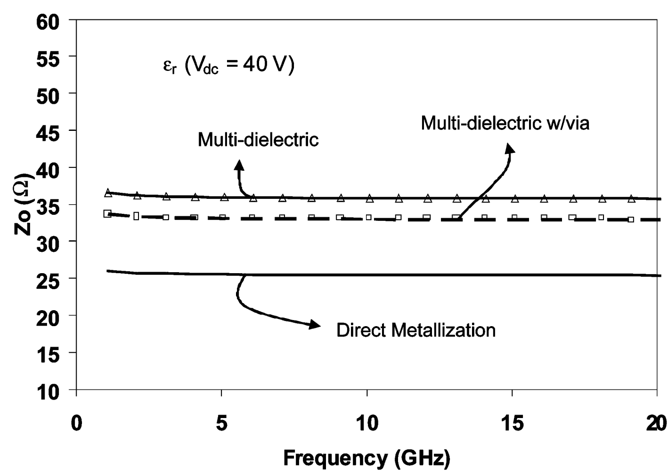

Fig. 12. Characteristic impedance Z_o for the biased case $\varepsilon_r(V_{\mathrm{dc}} = 40\ \mathrm{V})$, comparing the direct metallization design shown in Fig. 1, the multidielectric design shown in Fig. 6(a), and the multidielectric with via design shown in Fig. 6(b).

design with a low-permittivity layer between the signal conductors and ferroelectric film, it is expected that the low-permittivity layer would effectively "short out" and E-field in the ferroelectric layer [11], [12]. It is important, therefore, that we address appropriate dc biasing for the ferroelectric material layer.

The multidielectric case in Fig. 6(b), which includes the formation of a via through the silicon–dioxide layer, was analyzed to determine the feasibility of effectively polarizing the ferroelectric substrate [11]. In this case, biasing would involve the use of a bias tee. As may be seen from Figs. 9 and 10, even with the new biasing approach, the proposed multidielectric phase-shifter design continues to provide reduced attenuation as well as increased FoM.

The characteristic impedance is illustrated in Fig. 11 for the unbiased and Fig. 12 for the biased case for each of the three phase-shifter designs. The increase in characteristic impedance observed for the multidielectric designs is a result of the decrease in distributed capacitance based on the inclusion of the silicon dioxide layer.

The increase in characteristic impedance allows for improved impedance match and, hence, is expected to result in fewer oscillations in the reflection coefficient response.

The multidielectric with a via possessed an increase in attenuation, decrease in FoM, and decrease in characteristic impedance compared to the multidielectric design without a via; however, the via design still presents a substantial improvement (nearly a threefold increase in FoM) over the direct metallization case. If one is willing to reduce the complexity of ferroelectric biasing, then the multidielectric with a via phase shifter is an attractive alternative for phased-array antenna systems.

VII. Conclusion

A modified Green's function term for modeling ferroelectric CPW devices was presented. The previously unknown extrinsic parameter, w_{eff}, as reported in [1], has been quantified as the sum of the current crowding depths of both the signal

Authorized licensed use limited to: UNIV OF HAWAII LIBRARY. Downloaded on June 18,2010 at 22:24:49 UTC from IEEE Xplore. Restrictions apply.

and ground-plane conductors [2]. The newly derived Green's function provides a "first principles" approach to allow user the ability to accurately model high-permittivity ferroelectric CPW phase shifters.

Based on the observed results comparing the anisotropic and isotropic representation of the ferroelectric material, it was found the lateral component of the permittivity tensor, namely, the ε_{xx} component, dominated the device performance. The attenuation constant demonstrated no difference, while the phase shift displayed a slight difference of $\sim 1.1^{\circ}/\text{mm}$ at 20 GHz. These results indicate that the ferroelectric material may be modeled using either tensor or scalar representations without significant inaccuracies.

The coplanar ferroelectric design employing direct metallization of the electrodes with the ferroelectric material resulted in unacceptably high attenuation constant. To improve the device performance, we have introduced a multidielectric design that incorporated a thin layer of low-loss nontunable dielectric between the electrodes and ferroelectric layer. The developed "first principles" approach was used to model the multidielectric design. To improve the ferroelectric biasing capabilities, the multidielectric design was modified to include a via through the low-loss nontunable layer [11]. It should be noted that as the voltage drop across the capacitor stack under the ground planes of the CPW is much smaller than that under the signal conductor, the designs in Figs. 1 and 6(b) are similar from the dc biasing point-of-view, and that the significant microwave improvement was achieved without compromising biasing. The new via design demonstrated nearly a threefold increase in the FoM over the direct metallization case and, hence, presents itself as being attractive for implementation in phased-array antenna systems.

References

[1] C. M. Krowne, M. Daniel, S. W. Kirchoefer, and J. M. Pond, "Anisotropic permittivity and attenuation extraction from propagation constant measurements using an anisotropic full-wave Green's function solver for coplanar ferroelectric thin-film devices," *IEEE Trans. Microw. Theory Tech.*, vol. 50, no. 2, pp. 537–548, Feb. 2002.

[2] E. Carlsson and S. Gevorgian, "Effect of enhanced current crowding in a CPW with a thin ferroelectric film," *Electron. Lett.*, vol. 33, no. 2, pp. 145–146, 1997.

[3] G. L. Matthaei, K. Kiziloglu, N. Dagli, and S. Long, "The nature of the charges, currents, and fields in and about conductors having cross-sectional dimensions of the order of a skin depth," *IEEE Trans. Microw. Theory Tech.*, vol. 38, no. 8, pp. 1031–1036, Aug. 1990.

[4] F. Deflaviis, N. Alexopoulos, and O. Stafsudd, "Planar microwave integrated phase-shifter design with high purity ferroelectric material," *IEEE Trans. Microw. Theory Tech.*, vol. 45, no. 6, pp. 963–969, Jun. 1997.

[5] A. Kozyrev, A. Ivanov, A. Prudan, O. Soldatenkov, E. Hollman, V. Loginov, D. Ginley, and T. Rivkin, "Microwave phase shifter employing $SrTiO_3$ ferroelectric varactors," *Integr. Ferroelect.*, vol. 24, pp. 287–295, Mar. 1999.

[6] F. V. Keuls, R. Romanofsky, N. Varaljay, F. Miranda, C. Canedy, S. Aggarwal, T. Venkatesan, and R. Armes, "A Ku-band gold/$Ba_xSr_{1x}TiO_3/LaAlO_3$ conductor/thin-film ferroelectric microstrip line phase shifter for room-temperature communications applications," *Microw. Opt. Technol. Lett.*, vol. 20, no. 1, pp. 53–56, 1999.

[7] W. Kim, M. Iskander, and C. Tanaka, "High-performance low-cost phase shifter design based on ferroelectric materials technology," *Electron. Lett.*, vol. 40, no. 21, pp. 1345–1347, 2004.

[8] A. A. Mostafa, C. M. Krowne, and K. A. Zaki, "Numerical spectral matrix method for propagation in general layered media: Application to isotropic and anisotropic substrates," *IEEE Trans. Microw. Theory Tech.*, vol. MTT-35, no. 12, pp. 1399–1407, Dec. 1987.

[9] M. Iskander, *Electromagnetic Fields and Waves*. New York: Waveland Press, 1992.

[10] N. Alexopoulos, "Integrated-circuit structures on anisotropic substrates," *IEEE Trans. Microw. Theory Tech.*, vol. MTT-33, no. 10, pp. 847–881, Dec. 1985.

[11] W. Kim and M. Iskander, "An integrated phased array antenna design using ferroelectric materials and the continuous transverse stub technology," *IEEE Trans. Antennas Propag.*, vol. 54, no. 11, pp. 3095–3105, Nov. 2006.

[12] D. Chase, L. Chen, and R. York, "Modeling the capacitive nonlinearity in thin-film BST varactors," *IEEE Trans. Microw. Theory Tech.*, vol. 53, no. 10, pp. 3215–3220, Oct. 2005.

[13] K. C. Gupta, R. Garg, and I. J. Bahl, *Microstrip Lines and Slotlines*, 2nd ed. Norword, MA: Artech House, 1996.

Wayne Kim (A'05–M'05) received the B.S. degree from the University of Hawaii at Manoa, in 1998, the M.S. degree from the University of California at Los Angeles (UCLA), in 2001, both in electrical engineering, and is currently working toward the Ph.D. degree at the University of Hawaii at Manoa.

From 1998 to 2001, he was with TRW Space and Electronics (now Northrop Grumman), where he was involved in the development of indium phosphide bipolar transistors, as well as monolithic-microwave integrated-circuit (MMIC) design including high efficient power amplifiers. He holds several patents. His current research interests include developing phased-array antennas, smart antenna systems, and associated microwave components for wireless communications.

Mr. Kim was the second place recipient of the Student Paper Contest award of the 2004 Applied Computational Electromagnetics Society (ACES) Conference. He was also a recipient of the 2006 Achievement Rewards for College Scientists (ARCS).

Magdy F. Iskander (S'72–M'76–SM'84–F'93) is currently the Director of the Hawaii Center for Advanced Communications (HCAC), University of Hawaii at Manoa. He is a Co-Director of the National Science Foundation (NSF) Industry/University Joint Cooperative Research Center between the University of Hawaii, University of Arizona, Arizona State University, Rensselaer Polytechnic Institute (RPI), and more recently, The Ohio Sate University. Prior to joining the University of Hawaii at Manoa, he was the Engineering Clinic Endowed Chair Professor of the university. From 1997 to 1999, he was a Program Director of the Electrical and Communication System Division, National Science Foundation. He coedited a special issue on wireless communications of the *IEICE Journal* (Japan). He authored the textbook *Electromagnetic Fields and Waves* (Prentice-Hall, 1992; Waveland Press, 2001). He has authored or coauthored over 180 papers in journals. He holds seven patents. He has made numerous presentations at conferences. He is the founding editor of *Computer Applications in Engineering Education* (CAE) (Wiley).

Dr. Iskander was the 2002 president of the IEEE Antennas and Propagation Society (IEEE AP-S), the 2001 IEEE AP-S vice president, and a 1997–1999 and 2001–2006 Administrative Committee (AdCom) member. He was also a Distinguished Lecturer for the IEEE AP-S (1994–1997). He coedited two special issues devoted to wireless communications of the IEEE TRANSACTIONS ON ANTENNAS AND PROPAGATION. He was the recipient of the 1985 Curtis W. McGraw American Society for Engineering Education (ASEE) National Research Award, the 1991 ASEE George Westinghouse National Education Award, the 2000 University of Utah Distinguished Teaching Award, and the 2002 Kuhina (Ambassador) Award, University of Hawaii at Manoa.

Authorized licensed use limited to: UNIV OF HAWAII LIBRARY. Downloaded on June 18,2010 at 22:24:49 UTC from IEEE Xplore. Restrictions apply.

Clifford M. Krowne (S'73–M'74–SM'83) has been professionally affiliated with the Microelectronics Division, Lockheed Missiles and Space Company, Sunnyvale, CA, and the Watkins-Johnson Company, Palo Alto, CA. He was a faculty member with the Department of Electrical Engineering, North Carolina State University, Raleigh, and an Adjunct Professor of electrical engineering with the University of Maryland at College Park. Since 1982, he has been with the Microwave Technology Branch, Electronics Science and Technology Division, Naval Research Laboratory, Washington, DC. He has authored or coauthored approximately 190 or more conference and journal papers in solid-state electronics, microwave circuits, electromagnetics, and physics. He holds several patents. He has also authored major portions of four books for Academic Press in the Advances in Imaging and Electron Physics Series, as well as having contributed two chapters to Wiley's *Electrical and Electronics Engineering Encyclopedias*.

Authorized licensed use limited to: UNIV OF HAWAII LIBRARY. Downloaded on June 18,2010 at 22:24:49 UTC from IEEE Xplore. Restrictions apply.

An Integrated Phased Array Antenna Design Using Ferroelectric Materials and the Continuous Transverse Stub Technology

Wayne Kim, *Member, IEEE*, Magdy F. Iskander, *Fellow, IEEE*, and W. Devereux Palmer, *Senior Member, IEEE*

***Abstract*—In this paper, a new integrated phased array antenna system employing the ferroelectric materials technology for electronic beam steering capabilities is described. The design integrates a ferroelectric coplanar waveguide phase shifter with the continuous transverse stub (CTS) array. The phase shifter employs a multi-dielectric substrate and includes a thin layer of silicon dioxide between the signal conductors and the ferroelectric material to reduce the insertion losses and produce good impedance matching. The coplanar waveguide-based multi-dielectric layer design demonstrated an effective ferroelectric biasing architecture and exhibited an increase in figure of merit by up to 8 $^\circ/\mathrm{dB}$ from that of the direct metallization approach. An integrated two elements phased array antenna is developed and demonstrates linearly polarized radiation with $+/-20^\circ$ of beam scanning between the unbiased and biased states of the ferroelectric phase shifter.**

***Index Terms*—Continuous transverse stub (CTS) antenna, coplanar waveguide, ferroelectric, low cost, multiband antenna array, phase shifter.**

I. Introduction

PHASED array antennas have and will continue to play critical roles in the development of wireless and satellite communications systems. The advancement of future wireless and radar applications requires the use of phased array antennas that are low cost and exhibit high efficiencies. In spite of the significant advances in the phased array antennas technologies, there has always been a significant need for developing high performance phased array antennas with beam steering capabilities. In this paper we describe a design towards achieving this goal. It involves the integrated use of ferroelectric materials and the CTS antenna array technology.

The coplanar waveguide fed continuous transverse stub antenna (CPW-CTS) was first demonstrated in [1], and advantages of this new design include low cost, light weight, low profile (compared to reflector and lens antenna systems), and a very simple planar microstrip feed configuration. The low cost design is achieved through the use of printed circuit technologies as opposed to traditional waveguide methods used for the continuous transverse stub technology [2]. Furthermore, CTS technology is known to be tolerance insensitive and hence is also low cost in manufacturing.

Manuscript received February 2, 2006; revised July 24, 2006.

W. Kim and M. F. Iskander are with the Hawaii Center for Advanced Communications, College of Engineering, University of Hawaii at Manoa, Honolulu, Hawaii 96822 USA (e-mail: iskander@spectra.eng.hawaii.edu).

W. D. Palmer is with the U.S. Army Research Office, Research Triangle Park, NC 27709 USA.

Digital Object Identifier 10.1109/TAP.2006.883994

Our group has also recently developed a technique that employs a novel multidielectric approach to coplanar waveguide ferroelectric phase shifters where a layer of low loss, non-tunable dielectric such as silicon dioxide $(\mathrm{SiO_2})$ was placed in between the ferroelectric material $(\mathrm{Ba}_x\mathrm{Sr}_{1-x}\mathrm{TiO}_3$ (Barium Strontium Titanate) and the conductors. This approach significantly improved the insertion loss by nearly three fold in conjunction with maintaining significant fraction of the tunability [3].

In this paper, we describe an integrated phased array antenna approach that combines the multidielectric ferroelectric phase shifter design and the CTS antenna technology to form a phased array antenna with electronic beam scanning capabilities. Compared to other microstrip phased array antenna designs, the CPW-CTS has the advantage of low dispersion, being compact, and provides continuous analog beam steering [2]. In addition, the coplanar waveguide feed is easy to integrate with front-end receiver components.

A new approach for biasing the ferroelectric material in the coplanar multidielectric structure was developed and simulation results under dc bias conditions demonstrates that the potential distribution penetrates deep into the ferroelectric film and is fully pronounced under the signal conductor. This uniform distribution verifies that the dc voltage requirement for the multidielectric design is equivalent to the direct metallization architecture. In addition, the phase shifter performance under these new biasing arrangements was examined and an increase in the figure of merit (FOM) by up to $8^\circ/\mathrm{dB}$ above that of the direct metallization approach was achieved.

The paper is organized as follows: Section II describes the phase shifter design including the new biasing procedure and ways and means for accounting for current "crowding" and dielectric anisotropy when evaluating its performance. Section III focuses on the design of coplanar waveguide CTS array antennas and its integration with the ferroelectrics to achieve the desired beam steering capability. Section IV summarizes the findings and concludes the paper.

II. Phase Shifter Design

The use of ferroelectric materials was met with extreme challenges as the high value of the dielectric constant of these materials results in a significant reduction in the input impedance of the loaded devices; hence, unacceptably large values of ohmic losses. Our group has recently developed a technique to overcome this difficulty by employing a novel multilayer dielectric materials design that, while overcoming the return loss and insertion loss limitations of available designs, resulted in a challenging biasing arrangement [3]. If dc biasing is to be done

0018-926X/$20.00 © 2006 IEEE

Authorized licensed use limited to: UNIV OF HAWAII LIBRARY. Downloaded on June 09,2010 at 20:58:55 UTC from IEEE Xplore. Restrictions apply.

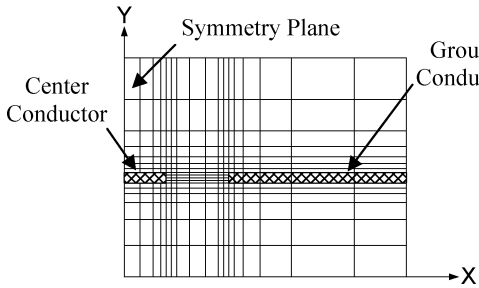

Fig. 1. Unequal arm grid showing grid spacing with a high confinement of cells near the conductor to gap interface (x-direction) in conjunction with high confinement of cells near the conductor regions (y-direction).

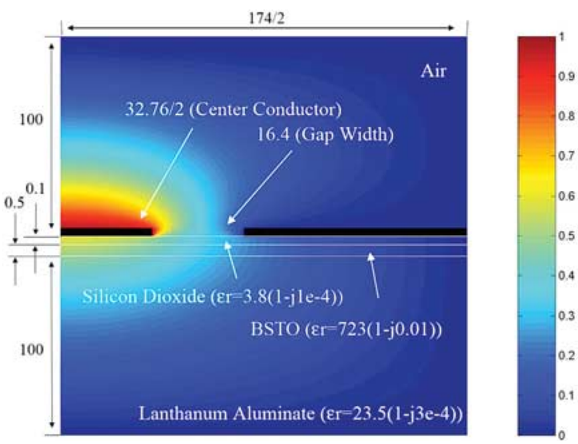

Fig. 2. Potential distribution over a cross section of the ferroelectric phase shifter where the phase shifter includes a thin layer of silicon dioxide between the conductors and the ferroelectric layer. The potential distribution employs symmetry, and the dimensions are given in microns.

through the regular biasing approach using a biasing tee, it is expected that much of the potential distribution will be concentrated in the SiO_2 layer above (rather than within) the ferroelectric layer. To help quantify the potential distribution across the ferroelectric substrate between bias states, and possibly lead to identifying a procedure for optimizing the biasing procedure, the method of finite differences was employed [4], [5].

Considering computational efficiency, an unequal arm grid was implemented taking into account the estimated concentration of charges. Shorter grids were used in regions where charges undergo rapid changes and wider grids in regions where the charges are relatively uniformly distributed or where the absolute value of the charge density is expected to be small. Along the x-direction in Fig. 1, a fine grid was formed near conductor-gap interfaces and a relatively coarser grid was formed away from these regions. Along the y-direction, a fine grid was formed near the conductors and substrate interfaces and a relatively coarser grid further away. If N segments are taken for the number of cells in a specified region, then the cell spacings may be mapped according to the relation

$$\begin{pmatrix} x_i \\ y_i \end{pmatrix} = -a\cos\frac{i\pi}{N}, \quad i=0,\ldots,N, \quad \begin{pmatrix} -a<x<a \\ -a<y<a \end{pmatrix} \tag{1}$$

where x_{i} and $\mathrm{y_i}$ are the local coordinates running along the x- or y-directions, respectively. The unequal arm grid employing symmetry is illustrated in Fig. 1.

With a $\mathrm{conductor\ thickness} = 1.5\ \mu\mathrm{m}$, and a ferroelectric permittivity of $\varepsilon_r = 723(1-\mathrm{j}0.01)$, Fig. 2 illustrates that

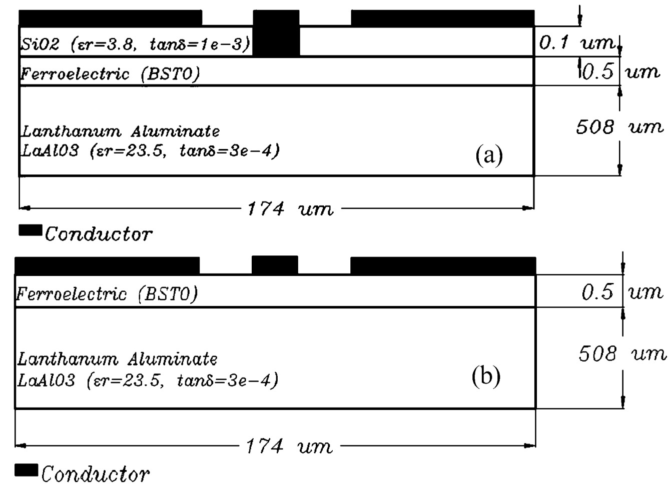

Fig. 3. (a) Cross section of ferroelectric phase shifter with the inclusion of a silicon oxide layer and the formation of a via hole under the signal conductor (b) phase shifter employing direct metallization. The metallization layers include: Cr/Ag/Au (250 Å, 14250 Å, 500 Å).

the potential distribution is primarily concentrated in the SiO_2 layer. Therefore, an alternative procedure is introduced to address the biasing issue as illustrated in Fig. 3(a). The new design includes the formation of a via through the silicon dioxide layer only under the center conductor while maintaining a thin layer of oxide under the ground plane regions. The direct contact between the center conductor and the ferroelectric layer allows for simple biasing. Simulation results of the potential distributions are shown in Fig. 4. These results compare the multidielectric design shown in Fig. 3(a) to the direct metallization design shown in Fig. 3(b) [6]. It can be seen that similar to the direct metallization case [6] with $\mathrm{V_{dc}} = 1\ \mathrm{V}$, the potential distribution penetrates deeper into the ferroelectric material for the multilayer design. These results indicate that adequate polarization across ferroelectric material may be realized with the formation of a via through the silicon dioxide layer, under the center conductor. Because the multidielectric design possessed the same dimensions for coplanar center conductor width, gap width, and ferroelectric thickness as that of the direct metallization design presented in [6], the new multidielectric design will also require $\mathrm{V_{dc}} = 40\ \mathrm{V}$ [6] to properly polarize the ferroelectric film.

We next examined the microwave performance of the new design Fig. 3(a) of the coplanar phase shifter. For this purpose, we used three simulation codes and compared the results with experimental data for the special case of direct metallization of the ferroelectric material. Specifically, we used a method of moments based code (LINPAR) [7] to determine the per unit length transmission line parameters L, C, R, and G, a full 3-D method of moments code WIPL-D [8], and a spectral matrix based code [6], modified by our group. Results from these three codes were compared with the experimental measurements reported in [6].

It should be noted that WIPL-D [8] models 3-D composite metallic and dielectric structures using wires and plates. The finite conductor thickness is modeled using thin solid boxes. The distributed loading of the metallic plates may be given by the conductivity of the metal *or* as surface impedance given by [8]

$$Z_s = \frac{1}{t\sigma_m} \tag{2}$$

Authorized licensed use limited to: UNIV OF HAWAII LIBRARY. Downloaded on June 09,2010 at 20:58:55 UTC from IEEE Xplore. Restrictions apply.

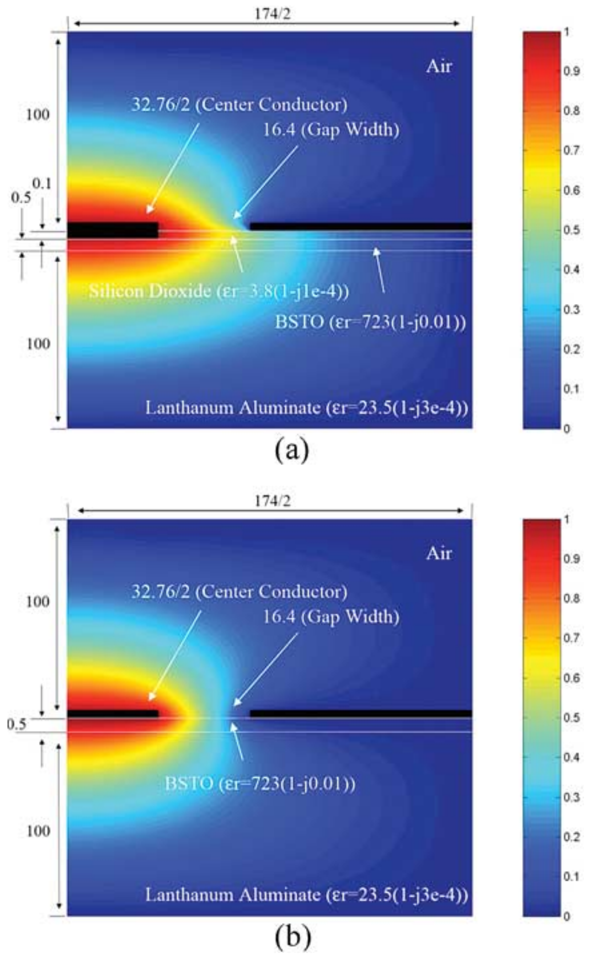

Fig. 4. Potential distribution over a cross section of the phase shifter for (a) multidielectric with via approach and (b) direct metallization approach. The potential distribution employs symmetry, and the dimensions are given in microns.

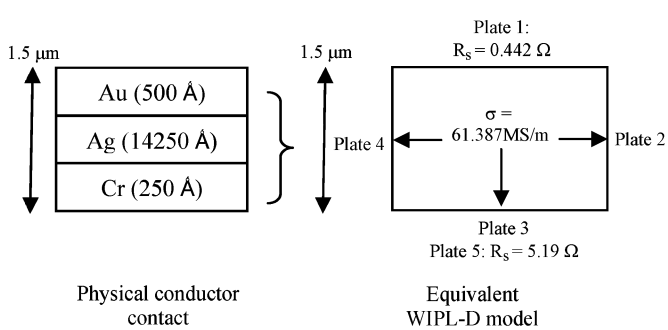

Fig. 5. Method for modeling metallization contacts in WIPL-D.

where t is the thickness of the metal and σ_m is the conductivity of the metal. The multiconductor combination which makes up the ohmic metal loss of the phase shifter device is modeled using metallic plates, each with a unique distributed loading depending on the layer it represents. Fig. 5 illustrates a method for modeling the metallic layer combination of Cr/Ag/Au (250 Å, 14250 Å, 500 Å). Plate 1 represents the gold (Au) metal layer, lies in the free space domain, and is assigned a surface impedance of 0.442 Ω where the conductivity is 45.21 MS/m. Plate 2 represents the silver (Ag) layer, plate 3 represents the silver (Ag) layer, and plate 4 represents the silver (Ag) layer. Each of the aforementioned plates is assigned a conductivity of 61.387 MS/m and is in the free space domain. Plate 5 represents the chromium (Cr) layer and overlaps plate 3. Plate 5 is in the ferroelectric substrate domain and is assigned a surface impedance of 5.19 Ω where the conductivity is 7.714 MS/m.

The quick variations of the electromagnetic field at the interface between the microstrip conductor and the dielectric cannot be properly approximated by the low-order polynomial expansions associated with dielectric plates. This edge effect can be properly taken into account if the edge of a dielectric plate connected to the edge of a microstrip conductor is modeled by a separate narrow strip [8]. The length of the phase shifter is arbitrary since there is no variation in the z-direction. For our design the line length was kept short at 1 mm in order to keep the number of unknowns low while not generating any port-to-port coupling. A total of 299 unknowns were used in the model for good convergence.

LINPAR models 2-D multiconductor transmission line structures by defining node coordinates at the interface of two homogeneous boundaries. A pulse is then assigned between two adjacent nodes and the method of moments is employed using pulse basis functions. Higher concentration of nodes is employed where charges undergo rapid changes or where the absolute value of the charge distribution is expected to be high. The frequency dependent series resistance is modeled using the following relation [7]:

$$R(f) = R(f_{\text{ref}}) \left(\frac{f}{f_{\text{ref}}} \right)^{r_e} \tag{3}$$

where f_{ref} is the reference frequency, r_e is the exponential term defining the frequency variation of the series resistance, and $R(f_{\text{ref}})$ is the series resistance evaluated and the reference frequency given by

$$R(f_{\text{ref}}) = \sqrt{\frac{\pi \mu f_{\text{ref}}}{\sigma}} \tag{4}$$

where μ is the conductor permeability (in H/m), which is practically always equal to μ_o, and σ is the conductor conductivity given in S/m. For the device in Fig. 3(b), $f_{\text{ref}} = 0.1$ GHz, r_e is 0.917 for the unbiased case, $\varepsilon_r(\text{V}_{\text{dc}} = 0\ \text{V}) = 723(1 - \text{j}0.01)$ and r_e is 0.855 for the biased case, $\varepsilon_r(\text{V}_{\text{dc}} = 40\ \text{V}) = 441.2(1 - \text{j}0.01)$. The conductor was made of pure silver with a conductivity of 61.387 MS/m. A total of 982 nodes were used in the model to provide good convergence.

The spectral matrix code [6] was formulated in MATLAB and the number of basis functions used to expand the x and z components of the electric field in the coplanar waveguide slots were set to $n_x = n_z = 3$ and the number of Fourier spectral terms was set to $n = 200$. It is important to note that in the spectral domain approach described in [6], it was necessary to introduce the following modifying diagonal term in the admittance Green's function to account for the finite thickness of the conductors. This modification was also implemented in our code

$$Gs3 = \frac{1}{\sigma w_{\text{eff}}} \left\{ (1+j)\frac{t}{4\delta} + c(f)\frac{w_{cs}}{w_{cs} + 2w_{\text{slot}}} \cdot \left[\frac{\frac{(1+j)w_{cs}}{\delta}}{\tanh\left[\frac{(1+j)w_{cs}}{\delta}\right]} \right] \right\} \tag{5}$$

Authorized licensed use limited to: UNIV OF HAWAII LIBRARY. Downloaded on June 09,2010 at 20:58:55 UTC from IEEE Xplore. Restrictions apply.

where

$$w_{\rm eff} = \delta_{\rm CentCond} + \delta_{\rm GndCond} \tag{6}$$

$$c(f) = \left(\frac{f}{f_o}\right)^{v} \quad \delta = \frac{1}{\sqrt{\pi f \mu_o \sigma}} \tag{7}$$

where $w_{\rm eff}$ is the summation of the current crowding depth of the center conductor $(\delta_{\rm CentCond})$ and the ground conductor $(\delta_{\rm GndCond})$ [9]. w_{cs} is the center conductor strip width and $w_{\rm slot}$ is the gap width of the coplanar waveguide device. $f_o = 10\,{\rm GHz}$, $w_{\rm eff} = 1.98\ \mu{\rm m}$, and $\nu = 0.373$ for the unbiased case and $f_o = 10$ GHz, $w_{\rm eff} = 2.97\ \mu{\rm m}$, and $\nu = 0.3428$ for the biased case. The values for $w_{\rm eff}$ obtained using the current crowding method [9] were in very good agreement with the values presented in [6] which were determined based on fitting measured data. The values determined in [6] were $w_{\rm eff}$ in [6] $= 2.004\ \mu{\rm m}$ for the unbiased case and $w_{\rm eff} = 3.021\ \mu{\rm m}$ for the biased case. All simulations were performed using a Pentium 4 processor with 3.75 GB of RAM.

Fig. 6 compares the simulation results from the three simulation codes together with experimental data from [6].

As pointed out in [6], the experimental data between about 5 to 11 GHz was questionable and therefore should be ignored. In all models, the attenuation appeared to be dominated by ohmic losses. In addition to possessing high attenuation primarily due to ohmic losses, the direct metallization design also exhibited low characteristic impedance as shown in Fig. 6(d).

Fig. 6(a)-(c) show excellent agreement between simulation and experimental data. Although measured results for both S_{21} phase angle and the normalized propagation constant were also available in [6] it was found that it is possible to replicate the propagation constant and phase angle data above 10 GHz because the S_{21} phase angle data was presented with a jump at 7 GHz. Data for the normalized propagation constant was presented in [6] between 10–20 GHz and as a result, Fig. 6(c) shows measured results between 10–20 GHz. By multiplying the normalized propagation constant by k_o, in [6, Fig. 6] (free space propagation constant), the propagation constant of the coplanar waveguide could be obtained. In [6], the unbiased ferroelectric case was modeled using a scalar permittivity given by $\varepsilon_r({\rm V_{dc}} = 0\ {\rm V}) = 723(1 - {\rm j}0.01)$, and the biased ferroelectric case was modeled using a tensor permittivity given by

$$\varepsilon_r(V_{dc} = 40\,{\rm V}) = \begin{bmatrix} 441.2 & 0 & 0 \\ 0 & 723 & 0 \\ 0 & 0 & 723 \end{bmatrix} - j \begin{bmatrix} 441.2 & 0 & 0 \\ 0 & 723 & 0 \\ 0 & 0 & 723 \end{bmatrix} 0.01. \tag{8}$$

We compare the tensor permittivity in (8) for the biased case to a scalar representation given by

$$\varepsilon_r(V_{\rm dc} = 40\,{\rm V}) = \begin{bmatrix} 441.2 & 0 & 0 \\ 0 & 441.2 & 0 \\ 0 & 0 & 441.2 \end{bmatrix} - j \begin{bmatrix} 441.2 & 0 & 0 \\ 0 & 441.2 & 0 \\ 0 & 0 & 441.2 \end{bmatrix} 0.01. \tag{9}$$

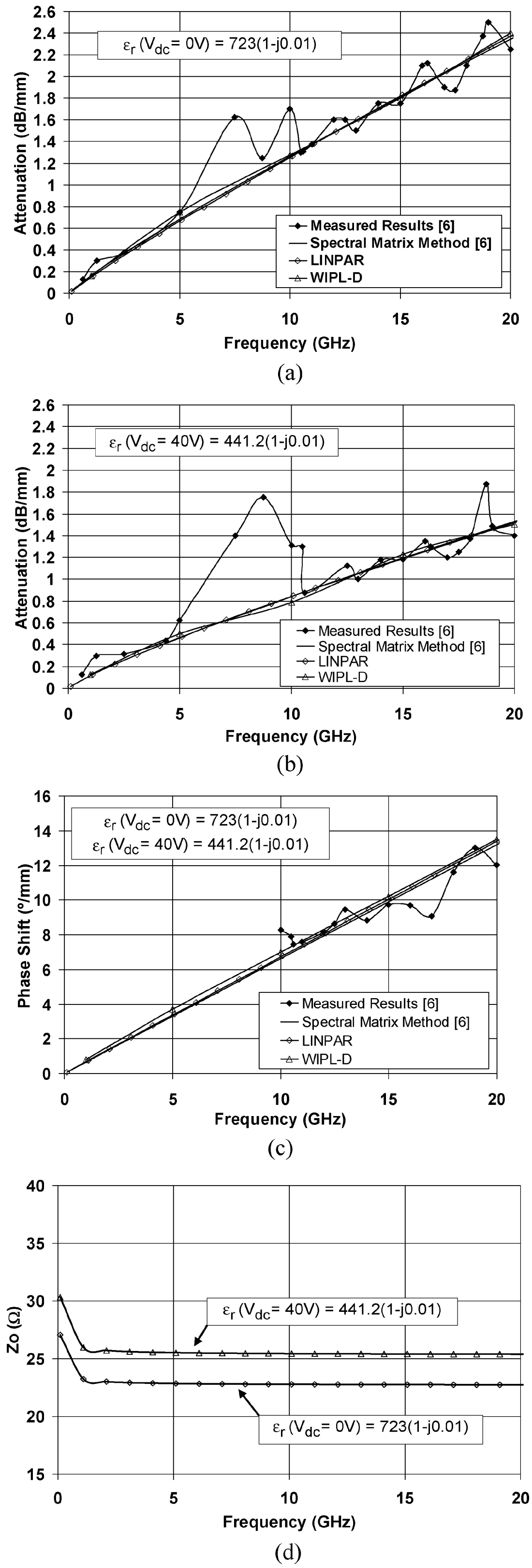

Fig. 6. Results of the direct metallization approach illustrated in Fig. 3(b), comparing measurement to the spectral matrix method [6], LINPAR, and WIPL-D: (a) attenuation for $\varepsilon_r({\rm V_{dc}} = 0\ {\rm V}) = 723(1 - {\rm j}0.01)$, (b) attenuation for $\varepsilon_r({\rm V_{dc}} = 40\ {\rm V}) = 441.2(1 - {\rm j}0.01)$, (c) phase shift, and (d) characteristic impedance.

Fig. 7(a) shows the attenuation constant and Fig. 7(b) shows the phase shift comparing the anisotropic and isotropic models. As

Authorized licensed use limited to: UNIV OF HAWAII LIBRARY. Downloaded on June 09,2010 at 20:58:55 UTC from IEEE Xplore. Restrictions apply.

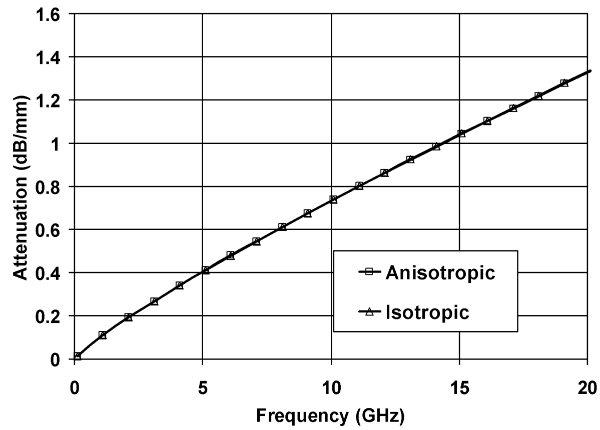

(a)

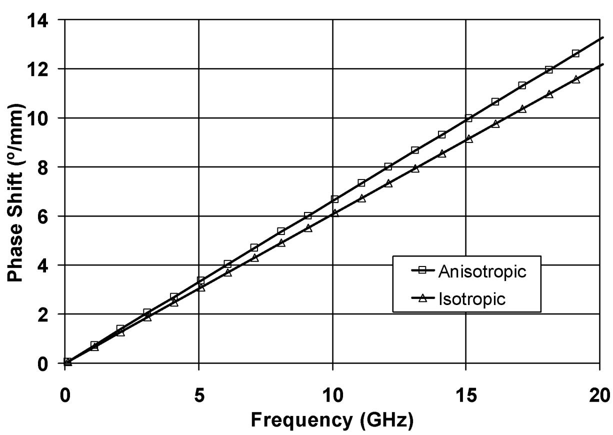

(b)

Fig. 7. (a) Attenuation and (b) phase shift versus frequency comparing the anisotropic and isotropic permittivity representations of the ferroelectric material.

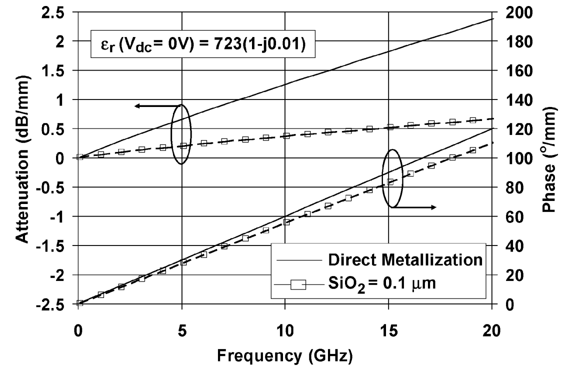

(a)

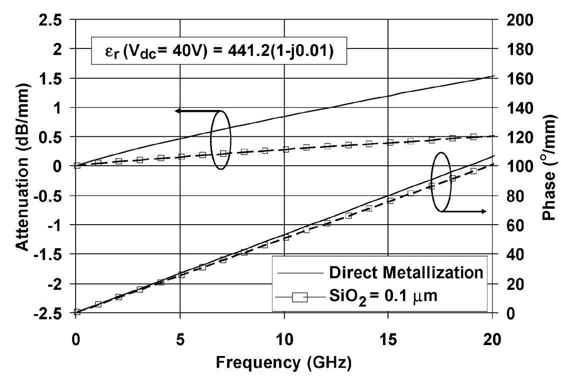

(b)

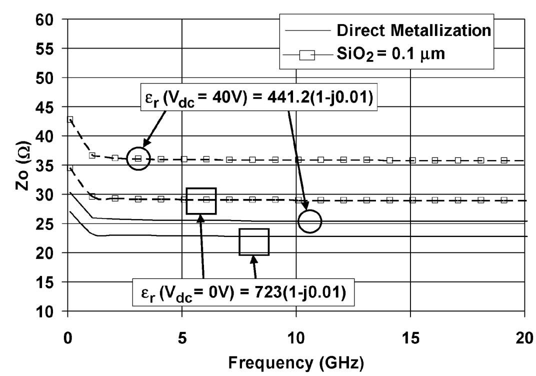

(c)

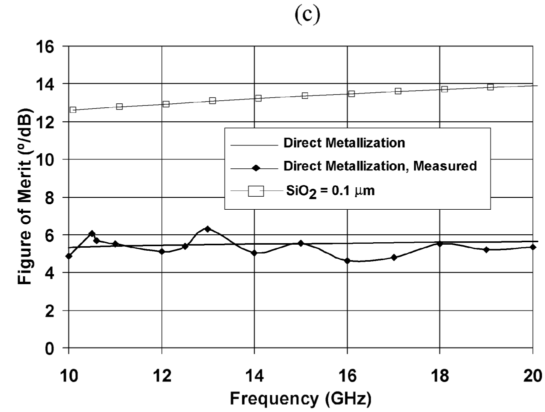

(d)

Fig. 8. Results of multidielectric design with 0.1 $\mu\mathrm{m}$ of silicon dioxide compared to the direct metallization case: (a) attenuation and phase for unbiased condition, (b) attenuation and phase for biased condition (c) characteristic impedance, and (d) figure of merit.

can be seen in Fig. 7(a), the attenuation constant for the tensor and scalar representation of the ferroelectric permittivity are in exact agreement (same curve).

The phase shift data shown in Fig. 7(b) changes by up to $\sim\ 1.1^{\circ}/\mathrm{mm}$ at 20 GHz and is not considered a significant difference. Additional simulation results in which elements of the tensor dielectric matrix were changed one element at a time showed that the lateral tensor element $(\varepsilon_{\mathrm{xx}})$ dominates the overall device operation as compared to the other tensor elements. The degree of anisotropy for the ferroelectric film under biased conditions is not substantial enough to cause significant deviation from the isotropic model and hence the device may be accurately modeled using the scalar representation.

With the validation of the simulation codes, it is important at this point to examine the phase shifter performance under this new biasing approach as shown in Fig. 3(a). For this purpose the new design with $\mathrm{SiO_2}\ =\ 0.1\ \mu\mathrm{m}$ was implemented and the simulation results were compared with the direct metallization approach shown in Fig. 3(b). WIPL-D was used to simulate the new phase shifter design. Fig. 8(a)–(d) show results of attenuation, characteristic impedance and figure of merit where WIPL-D was also used to model the direct metallization case. The ohmic metal loss was modeled according to the methods described in Fig. 5.

Fig. 8(d) shows that the figure of merit (FOM) improved by up to $8^{\circ}/\mathrm{dB}$ at 20 GHz, where the FOM is defined as the

Authorized licensed use limited to: UNIV OF HAWAII LIBRARY. Downloaded on June 09,2010 at 20:58:55 UTC from IEEE Xplore. Restrictions apply.

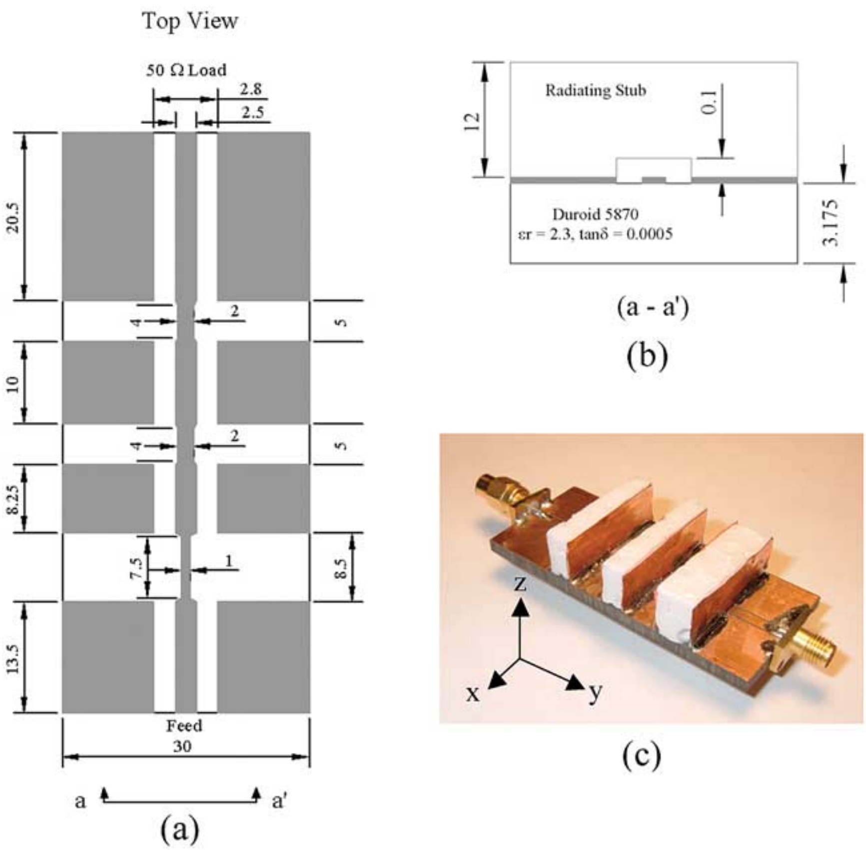

Fig. 9. Layout of the 3 elements CPW-CTS array, all dimensions in mm. (a) Top view, (b) front view and (c) fabricated prototype. Conductor thickness was 35 μm (1 oz.) electrodeposited copper with conductivity of 58.8 MS/m.

ratio between the amount of phase change and attenuation for the unbiased state. As it may be seen from Fig. 8, even with the new biasing approach (center conductor in contact with ferroelectric) the proposed multidielectric phase shifter design continues to provide reduced attenuation and increased characteristic impedance as well as an increase in the FOM. The increase in characteristic impedance is a result of the decrease in distributed capacitance with the inclusion of the SiO_2 layer. It may be noted that the phase for each ferroelectric state degraded slightly, resulting in a reduction in the overall phase shift. The overall FOM, however, is increased due to the relatively dominant decrease in attenuation.

III. CPW-CTS Array and Phased Array Antenna

First we extend the design of the single element coplanar waveguide continuous transverse stub (CPW-CTS) antenna presented in [1] to a traveling wave antenna with three series fed elements. The three element array was modeled using WIPL-D and a prototype was developed at *X*-band. Fig. 9(a)–(c) illustrate the dimensions of the array and show a photograph of the developed prototype. The dimensions of the coplanar waveguide feed and load lines were designed to provide 50 Ω impedance. The selected substrate was Duroid 5870 with a permittivity of 2.3 and $\tan\delta$ of 0.0005. The center to center stub spacings were $\sim \lambda_o/2$ and because of the low effective permittivity ($\varepsilon_{\rm reff} = 1.4$), also $\sim \lambda_g/2$ for a design frequency of 10 GHz. The parallel plate stubs couple power from the microstrip transmission line feed and are carefully positioned in the areas of current maximums. Since this is a traveling wave antenna the first stub is designed to couple a small amount of power while the last stub couples relatively more. This is done by adjusting the width of each stub. The design was also implemented such that induced currents J_z on each stub are out of phase which is just the condition required for the electric field E_y radiated by each stub to be in phase in the direction of maximum radiation producing linear polarization and superb polarization purity.

The measured and simulated S_{11} of the CPW-CTS array is shown in Fig. 10(a). The 10-dB bandwidth of the CPW-CTS array was ~4% and possesses narrow band characteristics, typical of resonant arrays with element spacing of $\sim \lambda_g/2$. The reflections from each stub combine in such a way as to cancel at the input of the array at only one frequency; hence the array has frequency dependent input impedance. The copolarized (E-plane, $y - z$ plane) and cross-polarized (H-plane, $x - z$ plane) radiation patterns are shown in Fig. 10(b) and illustrates that the linearly polarized array produced a broad side radiation pattern with a beam peak of 10.6 dBi at $-7.5°$ from broadside (towards feed direction) and a half power beam width of $\sim 36°$. The measured cross polarization level is below -20 dBi illustrating outstanding polarization purity. The slight deviation of the main beam from broadside towards the feed direction is a

Authorized licensed use limited to: UNIV OF HAWAII LIBRARY. Downloaded on June 09,2010 at 20:58:55 UTC from IEEE Xplore. Restrictions apply.

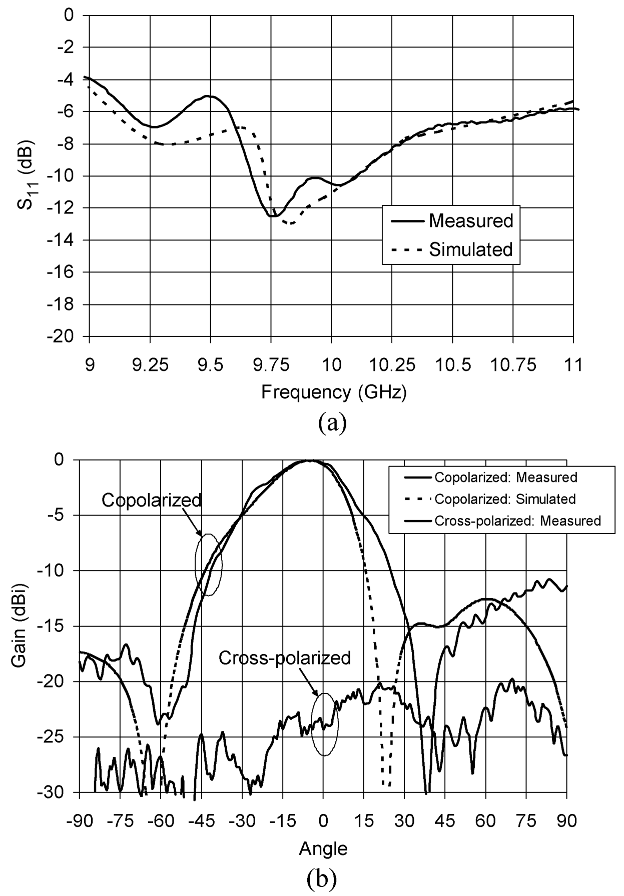

Fig. 10. Measured results of (a) S_{11} versus frequency (b) copolarized (E-plane, $y-z$ plane) and cross-polarized (H-plane, $x-z$ plane) radiation patterns at 10 GHz versus angle.

result of the small increase in radiated power by the first stub element.

With this confidence and experimental validation of the simulation results for both the phase shifter and the multielement CPW-CTS antenna array, we proceeded to simulate the desired integrated phased array antenna with beam steering capabilities. The newly designed ferroelectric phase shifter was integrated with the coplanar waveguide continuous transverse stub array to form a phased array antenna with electronic beam scanning capabilities. A detailed drawing of the developed phased array antenna employing two radiating stubs is illustrated in Fig. 11(a)–(d). The multidielectric ferroelectric phase shifter allows appropriate tuning of the phase velocity, hence varying the guide wavelength enabling electronic beam steering capabilities. The multidielectric coplanar waveguide phase shifter described in Section II provides adequate tunability, good impedance matching, and low attenuation and is an attractive candidate for phased array applications.

To enhance coupling from the microstrip feed to the radiating stubs, the ferroelectric material is removed from under the radiating stubs as illustrated in Fig. 11(b). The section under the radiating stubs is filled with low permittivity $\mathrm{SiO_2}$. Besides enhancing the radiation from the stubs, this procedure is expected to further reduce the sensitivity of the integrated design to manufacturing tolerances. The radiating stub elements are also "V" shaped which are narrow at the base and wider towards the top. The tapered geometry makes it possible to increase the distance and hence the phase shift between stubs. The narrow stub section couples power near the same current maximum on the transmission line feed. The center conductor of the coplanar waveguide penetrates the silicon oxide layer and is in direct contact with the ferroelectric layer as shown in Fig. 11(b).

Simulations were performed using WIPL-D [8]. Due to the very thin layers of the $\mathrm{SiO_2}$ as well as the ferroelectric layer, the computation "plates" run the risk of forming "non-convex" geometries where one dimension of the plate is much smaller than the other. This error can be overcome if the model contains plates with small dimensions, resulting in high concentration of plates in the ferroelectric sections and an overall increase in the number of unknowns. It was found that 12 plates for the multidielectric phase shifter provided the necessary convergence and accurate solution. Fig. 12 shows the WIPL-D model with a conductor thickness of 1.5 $\mu\mathrm{m}$ where the ohmic metal loss of the phase shifter is modeled according to the methods described in Fig. 5. The radiating stubs were made of copper foil with a conductivity of 58.8 MS/m. 5690 unknowns were used in the design.

Results in Fig. 13 show that with the center conductor width, $W = 13\ \mu\mathrm{m}$, gap width, $S = 300\ \mu\mathrm{m}$ (to provide a 50 Ω transmission line impedance), $A = 9.8$ mm, $B = 13$ mm, and $C = 8.0$ mm, a ferroelectric thickness $\mathrm{T} = 5\ \mu\mathrm{m}$, $\mathrm{SiO_2}$ thickness of 0.1 $\mu\mathrm{m}$, and a ferroelectric permittivity modulation between $\varepsilon_r(\mathrm{V_{dc}} = 0\ \mathrm{V}) = 723(1 - \mathrm{j}0.01)$ and $\varepsilon_r(\mathrm{V_{dc}} = 40\ \mathrm{V}) = 441.2(1 - \mathrm{j}0.01)$, approximately $+/-20^\circ$ of electronic beam scanning is observed. The gain is ~5 dBi for the unbiased case and is ~2.8 dBi for the biased case resulting in ~2.2 dB of scan loss at 10 GHz. The half power beam width is $\sim 47^\circ$ for the unbiased case and $\sim 46^\circ$ for the biased case. As shown in Fig. 13(b), the cross polarization remains below -20 dBi for both ferroelectric conditions and demonstrates good polarization purity, similar to that observed with the CPW-CTS array.

The CPW-CTS phased array is a non-resonant antenna array. The distance between radiating stub centers are not equal to $\lambda_g/2$ under either biased or unbiased ferroelectric states. It was designed to provide broadside radiation pattern at an intermediate value of λ_g between the biased and unbiased cases. Thus a broadside radiation pattern is not observed under either the biased or unbiased ferroelectric cases. Based on the condition that the stubs are not spaced $\lambda_g/2$ apart the reflections from the different stubs do not add up in phase and the total reflection coefficient at the input to the array is relatively small. Specifically, S_{11} for the unbiased case $(\varepsilon_r(\mathrm{V_{dc}} = 0\ \mathrm{V}) = 723(1 - \mathrm{j}0.01))$ was -12 dB, and for the biased case $(\varepsilon_r(\mathrm{V_{dc}} = 40\ \mathrm{V}) = 441.2(1 - \mathrm{j}0.01))$ was -18 dB.

While the above results illustrate the effectiveness of the proposed concept of integrated low cost phased array antenna, it should be noted that the proposed design provides ample opportunity for alternatives and optimizations to fit specific applications and needs. For example, a thinner ferroelectric substrate may be implemented to reduce the $\mathrm{V_{dc}}$ requirement of the phase shifter. In this case, we simulated another design with the thickness of the ferroelectric layer reduced to $\mathrm{T} = 0.5\ \mu\mathrm{m}$, instead

Authorized licensed use limited to: UNIV OF HAWAII LIBRARY. Downloaded on June 09,2010 at 20:58:55 UTC from IEEE Xplore. Restrictions apply.

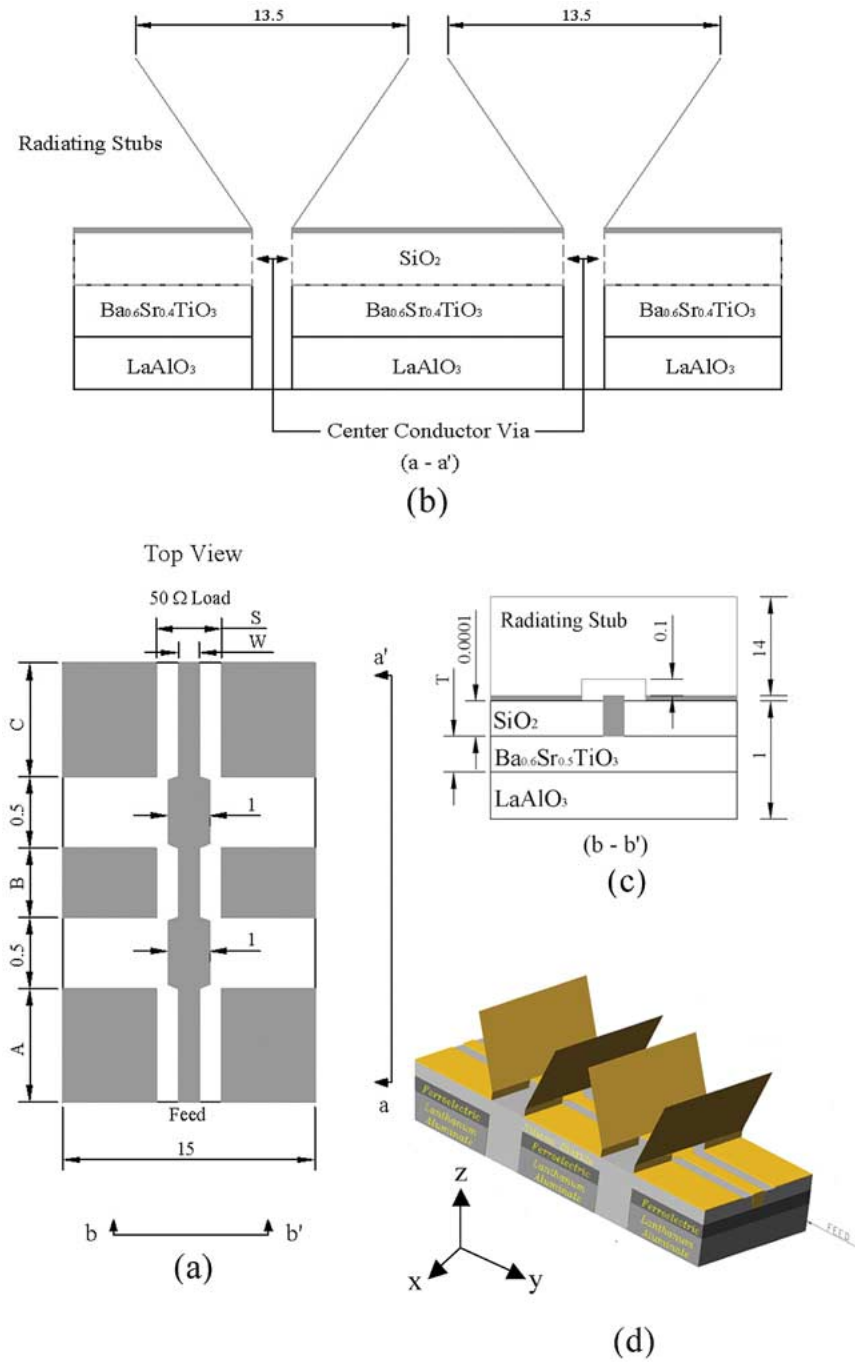

Fig. 11. Layout of the CPW-CTS phased array antenna. (a) Top view, (b) side view, (c) front view, and (d) perspective view, all dimensions in mm. The conductor thickness was 1.5 μm comprised of the multiconductor combination of Cr/Ag/Au (250 Å, 14250 Å, 500 Å).

of $\mathrm{T} = 5\ \mu\mathrm{m}$, and the obtained results are shown in Fig. 14. For this design, the dimensions $W = 10\ \mu\mathrm{m}$, $S = 50\ \mu\mathrm{m}$, $A = 9$ mm, $B = 17$ mm, $C = 8.5$ mm, and the thickness of SiO_2 layer is 0.1 μm. From Fig. 14 it may be seen that approximately $+/-15^\circ$ of electronic beam scanning was achieved. This is smaller than what was achieved when thicker ferroelectric layer was used, but the gain in this case is ~5.3 dBi for the unbiased case and is ~5.0 dBi for the biased case resulting in only ~0.3 dBi of scan loss, instead of 2.2 dBi scan loss for the earlier design, at 10 GHz. The half power beam width is $\sim 42^\circ$ for the unbiased case and $\sim 41^\circ$ for the biased case. As shown in Fig. 14, the cross polarization remains below −20 dBi for both ferroelectric conditions and also demonstrates good polarization purity. S_{11} for the unbiased case $(\varepsilon_r(\mathrm{V_{dc}} = 0\ \mathrm{V}) = 723(1 - \mathrm{j}0.01))$ was -27 dB, and for the biased case $(\varepsilon_r(\mathrm{V_{dc}} = 40\ \mathrm{V}) = 441.2(1-\mathrm{j}0.01))$ was -12 dB. In this case, since the distance between elements are longer (17 mm compared to 13 mm) than the previous case, 20 plates for the multi-dielectric phase shifter provided the necessary convergence.

These and similar design examples show that thinner ferroelectric layer may be employed thus leading to higher directive gain, lower scan loss, but would require an increase in the array

Authorized licensed use limited to: UNIV OF HAWAII LIBRARY. Downloaded on June 09,2010 at 20:58:55 UTC from IEEE Xplore. Restrictions apply.

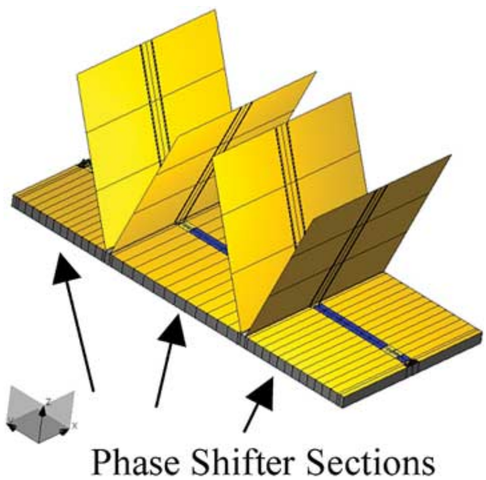

Fig. 12. WIPL-D model of two element CPW-CTS phased array illustrating the high concentration of plates in the multidielectric phase shifter sections.

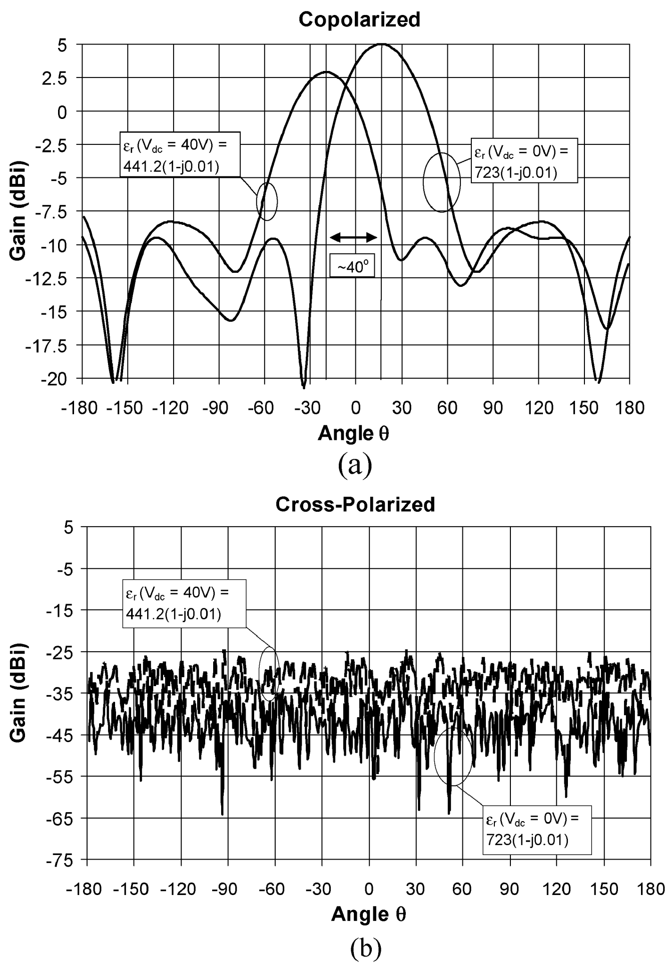

Fig. 13. (a) Co-polarized and (b) cross polarized radiation pattern of the phased array antenna shown in Fig. 11 at 10 GHz with $+/-20^\circ$ of beam scanning.

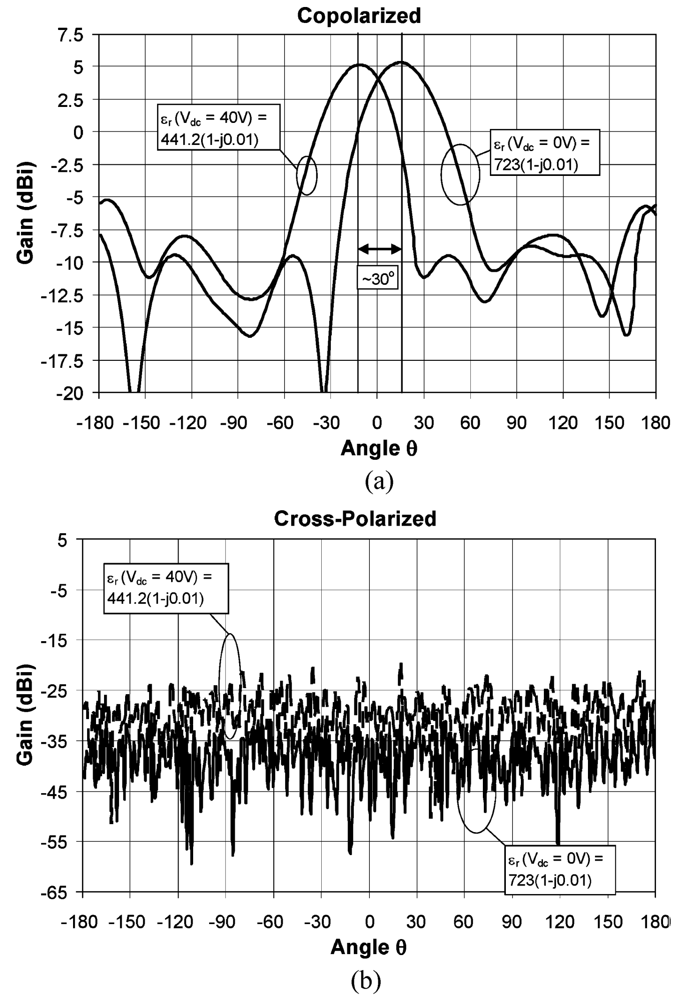

Fig. 14. (a) Co-polarized and (b) cross polarized radiation pattern of the phased array antenna shown in Fig. 11 at 10 GHz with $+/-15^\circ$ of beam scanning.

length. A thicker ferroelectric substrate, on the other hand, may be employed to reduce the overall array length; but this will result in a lower directive gain, increase in the scan loss, and will require larger dc bias, V_{dc}.

IV. Conclusion

A new biasing approach for the multidielectric layer phase shifter presented in [3] was developed and simulation results demonstrated its effectiveness in biasing the ferroelectric layer. The method of finite difference technique was used to quantify the potential distribution across the cross section of the ferroelectric device. It was found that the distribution was fully pronounced across the ferroelectric layer and that an equivalent voltage with that of the direct metallization case could be used to modulate the permittivity.

In this paper several modeling tools and numerical techniques were used to develop ferroelectric devices and phased array antennas. It is well known that the high permittivity and ferroelectric thin film technology makes modeling computationally intensive. We have presented several approaches to develop effective models. A first principles approach towards obtaining the effective width $(w_{\rm eff})$ parameter in the Green's function spectral domain algorithm was presented and was in excellent agreement to the values obtained from fitting measured results [6]. If, however, the frequency dependence of attenuation is desired, other unknown parameters namely ν and f_o in (4) are

Authorized licensed use limited to: UNIV OF HAWAII LIBRARY. Downloaded on June 09,2010 at 20:58:55 UTC from IEEE Xplore. Restrictions apply.

required to complete the analysis. The transmission line parameters obtained from LINPAR provides useful information; however as with the spectral domain method, modeling frequency dependent series resistance requires unknown parameters namely $f_{\max}$ and r_e in (3). The ability to parameterize individual metallic plates in WIPL-D allows the designer to generate an extremely close replica of the physical device and develop a very accurate model. For high attenuation devices such as ferroelectric phase shifters, a useful model for analyzing the ohmic metal loss was presented. However, the limitation of WIPL-D is that the dielectric domains are treated with isotropic permittivity.

The combination of the Green's function algorithm for analyzing the anisotropic characteristics of the ferroelectric material, LINPAR for determining the transmission line parameters and WIPL-D for full 3-D analysis provides a powerful combination for a first principles approach to ferroelectric device and antenna development. It was shown that the ferroelectric material characterized in [6] may be modeled with either an isotropic or anisotropic permittivity, thus allowing the use of WIPL-D. High frequency simulation of the new phase shifter design showed performance similar to the one reported earlier [3]. Specifically, improvement in both the attenuation and characteristic impedances were observed as well as an increase in FOM by up to $8^{\circ}/\mathrm{dB}$.

Furthermore, after experimentally verifying simulation results for the multielement CPW-CTS array, we presented results for an integrated phased array antenna with beam steering capabilities. Specifically, a two element phased array antenna with electronic beam scanning capabilities was designed at 10 GHz based on the integration of the multidielectric ferroelectric phase shifter and the coplanar waveguide continuous transverse stub array. The phased array antenna design is based on the new coplanar waveguide implementation described in [1]. The phased array produced nearly $+/-20^{\circ}$ (or 40°) of beam scanning in conjunction with possessing good impedance match. The use of a thinner ferroelectric layer results in a smaller scan of $+/-15^{\circ}$ but higher gain and lower scan loss.

Acknowledgment

The authors are indebted to the four reviewers and the associated editor who provided invaluable comments and suggestions that truly contributed to the value of this paper. Their efforts and the detailed evaluation of the manuscript are acknowledged and wholeheartedly appreciated.

References

[1] W. Kim and M. F. Iskander, "A new Coplanar Waveguide Continuous Transverse Stub (CPW-CTS) antenna for wireless communications," IEEE AWPL vol. 4, pp. 172–174, 2005 U.S. patent 7,079,082, Jul. 18, 2006.

[2] W. W. Milroy, "Continuous Transverse Stub (CTS) Element Devices and Methods of Making Same," U.S. Patent 5,266,961, Aug. 29, 1991.

[3] W. Kim, M. Iskander, and C. Tanaka, "High-performance low-cost phase-shifter design based on ferroelectric materials technology," *Electron. Lett.*, vol. 40, no. 21, pp. 1345–1347, 2004.

[4] M. Iskander, *Electromagnetic Fields and Waves*. Prospect Heights, IL: Waveland Press, 1992.

[5] N. Alexopoulos, "Integrated-circuit structures on anisotropic substrates," *IEEE Trans. Microw. Theory Tech.*, vol. MTT-33, no. 10, pp. 847–881, 1985.

[6] C. Krowne, M. Daniel, S. Kirchoefer, and J. Pond, "Anisotropic permittivity and attenuation extraction from propagation constant measurements using an anisotropic full-wave Green's function solver for coplanar ferroelectric thin- film devices," *IEEE Trans. Microw. Theory Tech.*, vol. MTT-50, no. 2, pp. 537–548, 2002.

[7] A. Djordjevic, M. Bazdar, T. Sarkar, and R. Harrington, *LINPAR for Windows*. Norwood, MA: Artech House, 1999.

[8] B. Kolundzija, J. Ognjanovic, and T. Sarkar, "WIPL-D: electromagnetic modeling of composite metallic and dielectric structures," Professional Version 6.

[9] E. Carlsson and S. Gevorgian, "Effect of enhanced current crowding in a CPW with a thin ferroelectric film," *Electron. Lett.*, vol. 33, no. 2, pp. 145–146, 1997.

Wayne Kim (S'98–M'00) received the B.S. degree from the University of Hawaii in 1998 and the M.S. degree from the University of California at Los Angeles in 2001, both in electrical engineering. He is currently working toward the Ph.D. degree at the University of Hawaii.

From 1998 to 2001, he was with TRW Space and Electronics (now Northrop Grumman) where he was involved in the development of indium phosphide bipolar transistors as well as MMIC design including high efficient power amplifiers. His research interests include developing phased array antennas, smart antenna systems, and associated microwave components for wireless communications. He has several patents.

Mr. Kim was the second place winner in the student paper contest for the Applied Computational Electromagnetics Society (ACES) conference in 2004. He was a recipient of the Achievement Rewards for College Scientists (ARCS) in 2006.

Magdy F. Iskander (F'93) is the Director of the Hawaii Center for Advanced Communications (HCAC), College of Engineering, University of Hawaii at Manoa, Honolulu, Hawaii. He is also a co-director of the NSF Industry/University joint Cooperative Research Center between the University of Hawaii, University of Arizona, Arizona State University, and the RPI in New York. He was a Professor of Electrical Engineering and the Engineering Clinic Endowed Chair Professor at the University of Utah for 25 years. He was also the Director of the Center of Excellence for Multimedia Education and Technology. From 1997–99 he was a Program Director, in the Electrical and Communication Systems Division at the National Science Foundation. While at NSF he formulated and directed a "Wireless Information Technology" initiative in the Engineering Directorate and funded over 29 projects in the microwave/millimeter wave devices, RF MEMS technology, propagation modeling, and the antennas areas. In 1986, he established the Engineering Clinic Program at the University of Utah to attract industrial support for projects for undergraduate engineering students and was the Director of this program since its inception. While in Utah, the program attracted more than 115 projects sponsored by 37 corporations from across the U.S. and resulted in an endowment for scholarships and a professorial chair held by the Director. Upon joining the University of Hawaii, he started a similar Engineering Clinic Program and in 2002–03 he had seven corporate sponsors. He was a member of the National Research Council Committee on Microwave Processing of Materials. He spent sabbaticals and other short leaves at Polytechnic University of New York; Ecole Superieure D'Electricite, France; UCLA; Harvey Mudd College; Tokyo Institute of Technology; Polytechnic University of Catalunya, Spain; and at several universities in China. He authored a textbook *Electromagnetic Fields and Waves* (Prentice Hall, 1992 and Waveland Press, 2001) edited *CAEME Software Books* (Vol. I, 1991, and Vol. II, 1994) and edited four other books on *Microwave Processing of Materials*, all published by the (Materials Research Society, 1990–1996). He is the Founding Editor of *Computer Applications in Engineering Education* (CAE). This journal is now in its 13th year, and received the Excellence in Publishing Award, by the Association of the American Publishers, in 1993.

Authorized licensed use limited to: UNIV OF HAWAII LIBRARY. Downloaded on June 09,2010 at 20:58:55 UTC from IEEE Xplore. Restrictions apply.

He has published over 180 papers in technical journals, has seven patents, and has made numerous presentations in technical conferences. His ongoing research contracts include "Propagation Models for Wireless Communication," funded by the Army Research Office and NSF; "Low-Cost Phased Array Antennas," funded by both the Army Research Lab and NSF; and several other research projects sponsored by corporate sponsors including Raytheon, Trex, Motorola, Kyocera Wireless, Corning, Inc., and BAE Systems. He also recently established a new indoor antenna range and wireless testbed lab facilities at the University of Hawaii as a result of an NSF Major Research Instrumentation (MRI) grant.

Dr. Iskander received the 1985 Curtis W. McGraw ASEE National Research Award, 1991 ASEE George Westinghouse National Education Award, 1992 Richard R. Stoddard Award from the IEEE EMC Society, the 2000 University of Utah Distinguished Teaching Award, and the 2002 Kuhina (Ambassador) Award from the Hawaii Visitors and Convention Bureau. He was a member of the 1999 WTEC panel on "Wireless Information Technology-Europe and Japan," and chaired two panels on "Asian Telecommunication Technology" sponsored by DoD and organized by the International Technology Research Institute (ITRI) in 2001 and 2003. He edited a special issue of the IEEE TRANSACTIONS ON ANTENNAS AND PROPAGATION ON WIRELESS COMMUNICATIONS TECHNOLOGY, May 2002, which included contributions from the NSF funded projects, in 2004 co-edited a special issue of the *IEICE journal* in Japan (September 2004) on recent progress in Wireless Communications, and co-edited the 2006 special issue of IEEE TRANSACTIONS ON ANTENNAS AND PROPAGATION ON WIRELESS COMMUNICATIONS. He organized the first (2001) and the second (2003) "Wireless Grantees Workshop" sponsored by NSF and held at the National Academy of Sciences, and in Honolulu, respectively. He is the 2002 President of the IEEE Antennas and Propagation Society, Vice President in 2001, and was a member of the IEEE APS AdCom from 1997 to 1999. He was the General Chair of the 2000 IEEE AP-S Symposium and URSI meeting in Salt Lake City, UT, the General Chair of the IEEE Conference on Wireless Communications Technology, in 2003, in Hawaii, the General Chair of the 2005 IEEE/ACES joint conference on Wireless Communications and Applied Computational Electromagnetics, and the General Chair for the 2007 IEEE Antennas and Propagation International Symposium in Honolulu, HI. He also edited the 1995 and 1996 proceedings of the International Conference on Simulation and Multimedia in Engineering Education. He was a Distinguished Lecturer for the IEEE AP-S (1994–97) and during this period he gave lectures in Brazil, France, Spain, China, Japan, and at a large number of U.S. universities and IEEE chapters.

W. Devereux Palmer (S'89–M'91–SM'01) was born in Augusta, GA, in 19[illegible]. He received the B.A. degree in physics and the M.S. and Ph.D. degrees in electrical engineering from Duke University, Durham, NC, in 1980, 1988, and 1991, respectively. His field of graduate study was electromagnetic theory, and design, construction, and testing of microwave circuits and systems for practical applications.

From 1991 to 2001, he served on the technical staff at MCNC Research and Development Institute where he worked on a number of technologies including silicon vacuum microelectronics for microwave power amplifiers, polymeric MEMS structures, high-Q HTS filters, wide-bandgap semiconductors for power electronics applications, radio and optical communications systems, and optical and electronic packaging. In 2000, he became the Director of the MCNC-RDI Optical and Electronic Packaging group, where he managed programs in development of lead-free flip-chip bumping processes, bumping and assembly of high-density tiled detector arrays for particle accelerators, and packaging for OC-768 optical components. He holds the position of Adjunct Professor in the Department of Electrical and Computer Engineering at Duke University where he collaborates on research activities with other faculty members and graduate students, serves on graduate examination committees, and taught introductory electromagnetics for four semesters. Since his assignment to the U.S. Army Research Office, Research Triangle Park, NC, in 2001, he manages extramural basic research programs in computational electromagnetics, microwave and millimeter-wave circuit integration, compact and multifunctional antenna design, low-power communications systems, and power electronics.

Dr. Palmer is a Professional Engineer registered in North Carolina and a member of URSI Commission C and Commission D, the American Vacuum Society, the Materials Research Society, and Sigma Xi. He serves as the 2006–2008 Chair of the USNC-URSI Commission C. Within the IEEE, he participates in the Antennas and Propagation; Components, Packaging, and Manufacturing Technology; Electron Devices; Microwave Theory and Techniques; Power Electronics; and Professional Communications societies, served on the Vacuum Devices Technical Committee from 1997 to 2003, and served as Guest Editor for the T-ED Special Issue on Vacuum Electronics (January 2001) and the T-MTT Special Issue on Multifunctional RF Systems (March 2005). He currently serves as Secretary for the Eastern North Carolina Section in Region 3, and is a founding member and past Chair of the ACME (AP/CPMT/MTT/ED) local chapter.

Authorized licensed use limited to: UNIV OF HAWAII LIBRARY. Downloaded on June 09,2010 at 20:58:55 UTC from IEEE Xplore. Restrictions apply.

A New Coplanar Waveguide Continuous Transverse Stub (CPW-CTS) Antenna for Wireless Communications

Wayne Kim, *Student Member, IEEE,* and Magdy F. Iskander, *Fellow, IEEE*

***Abstract*—To address the continuing demand for low-cost, lightweight and high-performance antennas, and multiband antenna arrays for wireless communications, we developed a new design of the continuous transverse stub (CTS) antenna technology. The design is based on a coplanar waveguide (CPW) feed which combines the advantages of the planar designs originally developed by Hughes Aircraft [1] and the newer 50 Ω coaxial version recently developed by our group [2]. To examine the feasibility of the approach, a one-element CPW-CTS antenna is designed and a prototype is built in the frequency range of 5.2–5.6 GHz. S-Parameters and radiation pattern results shows good agreement between the simulation results and the experimental data.**

***Index Terms*—Continuous transverse stub (CTS) antenna, coplanar waveguide, low cost, multiband array, wireless communications.**

I. Introduction

THE planar continuous transverse stub (CTS) antennas and antenna array were originally invented and patented by Hughes Aircraft Company in the early 1990s [1]. Benefits of the CTS antenna include compact size, light weight, low cost, increased directive gain with increased radiating elements, and high efficiencies. The CTS antenna finds applications in the areas of satellite communications and various military radar systems operating in the 1-20 GHz frequency band. A new coaxial version of the CTS technology with omnidirectional radiation pattern [2] and multiband operation [3] were recently reported. In particular, it was demonstrated that multiband performance at the 4.2 and 19.4 GHz frequency band with equivalent radiated power (~98%) and good impedance match is possible to achieve using this technology.

The coplanar waveguide CTS (CPW-CTS) antenna described in this paper makes use of the CTS technology in a planar microstrip configuration and produces a broadside radiation pattern with a maximum in the +z direction, perpendicular to the plane of the antenna. The coplanar CTS offer several advantages over previous designs including the planar and coaxial CTS. This includes: 1) broadside radiation pattern compared to the omni-directional pattern in the coaxial CTS case, 2) simple 50 Ω coaxial or microstrip transmission line feed compared to the waveguide feed for the planar design case [1], and 3) simple integration with microstrip 50 Ω circuitry in transceivers front-end which is not effectively possible in any of the earlier designs.

In addition, the CPW-CTS may realize high gain through a series array of elements with one feed, an advantage over high gain dipole antenna arrays which may require multiple feeds.

II. Simulated Models and Numerical Results

The operation of the CPW-CTS involves launching incident transmission line modes with a coplanar waveguide feed on a substrate with a low dielectric constant. The CPW feed have associated with them quasi TEM modes which are interrupted by the presence of a continuous transverse stub in conjunction with a discontinuous ground plane. The presence of the purely reactive transverse stub elements couples a longitudinal, z-directed displacement current across the parallel plate transmission line and coplanar waveguide interface (see Fig. 1). This induced current excites z-directed EM waves where the electric field is linearly polarized in the transverse direction (y-directed) to the stub elements. The CPW-CTS is a traveling-wave fed antenna.

The coupling values from the CPW to the radiating stubs are primarily dependent on the height (H1), width (W1), the transmission line width between radiating elements (CW1), the distance (L1) of the parallel plate stubs, and the transverse stub gap (H2). The gap distance between the transverse stubs (H2) is used to adjust the coupling capacitance to compensate the inductance of the purely reactive stub elements. The antenna is fed with a simple coplanar waveguide transmission line. The signal conductor width (CW), gap width (GW), and dielectric constant (ε_r) were chosen to provide 50 Ω feed impedance.

The feed point (L2) is positioned away from the edge of the stubs to maintain a good impedance match. L2 is carefully chosen to obtain the desired radiation pattern as a result of the axis of the feed line being oriented in line with the E-plane radiation pattern. The substrate height (SH) was chosen such that it improves the directive gain without severely influencing the incident transmission line modes and increasing reflections.

The length (L1), width (W1), and height (H1) were selected to be approximately a half wavelength, one wavelength, and one-third wavelength in the dielectric material that fills the stub, respectively. After extensive simulations, these values of CW and CW1 were carefully chosen to produce increased radiated power and at the same time maintain good impedance match. The ground width (W2) was approximately one-third

Manuscript received November 8, 2004; revised January 12, 2005.
The authors are with the Hawaii Center for Advanced Communications, College of Engineering, University of Hawaii at Manoa, Honolulu, HI 96822 USA (e-mail: kimwayne@hawaii.edu; magdy@hawaii.edu).
Digital Object Identifier 10.1109/LAWP.2005.848660

1536-1225/$20.00 © 2005 IEEE

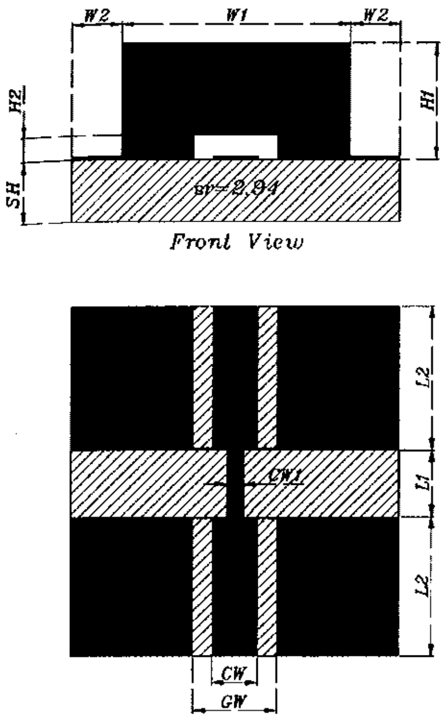

(a)

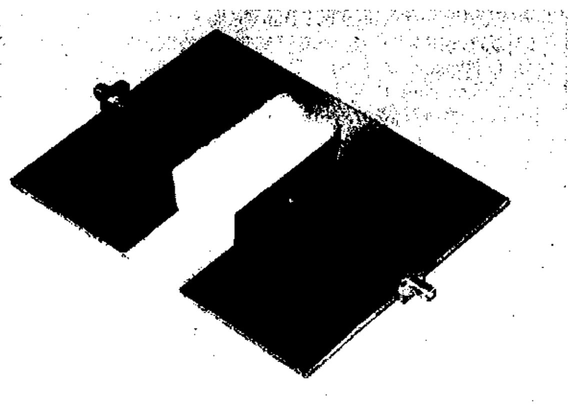

(b)

1. (a) Schematic of CPW-CTS and (b) fabricated prototype of the igned CPW-CTS. A Styrofoam spacer is inserted in the radiating stub to rately maintain the stub dimensions.

velengths. Large values of W2 were needed to reduce the desired back lobes, most notably in the H-plane radiation asurements.

III. Simulated and Experimental Results

or the simulation purposes we used WIPL-D, a full three-ensional electromagnetics simulator based on the method moments [4]. An antenna operating at 5.3 GHz was designed desired features include low input impedance, high radiated ver, and a broadside radiation pattern. The obtained design ensions after extensive simulations were as follows: W1 = 5 mm, W2 = 28.3 mm, H1 = 18.2 mm, H2 = 1.5 mm, $= \mathrm{CW1} = 4.7$ mm, GW = 5.97 mm, L1 = 27.3 mm, = 54.5 mm, SH = 3.01 mm, and $\varepsilon_r = 2.94$ (RT/Duroid

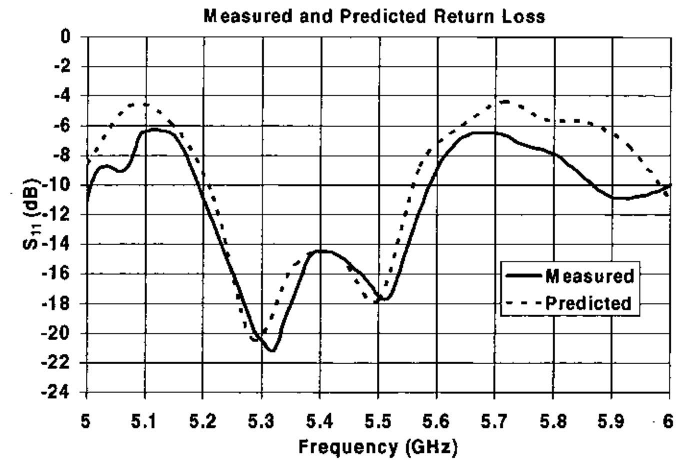

(a)

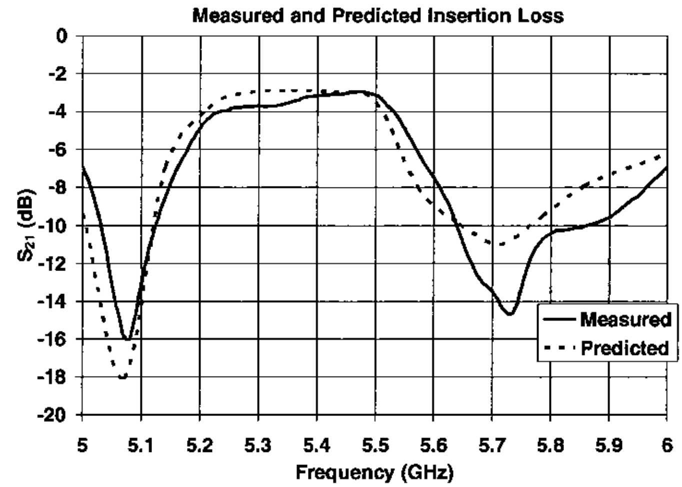

(b)

Fig. 2. Predicted and measured (a) return loss and (b) insertion loss.

6002). Fig. 2(a) and (b) show the measured and simulated return and insertion losses, respectively. As can be seen, S_{11} is better than -10 dB in the frequency range between 5.2 and 5.6 GHz and the radiated power ratio is greater than 40%. This radiated power ratio was calculated based on

$$Pwr_{\mathrm{rad}} \approx (1 - Pwr_{\mathrm{refl}} - Pwr_{\mathrm{trans}}) * 100\% \qquad (1)$$

where the reflected Pwr_{refl} and transmitted Pwr_{trans} powers are given by

$$Pwr_{\mathrm{refl,trans}} \approx 10^{\frac{S_{11,21}(\mathrm{dB})}{10}}. \qquad (2)$$

S_{11} and S_{21} are the reflection and insertion losses, respectively, from Fig. 2. The term transferred power is used to account for the amount of power received at the end of the antenna and after the radiating stub. Fig. 3 shows the measured and predicted E-plane and H-plane radiation patterns at 5.3 GHz. The measured E-plane beam peak was $-18°$ and the measured 3-dB beam width was 74.8°. The maximum back lobe was -14 dB from the maximum beam peak. The maximum back lobe of the measured H-plane was -17 dB down from the maximum beam peak. As may be seen, the measured data and simulated results

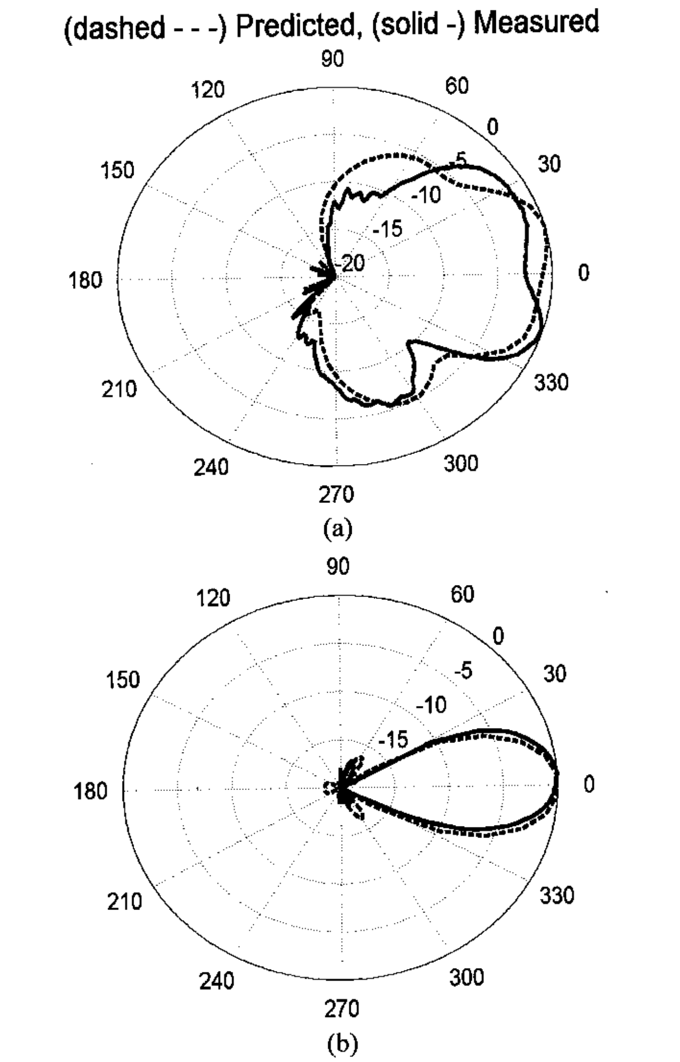

Fig. 3. Predicted and measured (a) E-plane and (b) H-plane radiation pattern.

are in good agreement and validate the predictability of the performance of this new antenna design.

The square stubs of the CPW-CTS antenna in Fig. 1(a) may be replaced with semicircular stubs in order to form a low-profile antenna with radial dimensions equivalent to the height (H1). Simulated results of such a configuration show identical results.

IV. Conclusion

A new coplanar waveguide CTS (CPW-CTS) antenna has been described. Advantages of this new design include low cost, low profile, light weight, and a very simple planar microstrip feed configuration. In this paper, we presented an example of a single element CPW-CTS design in the 5.2–5.6 GHz band. Both S-parameters and radiation pattern results were examined and good agreement between the experimental and simulation data were illustrated.

Specifically, the designed one-element antenna exhibited a well-formed broadside main beam at 5.3 GHz and good 50 Ω impedance match (−10 dB) from 5.2–5.5 GHz. For future work, the coplanar waveguide CTS antenna design could be loaded with multiple elements to form a series array for improved directive gain and narrow beam widths [2]. A multiple-element array could also be formed with frequency selective sections to enable multiband operation [3]. The planar design could be integrated with tunable ferroelectric materials to introduce multiband, electronic beam scanning capabilities [5], [6].

References

[1] W. W. Milroy, "Continuous Transverse Stub (CTS) Element Devices and Methods of Making Same," U.S. Patent 5 266 961, Aug. 29, 1991.

[2] M. F. Iskander, Z. Zhang, Z. Yun, and R. Isom, "Coaxial Continuous Transverse Stub (CTS) array," *IEEE Microw. Wireless Compon. Lett.*, vol. 11, no. 12, pp. 489–491, Dec. 2001.

[3] R. Isom, M. F. Iskander, Z. Yun, and Z. Zhang, "Design and development of multiband coaxial Continuous Transverse Stub (CTS) antenna arrays," *IEEE Trans. Antennas Propag.*, vol. 52, no. 8, pp. 2180–2184, Aug. 2004.

[4] B. Kolundzija, J. Ognjanovic, and T. Sarkar, *WIPL-D: Electromagnetic Modeling of Composite Wire and Plates Structures—Software and User's Manual*. Boston: Artech House, 2000.

[5] M. Iskander, Z. Zhang, Z. Yun, R. Isom, M. Hawkins, R. Emrick, B. Bosco, J. Synowczynski, and B. Gersten, "New phase shifters and phased antenna array designs based on ferroelectric materials and CTS technologies," *IEEE Trans. Microwave Theory Tech.*, vol. 49, no. 12, pp. 2547–2553, Dec. 2001.

[6] W. Kim, M. F. Iskander, and C. Tanaka, "High performance low cost phase shifters design based on the ferroelectric materials technology," *Electron. Lett.*, vol. 40, no. 21, pp. 1345–1347, Oct. 2004.

http://ip.com/patapp/US20050219136

US 20050219136A1

(19) United States
(12) Patent Application Publication
Iskander et al.
(10) Pub. No.: US 2005/0219136 A1
(43) Pub. Date: Oct. 6, 2005

(54) COPLANAR WAVEGUIDE CONTINUOUS TRANSVERSE STUB (CPW-CTS) ANTENNA FOR WIRELESS COMMUNICATIONS

(76) Inventors: **Magdy F. Iskander**, Honolulu, HI (US); **Wayne C. Kim**, Mililani, HI (US); **Jodie M. Bell**, Honolulu, HI (US)

Correspondence Address:
LEIGHTON K. CHONG
GODBEY GRIFFITHS REISS & CHONG
1001 BISHOP STREET, PAUAHI TOWER
SUITE 2300
HONOLULU, HI 96813 (US)

(21) Appl. No.: **11/087,116**

(22) Filed: **Mar. 21, 2005**

Related U.S. Application Data

(60) Provisional application No. 60/558,592, filed on Mar. 31, 2004.

Publication Classification

(51) **Int. Cl.**[7] **H01Q 13/00**

(52) **U.S. Cl.** **343/772**

(57) **ABSTRACT**

An improved continuous transverse stub (CTS) antenna has coplanar waveguide (CPW) feed elements spaced apart aligned in parallel and mounted perpendicular to a planar substrate base made of a low dielectric material. A continuous transverse stub extends perpendicularly through a clearance gap in the CPW feed elements on the ground plane of the substrate base. The antenna is fed with a simple coplanar waveguide transmission line formed by the parallel CPW elements. The antenna employs the coplanar waveguide with CTS technology, preferably in a planar microstrip configuration, to produce a broadside radiation pattern with a maximum in the +z direction, perpendicular to the plane of the antenna. The CPW-CTS antenna offers the advantages of a broadside radiation pattern, low input impedance, high radiation efficiency, low fabrication cost, use of simple coaxial or microstrip transmission line feed, and simple integration with microstrip circuitry in a transceiver front-end. The CPW-CTS antenna may be integrated in a single frequency band or in multiband arrays and could provide radiation beam steering capability when integrated with a substrate of tunable dielectric material such as BSTO.

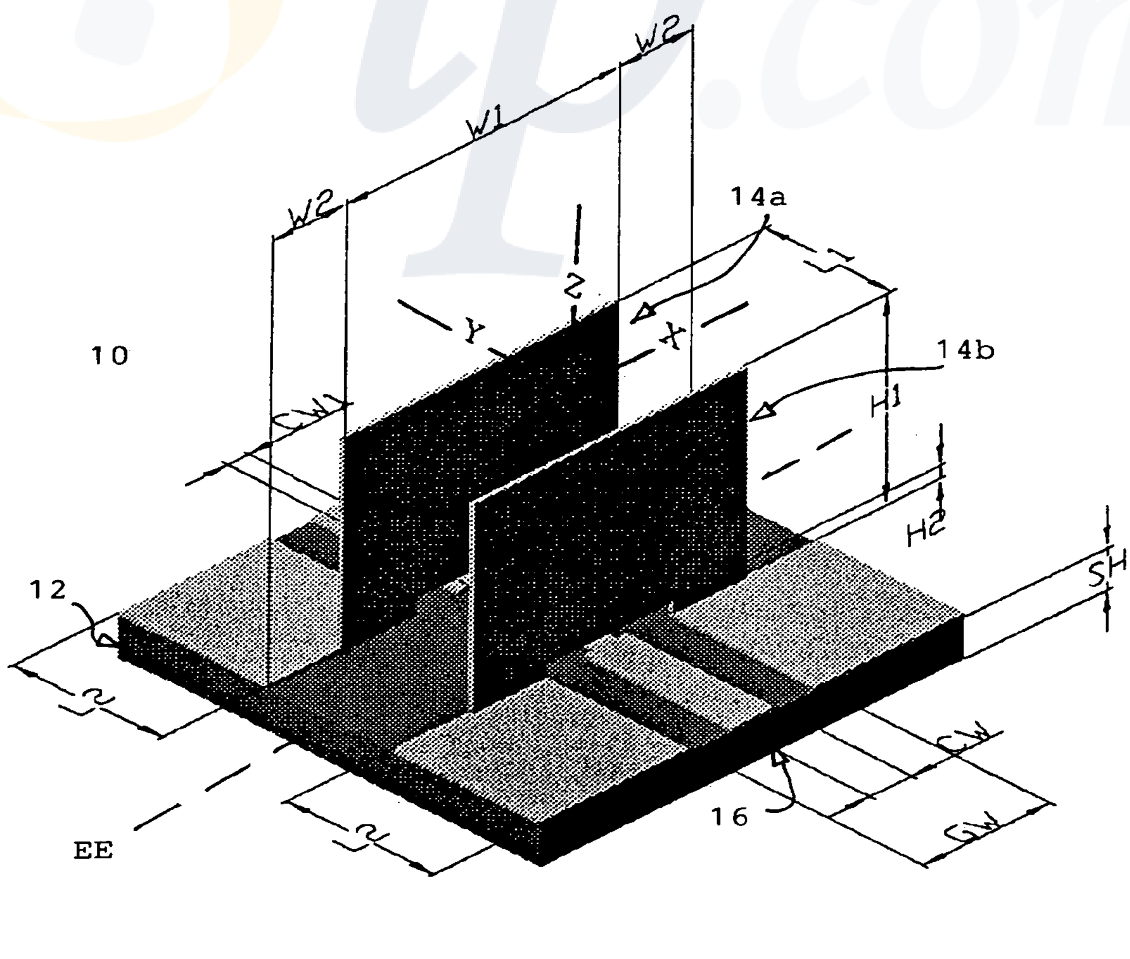

http://ip.com/patapp/US20050219136

FIG. 1(a)

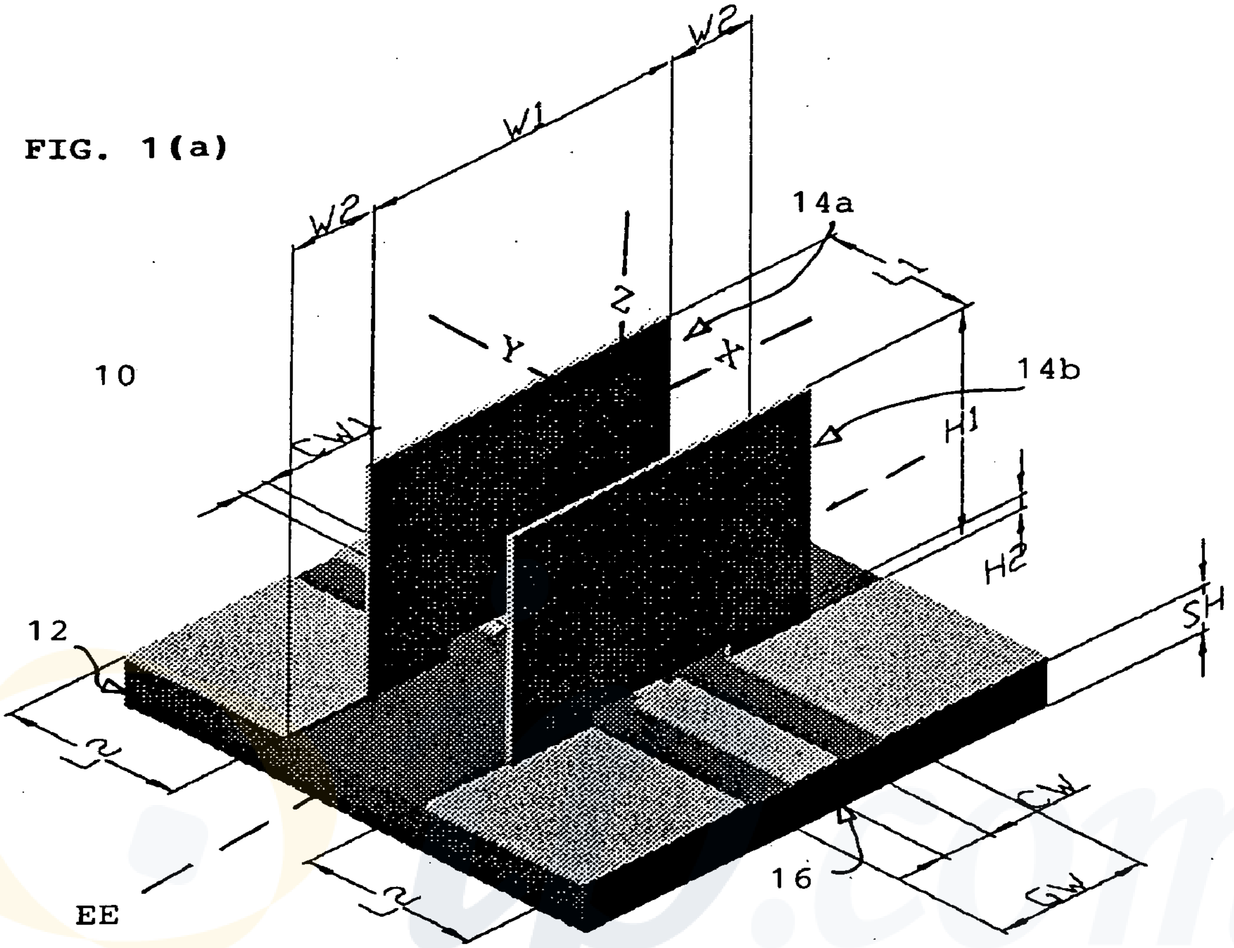

FIG. 1(b)

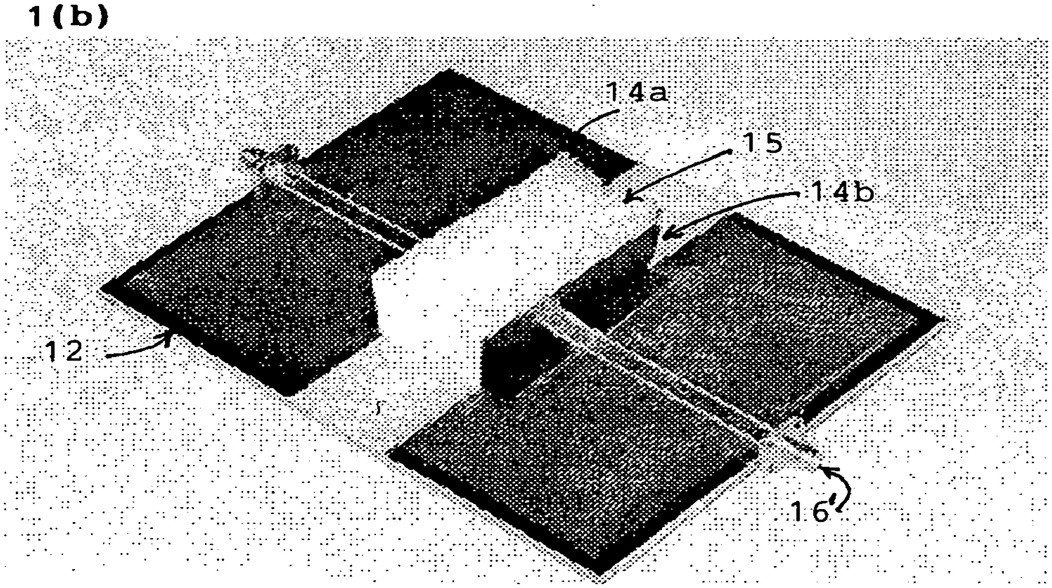

http://ip.com/patapp/US20050219136

FIG. 2(a)

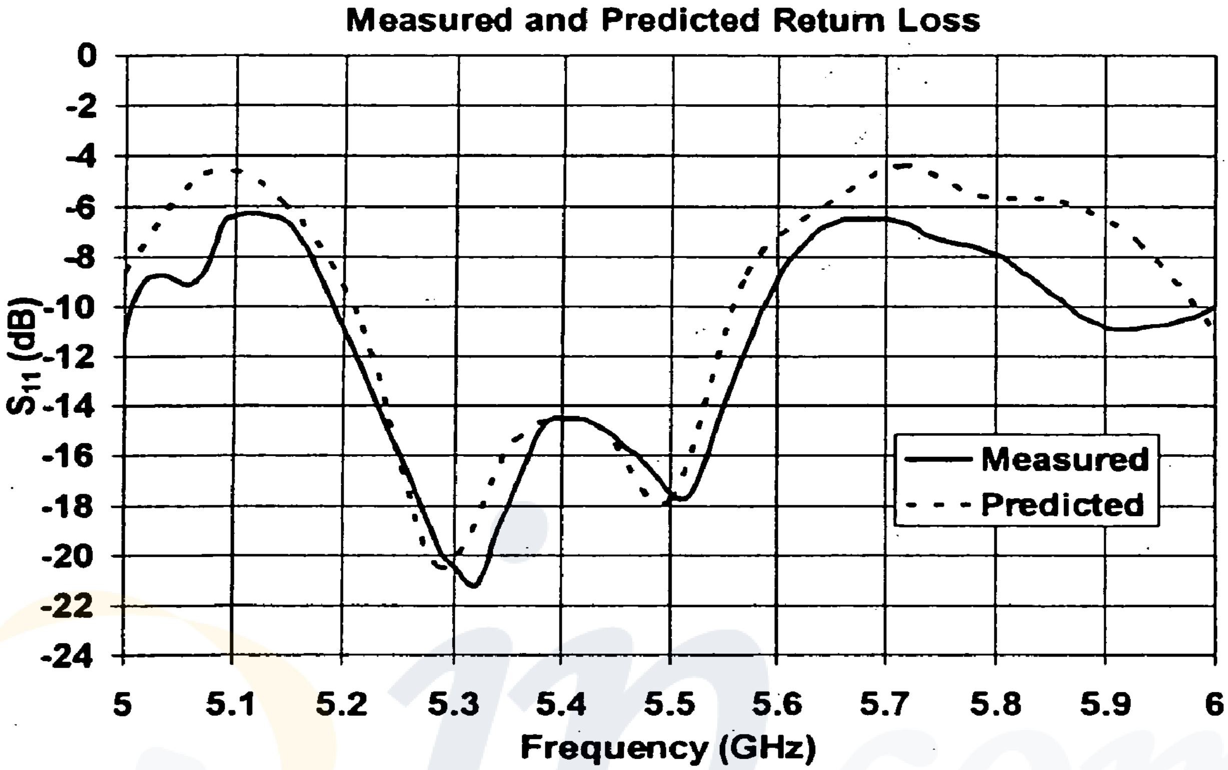

FIG. 2(b)

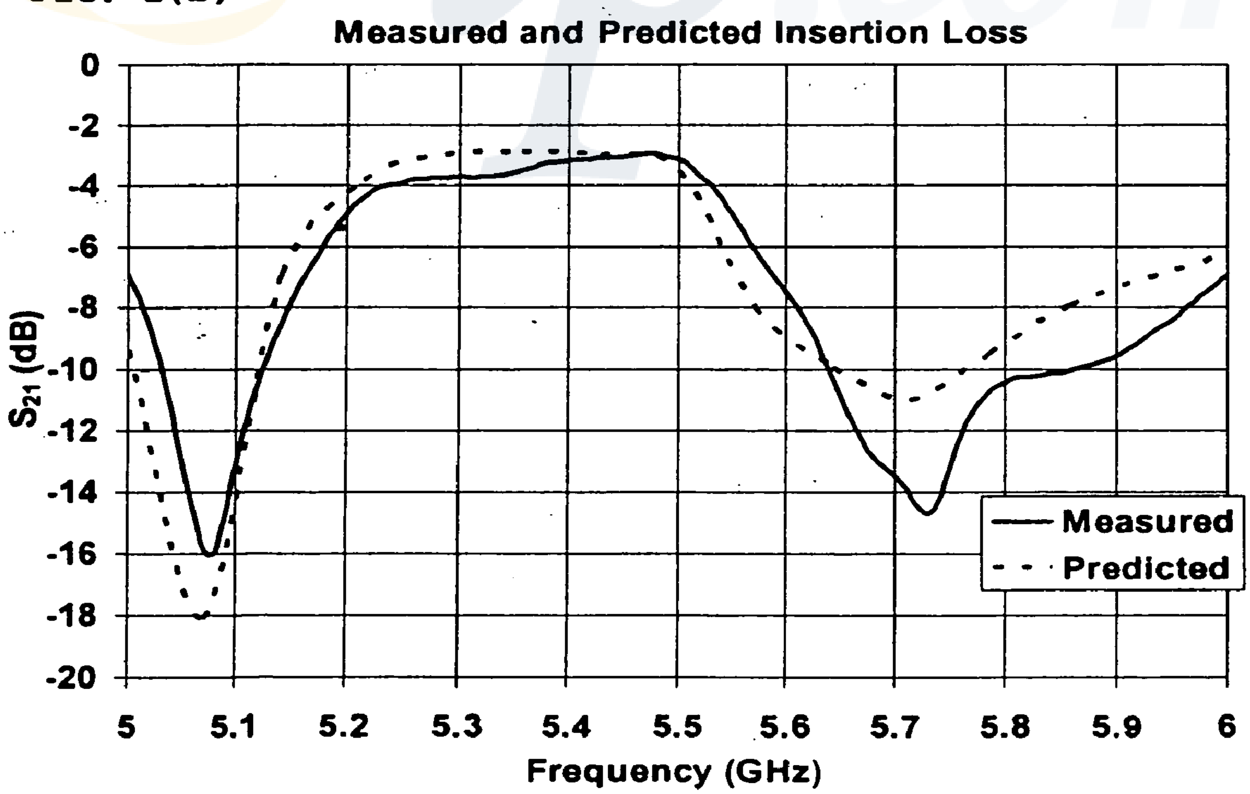

http://ip.com/patapp/US20050219136

FIG. 3(a) E-Plane Radiation Pattern

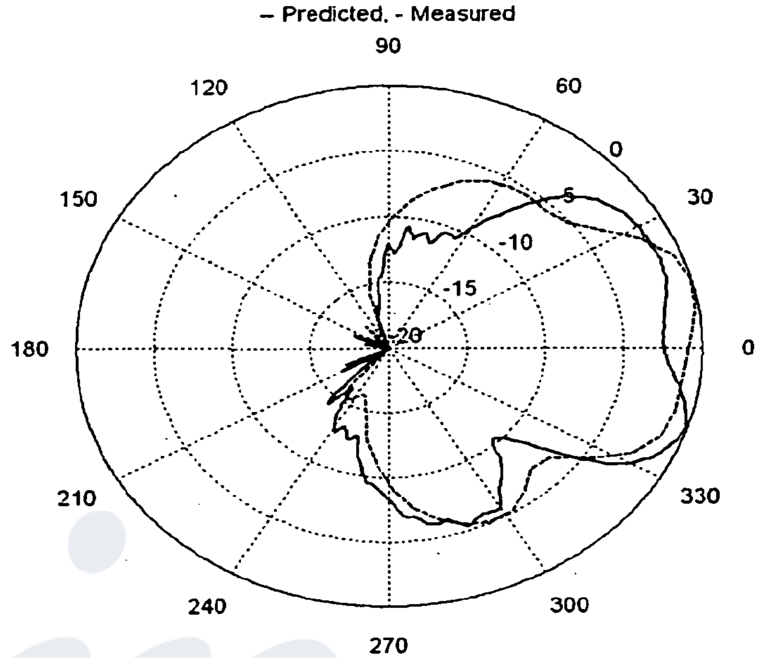

FIG. 3(b) H-Plane Radiation Pattern

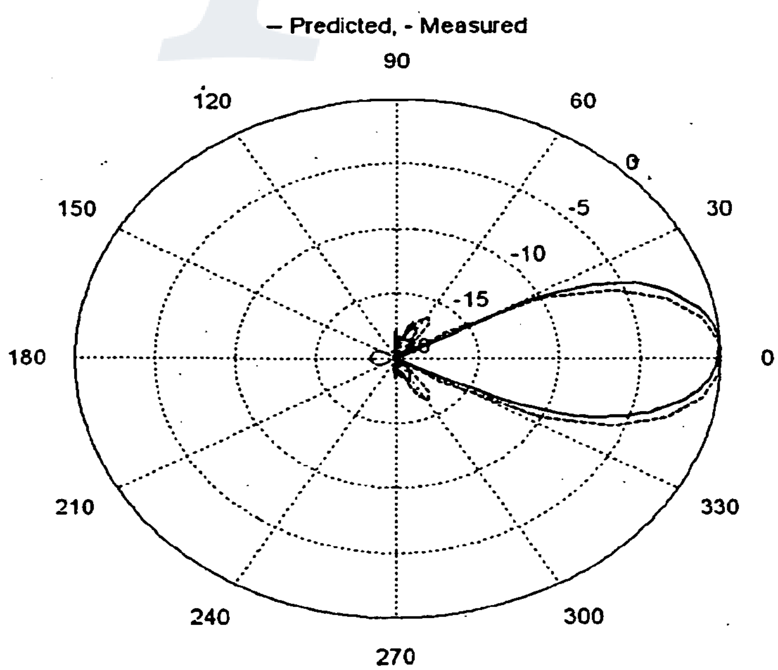

http://ip.com/patapp/US20050219136

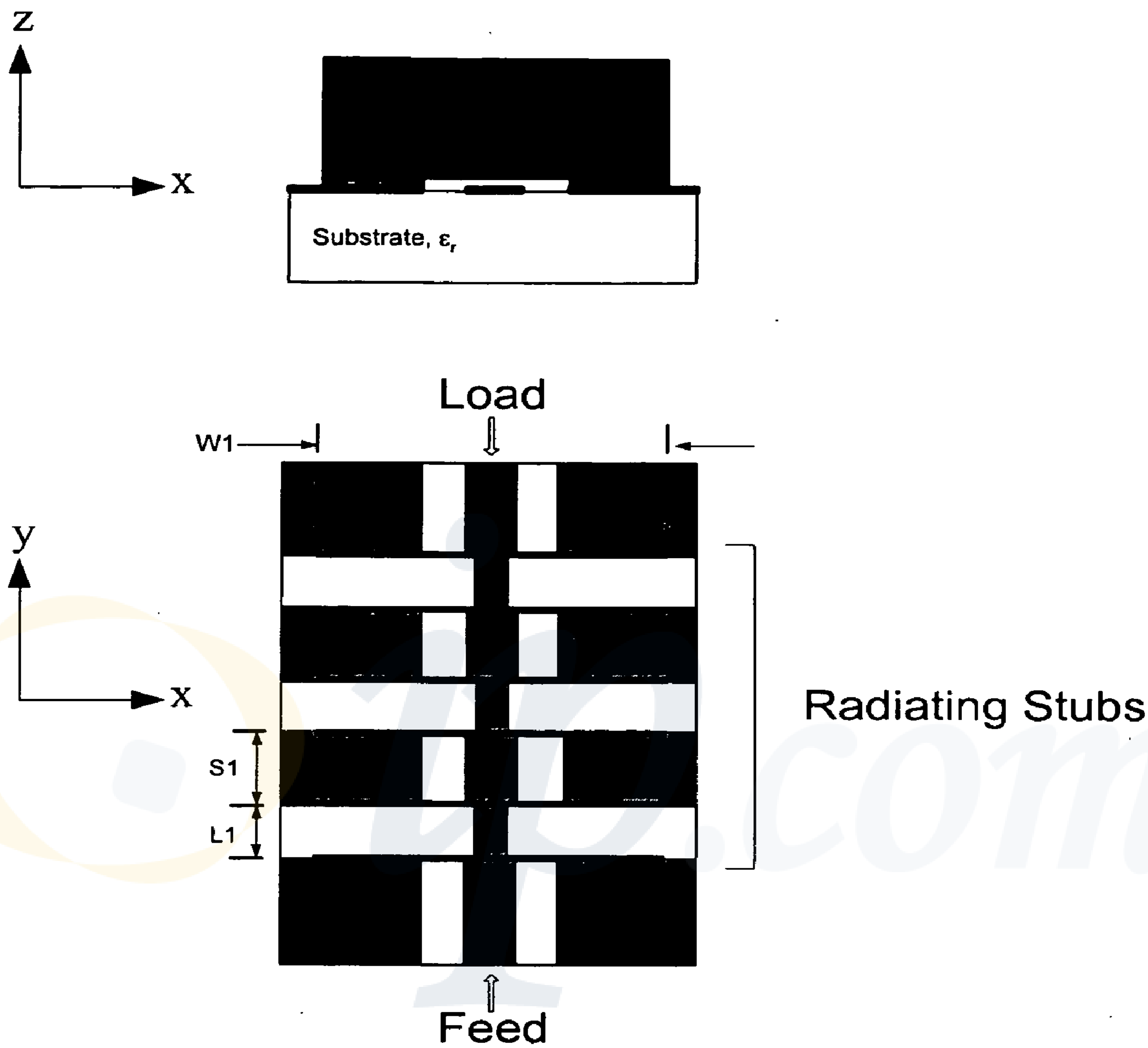

Figure 4

http://ip.com/patapp/US20050219136

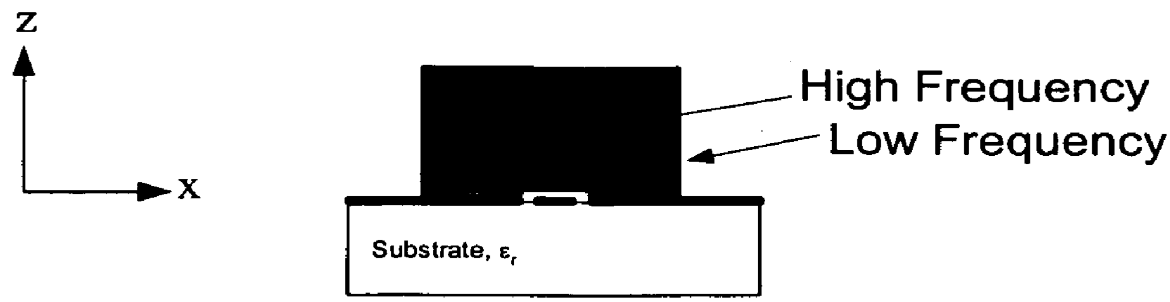

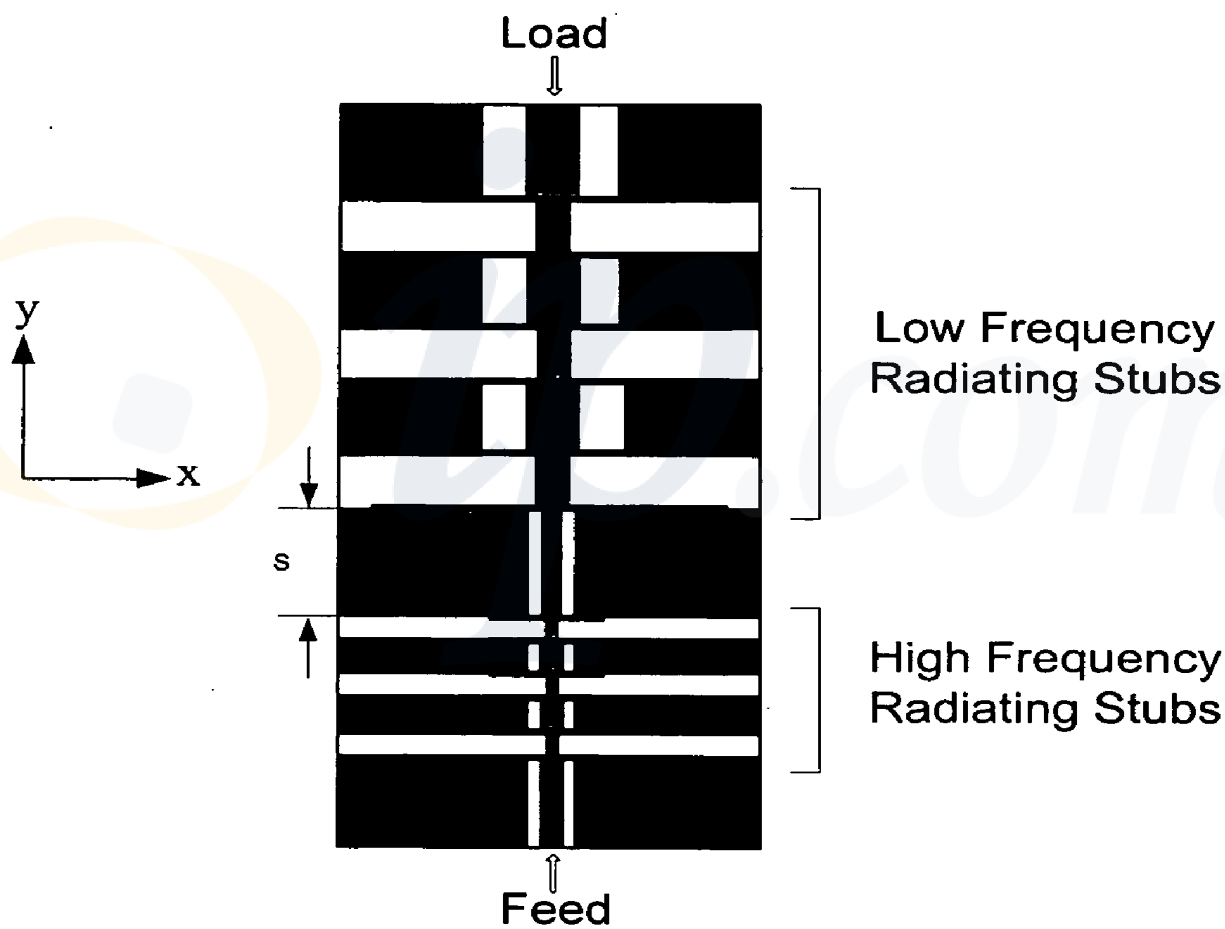

Figure 5

http://ip.com/patapp/US20050219136

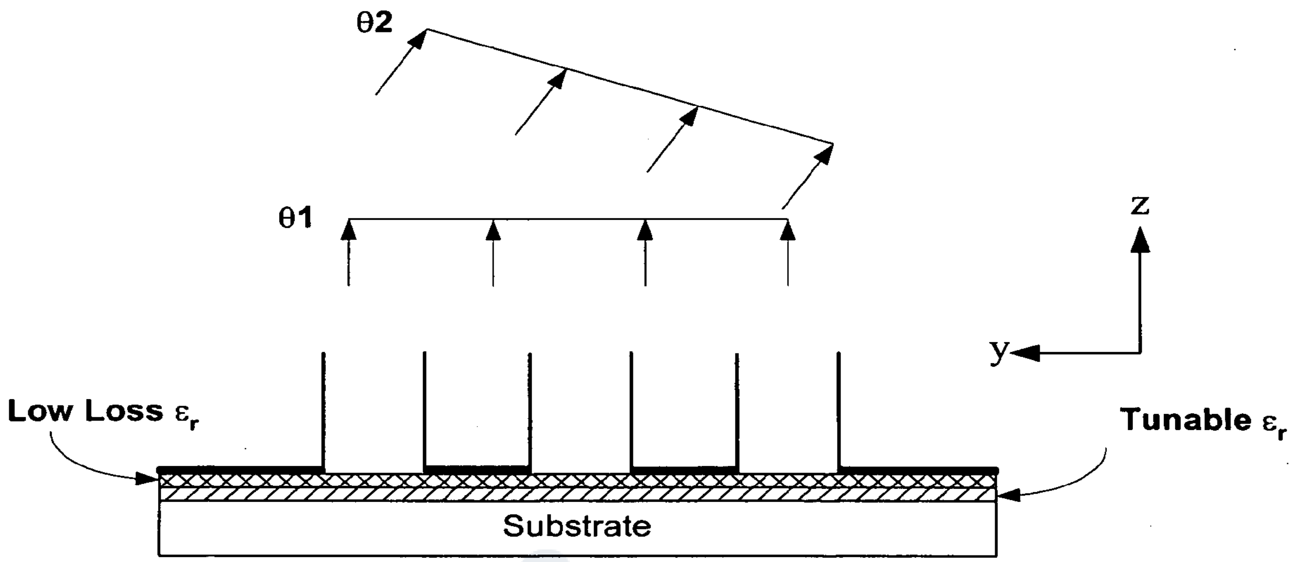

Figure 6

http://ip.com/patapp/US20050219136

COPLANAR WAVEGUIDE CONTINUOUS TRANSVERSE STUB (CPW-CTS) ANTENNA FOR WIRELESS COMMUNICATIONS

[0001] This U.S. patent application claims the priority of U.S. Provisional Application No. 60/558,592 filed on Mar. 31, 2004, entitled "Coplanar Continuous Transverse Stub (CTS) Antennas", by the same inventors.

TECHNICAL FIELD

[0002] This invention generally relates to continuous transverse stub (CTS) antennas, and more particularly, to an improved design that is mountable on a flat surface while being fed using a simple and low cost coaxial, microstrip, or coplanar transmission line and has multi-band capabilities and also low cost beam steering using ferroelectric technology.

BACKGROUND OF INVENTION

[0003] The planar continuous transverse stub (CTS) antenna and antenna array were originally invented and patented by Raytheon in the early 1990's, for example, in U.S. Pat. No. 5,266,961, by W. W. Milroy, issued 29 Aug. 1991, entitled "Continuous transverse stub (CTS) element devices and methods of making same". Benefits of the CTS antenna include compact size, lightweight, low cost, increased directive gain with increased radiating elements, and high efficiencies. The CTS antenna finds applications in the areas of mobile wireless and satellite communications and various military radar systems operating in the 500 MHz to 90 GHz frequency band.

[0004] A new coaxial version of the CTS technology with omni-directional radiation pattern is described in M. F. Iskander, Z. Zhang, Z. Yun, and R. Isom, "Coaxial Continuous Transverse Stub (CTS) Array," *IEEE Microwave and Wireless Components Letters,* vol. 11, no. 12, pp. 489-491, 2001, and in U.S. Pat. No. 6,201,509, of inventors in common herewith. A coaxial version of the CTS technology for multiband operation was reported in R. Isom, M. F. Iskander, Z. Yun, Z. Zhang, "Design and Development of Multiband Coaxial Continuous Transverse Stub (CTS) Antenna Arrays," *IEEE Trans. Antennas and Prop.,* vol. 52, no. 8, Aug. 2004. In particular, it was demonstrated that multiband performance at the 4.2 and 19.4 GHz frequency band with equivalent radiated power (~98%) and good impedance match is possible to achieve using this technology.

[0005] However, it is deemed desirable to improve the CTS antenna to be flat-mounted and have a broadside radiation pattern, low fabrication cost, simple coaxial, coplanar, or microstrip transmission line feed, and simple integration with microstrip circuitry in a transceiver front-end. With the flat implementation of the design, it is possible to provide beam steering capabilities through the integration of the antenna structure with a tunable dielectric substrate material as will be described in more details herein.

SUMMARY OF INVENTION

[0006] In accordance with the present invention, an improved continuous transverse stub (CTS) antenna has coplanar waveguide (CPW) feed elements spaced apart aligned in parallel with each other (x-directed) and mounted perpendicular to a planar substrate base made of a material of low dielectric constant. The CPW feed elements have associated with them quasi TEM modes which are interrupted by the presence of a continuous transverse stub on the ground plane of the substrate base. The presence of the purely reactive transverse stub elements couples a longitudinal, z-directed displacement current across the parallel plate transmission line and coplanar waveguide interface. This induced current excites z-directed EM waves where the electric field is linearly polarized in the transverse direction (y-directed) to the stub elements. The improved CPW-CTS antenna operates as a traveling-wave-fed antenna.

[0007] The transverse stub is preferably formed by a central portion of width (**CW1**) made of a conductive coating disposed on the ground plane surface with gap portions of width (CW) on each side thereof, providing a total stub gap width (GW). The CPW feed elements are preferably a pair of parallel plates spaced apart by a first length (**L1**) and having a width (**W1**) and height (**H1**) above the ground plane. The transverse stub extends perpendicularly through a clearance gap of height (**H2**) in the transverse direction across the ground plane. The clearance gap height (**H2**) is used to adjust the coupling capacitance to compensate the inductance of the purely reactive stub elements. The antenna is fed with a simple coplanar waveguide transmission line formed by the parallel CPW elements. The feed point (**L2**) is positioned away from the edge of the stubs to maintain a good impedance match. **L2** is carefully chosen to obtain the desired radiation pattern as a result of the axis EE of the feed line being oriented in line with the E-Plane radiation pattern. The substrate height (SH) is chosen for structural integrity and for improving the directive gain.

[0008] In a preferred embodiment, the signal conductor width (CW), total stub gap width (GW), and dielectric constant ($\in_r$) were chosen to provide 50 ohms feed impedance. The length (**L1**), width (**W1**), and height (**H1**) of the parallel plates were selected to be approximately a half wavelength, one wavelength, and one-third wavelength, respectively. The values of CW and CW**1** were carefully chosen and after extensive simulations to produce increased radiated power and at the same time maintain good impedance match. The width (**W2**) of the opposite outward portions from the plates is selected to reduce undesired back lobes, most notably in the H-Plane radiation measurements.

[0009] The CPW-CTS antenna of the present invention employs the coplanar waveguide with CTS technology, preferably in a planar microstrip configuration, to produce a broadside radiation pattern with a maximum in the +z direction, perpendicular to the plane of the antenna. The coplanar CTS offers the advantages over previous designs of a broadside radiation pattern, low input impedance, high radiated power, low fabrication cost, use of simple coaxial or microstrip transmission line feed, and simple integration with microstrip circuitry in a transceiver front-end.

[0010] Other objects, features, and advantages of the present invention will be explained in the following detailed description having reference to the appended drawings.

BRIEF DESCRIPTION OF DRAWINGS

[0011] **FIG. 1**(*a*) shows a schematic of a coplanar waveguide continuous transverse stub (CPW-CTS) antenna,

http://ip.com/patapp/US20050219136

and **FIG. 1**(*b*) shows a fabricated prototype example of the CPW-CTS antenna in accordance with the present invention.

[0012] **FIG. 2**(*a*) is a chart showing measured to predicted values for return loss, and **FIG. 2**(*b*) is a chart showing measured to predicted values for insertion loss.

[0013] **FIG. 3**(*a*) is a chart showing measured to predicted values for E-Plane radiation pattern, and **FIG. 3**(*b*) is a chart showing measured to predicted values for H-Plane radiation pattern.

[0014] **FIG. 4** shows an example of a coplanar waveguide continuous transverse stub array.

[0015] **FIG. 5** shows an example of a multiband coplanar waveguide continuous transverse stub.

[0016] **FIG. 6** shows an example of a CPW-CTS array with beam steering capabilities.

DETAILED DESCRIPTION OF INVENTION

[0017] The present invention provides an improvement upon previously known CTS technology, for example, as described in U.S. Pat. No. 6,201,509, to a named inventor in common herewith, which is incorporated by reference in its entirety herein. The CTS antenna employs a continuous transverse stub to form reactive or radiating elements for microwave, millimeter-wave, and quasi-optical filters and antennas. Purely reactive elements are formed by leaving a conductive coating on the surface of the stub elements to form radiating elements. The conductive material may be a ferroelectric material. The stub may be formed with individual stub elements separated from each other by air gaps or an appropriate material.

[0018] Referring to **FIG. 1**(*a*), a schematic diagram illustrates a co-planar waveguide, continuous transverse stub (CPW-CTS) antenna **10** in accordance with the present invention. The CPW-CTS antenna **10** has a planar substrate base **12** made of a material with a low dielectric constant, and a pair of coplanar waveguide (CPW) feed elements **14***a,* **14***b* extending longitudinally in the X-direction aligned in parallel with each other and mounted perpendicular to the plane of the substrate base **12**. The CPW feed elements **14***a,* **14***b* have associated with them quasi TEM modes which are interrupted by the presence of a continuous transverse stub element **16** formed on the ground plane. The presence of the purely reactive transverse stub elements couples a longitudinal, z-directed displacement current across the parallel plate transmission line and coplanar waveguide interface. This induced current excites z-directed EM waves where the electric field is linearly polarized in the transverse direction (Y-direction) to the stub elements, so that the CPW-CTS antenna operates as a traveling-wave-fed antenna.

[0019] The coupling values from the CPW elements to the stub radiating elements are primarily dependent on the following dimensional parameters:

[0020] Height (H1) of the top of the CPW feed elements above the ground plane

[0021] Gap clearance height (H2) of the CPW feed elements over the ground plane

[0022] Width (W1) of CPW elements across the ground plane

[0023] Width (W2) on each side externally from the width of CPW elements

[0024] Distance (L1) between parallel CPW elements

[0025] Distance (L2) on each side externally from the CPW elements

[0026] Central portion width (CW1) between stub radiating elements

[0027] Signal conductor width (CW) of stub radiating elements

[0028] Total stub gap width (GW) of central portion and stub radiating elements

[0029] Dielectric constant ($\in_r$) of conductive material for transverse stub

[0030] Substrate height (SH)

[0031] The transverse stub is preferably formed by a central portion of width (CW1) made of a conductive coating disposed on the ground plane surface with gap portions of width (CW) on each side thereof, providing a total stub gap width (GW). The CPW feed elements are preferably a pair of parallel plates spaced apart by a first length (L1) and having a width (W1) and height (H1) above the ground plane. The transverse stub extends perpendicularly through a clearance gap of height (H2) in the transverse direction across the ground plane. The clearance gap height (H2) is used to adjust the coupling capacitance to compensate the inductance of the purely reactive stub elements. The antenna is fed with a simple coplanar waveguide transmission line formed by the parallel CPW elements. The feed point (L2) is positioned away from the edge of the stubs to maintain a good impedance match. L2 is carefully chosen to obtain the desired radiation pattern as a result of the axis EE of the feed line being oriented in line with the E-Plane radiation pattern. The substrate height (SH) is chosen for structural integrity and for improving the directive gain.

[0032] In a preferred embodiment, the signal conductor width (CW), total stub gap width (GW), and dielectric constant ($\in_r$) were chosen to provide 50 ohms feed impedance. The length (L1), width (W1), and height (H1) of the parallel plates were selected to be approximately a half wavelength, one wavelength, and one-third wavelength, respectively. The values of CW and CW1 were carefully chosen and after extensive simulations to produce increased radiated power and at the same time maintain good impedance match. The width (W2) of the opposite outward portions from the plates is selected to reduce undesired back lobes, most notably in the H-Plane radiation measurements.

[0033] For simulation testing of the operating characteristics of the CPW-CTS antenna, a WIPL-D electromagnetic modeling program was used. It is a full 3-D electromagnetic simulation based on the method of moments, e.g., as described by Kolundzija, B., Ognjanovic, J. and Sarkar, T., *WIPL-D: Electromagnetic Modeling of Composite Wire and Plates Structures—Software and User's Manual,* Artech House, Boston, 2000. An antenna operating at 5.3 GHz was designed and desired features include low input impedance, high radiated power, and a broadside radiation pattern. The

http://ip.com/patapp/US20050219136

design dimensions obtained after extensive simulations were as follows:

[0034] H1=18.2 mm

[0035] H2=1.5 mm

[0036] W1=54.5 mm

[0037] W2=28.3 mm

[0038] L1=27.3 mm

[0039] L2=54.5 mm

[0040] CW=CW1=4.7 mm

[0041] GW=5.97 mm

[0042] Dielectric constant $\in_r$=2.94 (RT/Duroid 6002)

[0043] SH=3.01 mm.

[0044] A prototype of the CPW-CTS antenna was fabricated using the above simulation-designed parameters, as shown in **FIG. 1**(*b*). A coaxial tube type of transverse stub 16' (as described in U.S. Pat. No. 6,201,509) was used in this prototype. In the figure, a styrofoam spacer **14** is shown inserted over the radiating stub 16' between the CPW elements **14***a*, **14***b* to accurately maintain the radiating dimensions of the design distance between elements.

[0045] Referring to FIGS. **2**(*a*) and **2**(*b*), the charts of frequency (GHz) to signal (dB) show good agreement between the measured and the predicted (simulated) return and insertion losses, respectively. As can be seen, S_{11} was better than −10 dB between 5.2 and 5.6 GHz with a radiated power ratio greater than 40%, where the radiated power ratio is given by:

$$Pwr_{rad} \approx \frac{Pwr_{rad} - Pwr_{refl} - Pwr_{trans}}{Pwr_{tot}} * 100\% \tag{1}$$

[0046] The term transferred power is used to account for the amount of power received at the end of the antenna and after the radiating stub.

[0047] FIGS. **3**(*a*) and **3**(*b*) shows good agreement between the measured and the predicted E-Plane and H-Plane radiation patterns at 5.3 GHz, respectively. The measured E-Plane beam peak was −18° and the measured 3-dB beam width was 74.8°. The maximum back lobe was −14 dB from the maximum beam peak. The maximum back lobe of the measured H-Plane was −17 dB down from the maximum beam peak. The good agreement between predicted and measured results validates the predictability of the performance of this new antenna design.

[0048] Other design selections and modifications may be made to optimize the dimensions, characteristics, and/or performance of the CPW-CTS antenna. For example, the square stubs of the CPW-CTS antenna shown in **FIG. 1**(*a*) may be replaced with semi-circular stubs in order to form a low profile antenna with radial dimensions equivalent to the height (H1). Simulated results of such a configuration showed identical results.

[0049] Example of CPW-CTS Antenna Array

[0050] The invented continuous transverse stub design can be integrated in an array arrangement as shown in **FIG. 4** to increase the gain and narrow the beam width of the overall antenna. Increased gain may be achieved by increasing the amount of stub elements. Accomplishing this using a single feed in the antenna arrangements provides a significant advantage in simplicity of implementation and low cost of fabrication. The coupling from the microstrip to the radiating elements is primarily dependent on the parallel plate spacing (L1) and width (W1). The element to element spacing (S1) controls the amount of mutual coupling between each element. Element spacings are chosen to be approximately equal to an integral number of wavelengths (typically one) within the coplanar waveguide region. With increased elements, appropriate variation of the plate spacing (L1) and element to element spacings (S1) are required to achieve the desired radiated power based on the series nature of the array.

[0051] Example of CPW-CTS Multiband Array

[0052] A multiband planar array for microwave and millimeter wave applications may be constructed through appropriate selection of inter-element spacings and continuous transverse stub parameters. The selected frequency bands may be well separated due to the dispersionless nature of the air filled parallel plate transmission line structure and the frequency independent orthogonality of the coplanar waveguide modes. A six element multiband (two bands in this case with three elements array in each band) coplanar waveguide continuous transverse stub is shown in **FIG. 5**. Periodically-spaced continuous transverse stub elements designed to operate at the appropriate frequency bands are arranged with the high frequency radiators closest to the feed and low frequency radiators farthest from the feed. In this case the first three elements radiate at high frequency and last three radiate at lower frequencies. Typical planar array developments require the design of separate subarrays for each frequency band then merged to form the multiband array. Appropriate multiband performance is achieved with proper selection of the sub array spacing (S). Based on the wavelength dependence of the parallel plate elements and inter-element spacings, the subarray designed for higher frequencies will be relatively smaller compared with those for lower frequencies. Extended frequency bands may be realized using the aforementioned techniques.

[0053] Example of CPW-CTS Array With Beam Steering Capabilities

[0054] The coplanar implementation of the continuous transverse stub technology also lends itself to effective and low cost designs of antenna arrays with beam steering capabilities. As shown in **FIG. 6**, by including a layer of tunable dielectric materials such as Barium Strontium Oxide (BSTO), and providing the necessary biasing arrangement required to provide proper modulation of the dielectric constant, the radiation pattern of the array may be steered along the axis of the array. To help with the reduction of the insertion loss of the developed devices, a multilayer arrangement including a low loss dielectric between the conductors and the Barium Strontium Oxide layer (as shown in **FIG. 6**) may be implemented. For more details on BSTO technology for CTS antenna arrays, see W. Kim, M. Iskander, and C. Tanaka, "High-performance low-cost phase-shifter design

http://ip.com/patapp/US20050219136

based on ferroelectric materials technology", *IEE Electronic Letters,* 2004, vol. 40, no. 21, pp. 1345-1347.

[0055] The coplanar waveguide continuous transverse stub array has many performance, reproducibility, and application advantages over conventional slotted waveguide array, printed patch array, and reflector and lens antenna approaches in applications for which planar arrays have been inappropriate due to traditional bandwidth and/or cost limitations. Producibility advantages include considerable insensitivity to dimensional and limited material properties variations and simplified fabrication and processing procedures and ease of integration in the transceiver systems. This all leads to the low cost advantage of this technology. Making antenna components with BSTO ceramics with reliable dimensions in cylindrical geometries is currently achievable, and the planar structure of this CPW-CTS antenna configuration will facilitate this with ease.

[0056] In summary, a new coplanar waveguide CTS (CPW-CTS) antenna has been described. Advantages of this new design include low cost, low profile, light weight, and a very simple planar microstrip feed configuration. The design was validated by comparing measured results of a designed prototype against simulation results for a single element CPW-CTS design in the 5.2 to 5.6 GHz band. Both S-parameters and radiation pattern results were examined and good agreement between the experimental and simulation data were illustrated. Specifically, the designed one-element antenna exhibited a well-formed broadside main beam at the 5.3 GHz and good 50 ohms impedance match (−10 dB) from 5.2 to 5.5 GHz.

[0057] For further development, the coplanar waveguide CTS antenna design can be loaded with multiple elements to form a series array for improved directive gain and narrow beam widths. A multiple element array could also be formed with frequency selective sections to enable multiband operation. The planar design could be integrated with tunable ferroelectric materials to introduce multiband, electronic beam scanning capabilities, for example, as discussed in M. Iskander, Z. Zhang, Z. Yun, R. Isom, M. Hawkins, R. Enrick, B. Bosco, J. Synowczynski, and B. Gersten, "New phase shifters and phased antenna array designs based on ferroelectric materials and CTS technologies,"*IEEE Trans. Microwave Theory Tech.,* vol. 49, no. 12, December 2001, and W. Kim, M. F. Iskander, "High Performance Low Cost Phase Shifters Design Based on the Ferroelectric Materials Technology,"*IEE Electronic Letters,* 2004, vol. 40, no. 21, pp. 1345-1347.

[0058] It is understood that many modifications and variations may be devised given the above description of the principles of the invention. It is intended that all such modifications and variations be considered as within the spirit and scope of this invention, as defined in the following claims.

1. An improved continuous transverse stub (CTS) antenna comprising:

(a) a planar substrate base made of material of a low dielectric constant;

(b) a pair of coplanar waveguide (CPW) feed elements spaced apart by a given distance aligned in parallel with each other and mounted perpendicularly on a ground plane surface of the substrate base, wherein said CPW feed elements form a parallel feed transmission line through a coplanar waveguide interface; and

(c) a continuous transverse stub disposed on the ground plane surface of the substrate base extending in a transverse direction perpendicularly through a clearance gap formed through the CPW feed elements, wherein said transverse stub acts as a reactive, radiating member in conjunction with the feed transmission line of the coplanar waveguide interface for operation as a traveling-wave-fed antenna.

2. An improved continuous transverse stub (CTS) antenna according to claim 1, wherein the CPW feed elements have a first height **(H1)** above the ground plane surface and a first width **(W1)** across the ground plane surface, a gap height **(H2)** of the clearance gap above the ground plane surface, a second width **(W2)** of opposite outward portions on the ground plane surface on each outward side of the CPW feed elements, a first length **(L1)** between the parallel CPW feed elements, and a second length **(L2)** of opposite outward portions on the ground plane surface on each outward side of the CPW feed elements.

3. An improved continuous transverse stub (CTS) antenna according to claim 2, wherein the clearance gap height **(H2)** is used to adjust a coupling capacitance to compensate for inductance of the reactive transverse stub.

4. An improved continuous transverse stub (CTS) antenna according to claim 2, wherein the second length **(L2)** of the outward portions from the CPW feed elements is selected to maintain a good impedance match.

5. An improved continuous transverse stub (CTS) antenna according to claim 2, wherein the preferred first length **(L1)**, first width **(W1)**, and first height **(H1)** are selected to be approximately a half wavelength, one wavelength, and one third wavelength of a traveling wave sent on the feed transmission line.

6. An improved continuous transverse stub (CTS) antenna according to claim 2, wherein the CPW feed elements are a pair of rectangular plates in parallel having the first length **(L1)** between them and each having the first width **(W1)** and first height **(H1)**.

7. An improved continuous transverse stub (CTS) antenna according to claim 2, wherein the CPW feed elements are a pair of semi-circular plates in parallel having the first length **(L1)** between them and each having the first width **(W1)** and first height **(H1)** at its apex.

8. An improved continuous transverse stub (CTS) antenna according to claim 2, wherein the width **(W2)** of the opposite outward portions on each side of the first width **(W1)** of the CPW feed elements is preferably one third wavelength of a traveling wave sent on the feed transmission line to reduce undesired back lobes.

9. An improved continuous transverse stub (CTS) antenna according to claim 1, wherein the transverse stub is formed by a central portion of width **(CW1)** made of a conductive coating extending longitudinally in the transverse direction on the ground plane surface through the clearance gap formed through the CPW feed elements, and a pair of stub gaps of width **(CW)** on each side of the central portion separating it from opposite outward portions on the ground plane surface on each outward side of the pair of gaps.

10. An improved continuous transverse stub (CTS) antenna according to claim 9, wherein the central portion width **(CW1)**, signal conductor width **(CW)** of the pair of

http://ip.com/patapp/US20050219136

stub gaps, total stub gap width (GW), and dielectric constant ($\in_r$) of the stub material are chosen to provide 50 ohm feed impedance.

11. An improved continuous transverse stub (CTS) antenna according to claim 1, wherein the CPW feed elements have a first height (**H1**) above the ground plane surface and a first width (**W1**) across the ground plane surface, a gap height (**H2**) of the clearance gap above the ground plane surface, a second width (**W2**) of opposite outward portions on the ground plane surface on each outward side of the CPW feed elements, a first length (**L1**) between the parallel CPW feed elements, a second length (**L2**) of opposite outward portions on the ground plane surface on each outward side of the CPW feed elements, and wherein the transverse stub is formed by a central portion of width (**CW1**) made of a conductive coating extending longitudinally in the transverse direction on the ground plane surface through the clearance gap formed through the CPW feed elements, and a pair of stub gaps of width (CW) on each side of the central portion separating it from opposite outward portions on the ground plane surface for a total stub gap width (GW), said antenna being designed for operating at 5.3 GHz and having the following approximate values selected to provide for low input impedance, high radiated power, and a broadside radiation pattern:

H1=18.2 mm

H2=1.5 mm

W1=54.5 mm

W2=28.3 mm

L**1**=27.3 mm

L**2**=54.5 mm

CW=CW**1**=4.7mm

GW=5.97 mm

Dielectric constant ($\in_r$)=2.94 (RT/Duroid 6002)

SH=3.01 mm.

12. An improved continuous transverse stub (CTS) antenna according to claim 1, formed as a coplanar waveguide continuous transverse stub array.

13. An improved continuous transverse stub (CTS) antenna according to claim 1, formed as a multiband coplanar waveguide continuous transverse stub antenna.

14. An improved continuous transverse stub (CTS) antenna according to claim 1, formed as a CPW-CTS array with beam steering capabilities.

* * * * *